

# **FABRICATION AND CHARACTERIZATION OF COMPOSITE MEMBRANES AS DRUG-DELIVERING DURAPLASTY FOR STROKE TREATMENT**

Hollis McCulloch

A thesis submitted to the Faculty of Graduate and Postdoctoral Studies  
in partial fulfillment of the requirements for the degree of

**MASTER OF APPLIED SCIENCE**

in Biomedical Engineering

Faculty of Engineering

University of Ottawa

Ottawa, Canada

February 2019

© **Hollis McCulloch, Ottawa, Canada, 2019**

## Abstract

Stroke is a very prevalent issue in the world today with extremely limited treatment options. Load drug delivery and stem cell therapy are areas currently under development for the treatment of stroke. A stroke causes brain swelling and often a decompressive craniectomy is performed to prevent further damage. Then, a duraplasty is implanted to replace the surgically-damaged protective layers around the brain. The purpose of this project was to develop a synthetic duraplasty which can also be used as a drug-delivery system to promote endogenous stem cell therapy to treat stroke. The proposed duraplasty was a composite membrane composed of microspheres embedded in blended biosynthesized cellulose. Both single-walled microspheres (SWMS) and double-walled microspheres (DWMS) were fabricated and characterized. Then, they were incorporated into the composite membranes which were further characterized. The DWMS composite membranes were a similar thickness to human dura mater. They had the lowest swelling ratio implying that their initial drug release would be lower than the other samples. They were the strongest membranes and they still maintained some elasticity. The DWMS had a higher drug encapsulation efficiency than the SWMS and the DWMS composite membrane drug release profile showed the lowest initial burst and provided a prolonged zero-order release. Therefore, it was determined that the DWMS composite membranes were the ideal drug-releasing duraplasty.

## Statement of originality

The content presented in this document is the product of original work performed by the author at the University of Ottawa under the supervisor of Professor Xudong Cao.

In partial fulfillment of the requirements for the degree of Master of Science (Biomedical Engineering) at the University of Ottawa, this work was presented at the Ottawa Carleton Institute for Biomedical Engineering Seminar Series:

Holly McCulloch, Taisa R. Stumpf and Xudong Cao, Development of duraplasty for long term release of regenerative factors to repair brain tissue post stroke. Ottawa Carleton Institute for Biomedical Engineering, October 2018.

A poster on the same topic was also presented at the 68<sup>th</sup> annual Canadian Chemical Engineering Conference:

Holly McCulloch, Taisa R. Stumpf and Xudong Cao, Development of duraplasty for long term drug release to repair brain tissue post stroke. CSChE2018, October 2018.

## Statement of contribution

The entirety of this document was written by the author. All figures and tables were created by the author unless otherwise mentioned in the caption. The work presented was largely performed by the author including fabrication and characterization of the microspheres and composite membranes. The blank BBC membranes were designed and initially characterized by Taisa R. Stumpf. The cryo-sectioning of the double-walled microspheres was partially performed by Tongda Li.

## Acknowledgements

First, I would like to thank my supervisor Dr. Xudong Cao for his consistent support throughout this journey. I am very grateful for the opportunities that he has provided and for his enthusiasm about the project.

Second, I would like to thank Taisa R. Stumpf for her patience and motivation during this process. I would also like to thank Hesham Ismail and Tongda Li for all their help with this work as well as the other members of my lab for being so kind and providing moral support.

Third, I would like to thank my family and friends. Thank you for always encouraging and believing in me.

# Table of Contents

Abstract .....	ii
Statement of originality .....	iii
Statement of contribution .....	iv
Acknowledgements .....	v
List of Abbreviations.....	viii
List of Figures .....	ix
List of Tables.....	xi
1. Introduction.....	1
2. Literature Review .....	4
2.1 Stroke.....	4
2.1.1 Approaches to Overcome Stroke .....	4
2.1.1.1 Stem Cell Therapy.....	5
2.1.1.2 Decompressive Craniectomy (DC) .....	9
2.2 Protective layers of the brain .....	9
2.3 Duraplasty.....	10
2.3.1 Duraplasty Types .....	11
2.3.1.1 Autograft .....	11
2.3.1.2 Allograft .....	11
2.3.1.3 Xenograft.....	12
2.3.1.4 Synthetic Duraplasty .....	12
2.4 Hydrogels .....	14
2.4.1 Post-Stroke Treatment Using Hydrogels .....	14
2.4.2 Cellulose .....	17
2.4.2.1 Properties.....	18
2.4.2.2 Tissue Engineering Applications of BC.....	19
2.4.2.3 Drug Delivery Applications of BC .....	24
2.5 Microspheres .....	24
2.5.1 Types of Microspheres.....	24
2.5.1.1 Single-walled microspheres (SWMS).....	26
2.5.1.2 Double-walled microspheres (DWMS).....	27
2.5.2 Incorporation into Hydrogels.....	30

2.6 Purpose .....	35
2.6.1 Motivation.....	35
2.6.2 Objectives .....	35
3. Materials and Methodology .....	37
3.1 Materials .....	37
3.1.1 Microspheres.....	37
3.1.2 Membranes.....	37
3.2 Methodology.....	38
3.2.1 Microsphere Protocol.....	38
3.2.1.1 Preparation of Single-Walled Microspheres (SWMS).....	38
3.2.1.2 Preparation of Double-Walled Microspheres (DWMS) .....	39
3.2.2 Encapsulation Efficiency .....	41
3.2.3 Microsphere Size Analysis .....	42
3.2.4 DWMS Polymer Layer Characterization.....	42
3.2.5 Composite Blended Biosynthesized Cellulose (BBC) Membrane Production Protocol.....	42
3.2.6 Microsphere Retention.....	44
3.2.7 Swelling Ratio Protocol .....	45
3.2.8 Mechanical Test Protocol .....	45
3.2.9 Drug Release.....	46
3.2.10 Statistical Analysis.....	46
4. Results and Discussion .....	48
4.1 Preparation and Characterization of Microspheres .....	48
4.2 Production and Characterization of Composite Membranes.....	58
4.3 Drug Retention and Release .....	70
5. Conclusions.....	79
6. References.....	81
Appendix .....	110

## List of Abbreviations

BBB	Blood brain barrier
BBC	Blended biosynthesized cellulose
BC	Biosynthesized cellulose
BCA	Micro bicinchoninic acid
BDNF	Brain-derived neurotrophic factor
bFGF	Basic fibroblast growth factor
BSA	Bovine serum albumin
CNS	Central nervous system
CsA	Cyclosporin
CSF	Cerebral spinal fluid
DC	Decompressive craniectomy
DCM	Dichloromethane
DWMS	Double-walled microspheres
EA	Ethyl acetate
ECM	Extracellular matrix
EE	Encapsulation efficiency
EGF	Epidermal growth factor
ELISA	Enzyme-linked immunosorbent assay
FDA	US Food and Drug Administration
FGF-2	Fibroblast growth factor-2
HAMC	Hyaluronan and methylcellulose
NGF	Nerve growth factor
NPC	Neural progenitor cells
NSC	Neural stem cells
PBS	Phosphate buffer solution
PEG	Poly (ethylene glycol)
PLGA	Poly (lactic-co-glycolic acid)
PLLA	Poly (L-lactide acid)
PVA	Poly (vinyl alcohol)
SEM	Scanning electron microscope
SR	Swelling ratio
SVZ	Subventricular zone
SWMS	Single-walled microspheres
TE	Tissue engineering
UTS	Ultimate tensile strength
VEGF	Vascular endothelial growth factor

## List of Figures

Figure 1. Schematic showing exogenous (left) and endogenous (right) stem cell therapy for stroke treatment using neural stem cells (NSC). Reproduced from [85] License: CC BY 3.0.6	
Figure 2. The protective layers around the brain. Reproduced from [123]. License: Public Domain.....	10
Figure 3. Chemical structure of cellulose [171, 172, 169, 173].....	17
Figure 4. Chemical structure of PLGA where x refers to the number of units of lactic acid and y refers to the number of units of glycolic acid [239, 241].....	25
Figure 5. Possible configurations based on spreading coefficient theory; from left to right: complete encapsulation, partial encapsulation and non-encapsulation [265]. .....	30
Figure 6. Schematic of SWMS fabrication. ....	39
Figure 7. Schematic of DWMS formation. ....	41
Figure 8. Schematic of BBC composite membrane fabrication.....	44
Figure 9. Morphological characterization of the SWMS. A. Histogram of the size distribution of the blank and BSA-loaded SWMS; B. A representative SEM image of blank SWMS; C. A representative SEM image of BSA-loaded SWMS. ....	50
Figure 10. Representative SEM images of cross-sectioned DWMS showing the two distinct polymer layers. ....	52
Figure 11. Morphological characterization of the DWMS. A. Histogram of the size distribution of the blank and BSA-loaded DWMS; B. A representative SEM image of blank DWMS; C. A representative SEM image of BSA-loaded DWMS.....	55
Figure 12. Representative cross-sectioned SEM images of DWMS before and after washing with ethyl acetate (EA) where the arrows indicate the core of the DWMS. ....	57
Figure 13. Representative SEM images of high and low cellulose content control membranes and the commercially available Duraform®. All the above SEM images are at 225 x magnification.....	59
Figure 14. Representative SEM images of top and bottom of the SWMS composite membranes with varying amount of SWMS (0.1 g, 0.05 g and 0.025 g) and high and low cellulose concentrations. All the above SEM images are at 260 x magnification. ....	61
Figure 15. Swelling ratio of the composite membranes, control BBC membranes and Duraform® (N=8); A: SR at 24 hours of control BBC membranes and Duraform®; B: SR over time of high cellulose concentration membranes containing various amounts of SWMS; C: SR over time of high cellulose concentration membranes containing various amounts of DWMS. ....	64
Figure 16. The mechanical testing of the composite and control membranes and the commercially available Duraform® (N=8); A: The average ultimate tensile strength; B: The average Young's modulus; C: The average elongation-at-break. ....	69
Figure 17. The retention percentage of the varying amounts of SWMS and DWMS into the high and low cellulose content composite membranes (N=8). ....	72
Figure 18. Cumulative BSA released from the various amounts of SWMS alone and incorporated into the SWMS composite membranes (N=6). ....	75
Figure 19. Cumulative released BSA amount from various amounts of DWMS and DWMS composite membranes (N=6). ....	77

Figure 20. Representative SEM images after 42 days of release testing to demonstrate degradation; A: SWMS composite membrane; B: SWMS alone. .... 78  
Figure 21. Cumulative BSA released from various amounts of 1:1 DWMS (N=6). .... 110  
Figure 22. Percent cumulative BSA release from various amounts of SWMS and DWMS incorporated into the composite membranes (N=6). .... 111

## List of Tables

Table 1. Summary of several hydrogels used for stroke treatment.....	15
Table 2. Summary of several tissue engineering applications of BC .....	20
Table 3. Summary of several microsphere and hydrogel composites.....	32
Table 4. Average thickness of membranes when fully saturated with water (N=10). .....	66
Table 5. Average encapsulation efficiency of both SWMS and DWMS.....	71
Table 6. Initial burst release after 24 hours.....	77

# 1. Introduction

Stroke is currently a leading cause of long-term disability and death in the world [1, 2]. There are limited treatment options post-stroke mainly due to the challenge of getting drugs past the blood-brain barrier (BBB) and to the site of the stroke [3, 4, 5, 6]. While systemic thrombolytic therapy has been shown to be an effective treatment, unfortunately it has a very limited treatment window of 4.5 hours [7, 8, 9, 10, 11, 12]. Endogenous and exogenous stem cell based therapies are under investigation as potential stroke treatment options [6, 13, 14, 15, 16]. In addition, several injectable hydrogels loaded with different drugs to promote stem cell therapy have been used to attempt to treat stroke with varying degrees of success. The main problem with injectable hydrogels is that a burr hole must be drilled into the skull, so they are highly invasive [17, 18, 19, 20, 21]. Decompressive craniectomies are often performed on stroke patients to release the built-up pressure inside their skull caused by the stroke [22, 23]. While this procedure is invasive, it has been shown to greatly reduce the mortality rate of stroke patients [116, 117, 118, 119, 120]. After this procedure, a duraplasty is used to replace the surgically-damaged meninges, the protective layers around the brain. The purpose of this thesis was to create a long-term, zero-order drug releasing duraplasty for future use as an endogenous stem cell stroke therapy. The drug-loaded duraplasty could be used to enhance stroke recovery through stimulating endogenous stem cells to promote neural regeneration.

The hydrogel used to make the duraplasty membrane was biosynthesized cellulose (BC) due to its unique properties, such as high chemical purity and biocompatibility [24, 25, 26, 27, 28, 29, 30, 31, 23, 32]. BC has been used for a variety of previous tissue engineering applications

including for drug delivery and as a scaffolding material [33, 34, 35, 36, 37, 38, 39, 40, 41, 42]. Our lab successfully designed a duraplasty using BC [43]. The membrane itself showed excellent physical and mechanical properties, however the drug release of the fabricated membrane, when the drug was simply loaded onto the top of the membrane, only lasted for less than 7 days [43]. Since the duraplasty is intended to be a permanent implant, ideally, we would have better temporal control over the drug release in order to achieve the optimal therapeutic effect to further improve our duraplasty's potential application as a stroke treatment. Therefore, microspheres, spheres composed of degradable materials which can encapsulate drugs and other molecules, were incorporated into the duraplasty to create composite membranes. Microspheres have been used very successfully in tissue engineering for drug delivery applications since their release profiles are easily modifiable [44, 45, 46, 47, 48, 49, 50, 51, 52, 53]. They can deliver drugs for a prolonged period, but they suffer from high initial burst: a large amount of drug released in the first 24 hours [54, 55, 56]. The initial burst is caused by the drug which has not been encapsulated within the microspheres, but instead is located on the surface and therefore quickly diffuses into the surroundings once the microspheres are submerged [54, 55, 56]. Microspheres have been used in conjunction with a variety of hydrogels in order to combine their benefits [57, 58, 18, 59, 60, 61, 19, 62, 45, 63]. The combination of these materials has the potential to create a duraplasty with a sustained release profile.

The purpose of this work was to create a sustained drug-releasing duraplasty for future use as a stroke treatment. This was achieved by incorporating drug-loaded microspheres into a BC membrane and testing the efficacy of the drug release. Both single-walled microspheres

(SWMS) and double-walled microspheres (DWMS) were incorporated into the membranes to make SWMS composite membranes and DWMS composite membranes respectively and determine which composite membrane was the optimal drug-delivering duraplasty.

## 2. Literature Review

### 2.1 Stroke

Stroke is a major health concern in the world today, being the second leading cause of death and the third leading cause of long-term disability in adults in Canada [1, 64]. It is also associated with high financial cost due to the burden on the health-care system [65]. It is characterized by a sudden death of cells in the brain due to a disrupted blood supply depriving those cells of the needed oxygen and nutrients to survive. There are two major kinds of stroke: ischemic and hemorrhagic. An ischemic stroke is caused by a blood clot in a blood vessel in the brain blocking the blood supply to that area. This causes rapid death of the surrounding brain tissue, including the neurons, astroglia and oligodendroglia [64]. In comparison, a hemorrhagic stroke is caused by the rupture of a weakened cranial blood vessel resulting in an intracerebral hemorrhage where blood accumulates in the tissue around the rupture [22]. Ischemic strokes are in the clear majority, accounting for around 80% of all cases worldwide [66].

#### 2.1.1 Approaches to Overcome Stroke

There are a limited number of therapeutic approaches currently available for stroke treatment. The only FDA-approved ischemic stroke treatment is reperfusion, also called systemic thrombolytic therapy [7, 8, 9, 10, 11]. In this approach, tissue plasminogen activator is used to restore blood flow to the area by breaking the clot through activation of the proteolytic enzyme plasminogen [67]. Many studies have shown the effectiveness of this treatment if it is used during the limited therapeutic window [68, 69, 12, 70]. However, the therapeutic window

is only within 4.5 hours from onset of the stroke, which means that only a very small minority of patients are eligible for this treatment [64]. This leaves most stroke patients with no treatment, resulting in a high number of people living with long-term disabilities due to a stroke today [3, 4, 5]. In 2017, there were more than 400 000 Canadians living with long-term disabilities due to a stroke and that number is expected to double in the next 20 years [71]. It is of utmost importance that new therapeutic strategies be developed that do not rely so heavily on early detection and that aid in long-term recovery [64].

#### 2.1.1.1 Stem Cell Therapy

Stem cell therapy is a treatment option for stroke that is currently undergoing development. Stem cells are immature cells which have remarkable self-renewal capabilities and can differentiate into several different cell types throughout a lifetime [64, 72]. The purpose of stem cell therapy is to replace the damaged cells at the site of the stroke in the infarcted tissue, where the cells were damaged beyond repair [73, 64]. In addition, it assists in the recovery of the ischemic penumbra, where the cells are damaged but there is still potential for recovery through trophic support [73, 64]. Stem cell therapy has the potential to help re-establish functional neuronal circuitry and replace glial cells, including astroglia and oligodendroglia, to re-establish proper nerve conduction [64].

There are several potential sources for stem cells including: embryonic, fetal and adult stem cells [73, 64]. Both embryonic and fetal stem cells were implanted into native and ischemic stroke brains in rats and survived well and resulted in improved stroke outcomes [74, 75, 76, 77, 78, 79, 64]. Therefore, the stem cell treatment option has potential. However, the use of either of these types of stem cells has huge ethical issues and associated restrictions, so it is

adult stem cells that are the main research focus for stroke treatment. Research has shown that adult stem cells are present in the adult central nervous system (CNS) [64]. They provide progenitor cells to support normal cell turnover [80, 81, 82]. Adult stem cells, like all stem cells, have an amazing capacity for self-renewal and differentiation into organ-specific lineages, which makes them an excellent option for stroke treatment [83, 84].

There are two approaches for adult stem cell therapy in stroke treatment: an exogenous or an endogenous approach as shown in Figure 1 [65, 64].

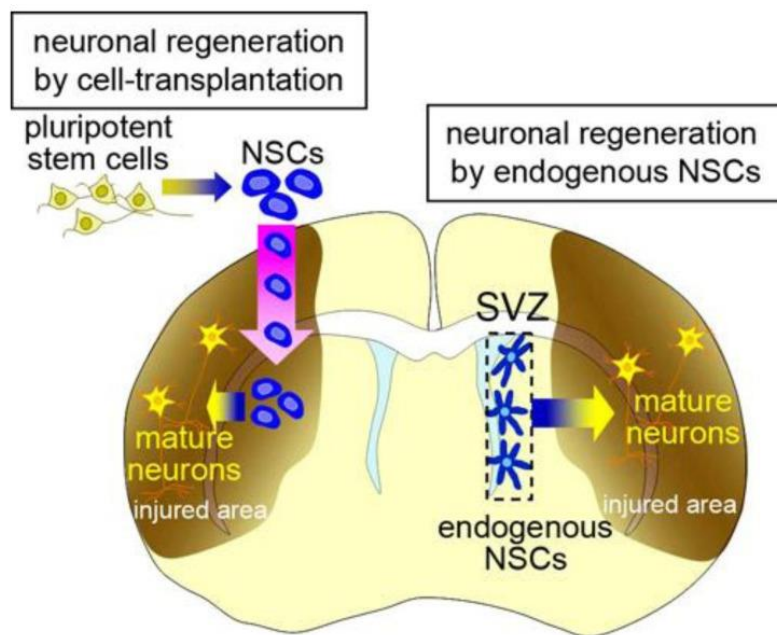


Figure 1. Schematic showing exogenous (left) and endogenous (right) stem cell therapy for stroke treatment using neural stem cells (NSC). Reproduced from [85] License: CC BY 3.0.

Exogenous stem cell therapy propagates stem cells in culture before purification and local or systemic administration [64]. Research for exogenous stem cell therapy as a stroke treatment is ongoing. Li *et al.* found that the rats treated with human bone marrow stromal cells had a

significantly better recovery when compared to the control rats [16]. They found a statistically significant increase in brain-derived neurotrophic factor and nerve growth factor as well as a decrease in apoptotic cells in the ischemic boundary zone [16]. Nelson *et al.* reported on their phase 1 clinical trial findings which showed that implanted clonal human neuronal grafts were able to survive in the human brain for over two years [15]. It has been shown that implanted neural cells are safe in animal models and can improve stroke outcomes in rats [14]. Kondziolka *et al.* showed that human neural cells implanted into stroke patients were safe [14]. Bang *et al.* showed that intravenous infusion of autologous mesenchymal stem cells into stroke patients was both possible and safe and resulted in improved functional outcomes using the Barthel index [6]. A major disadvantage of exogenous stem cell therapy is the fact that neural stem cells lose their differentiation capacity *in vitro* over time, which constrains their ability to be functional grafts [86, 87].

Endogenous stem cell therapy utilizes the adult stem cells already present in the CNS [88, 83, 89, 84, 90]. It has been shown in animal models that traumatic brain injuries, including stroke, promote neurogenesis from the neural stem cells (NSC) located in the subventricular zone (SVZ) [91, 92, 93, 94]. The NSC migrate to the damaged area of the brain and then differentiate into neurons to replace the neurons that died during the stroke [81].

Growth factors have also been shown to be able to promote SVZ neurogenesis, causing migration of the NSC to the site of the injury and NSC proliferation in the penumbra region [95, 80, 96]. Several different growth factors are currently being studied including: fibroblast growth factor-2 (FGF-2) [97, 98, 99], vascular endothelial growth factor (VEGF) [100, 101], brain-derived neurotrophic factor (BDNF) [102, 103], erythropoietin [104], epidermal growth

factor (EGF) [105] and stem cell factor [98]. Several other drugs are also being studied to determine their impact on endogenous stem cell therapy including caspase inhibitors [106] and anti-inflammatory drugs [107, 108].

In a rat model, VEGF has been shown to promote migration of NSC from the SVZ to the site of the injury [109]. This led to a 35 % reduced infarct volume after 3 days and associated functional recovery determined through the improvement of two motor tests and one sensory test [95]. FGF-2 and EGF increased neurogenesis in the SVZ, helped restore long-term potentiation, and were associated with an improved spatial orientation [110]. Erythropoietin has also been shown to be able to increase neurogenesis through the upregulation of VEGF and BDNF [111]. A double-blind study was performed on 40 patients that showed better stroke outcomes in erythropoietin-treated patients compared to the control group [112]. The outcome was evaluated through an increased functional recovery and a reduction in the infarct size [112].

The question remains of how to place the growth factors into the brain so that they can induce endogenous stem cell therapy. This is especially challenging after a stroke, because there are astrocytes and microglia at the site of the injury releasing pro-inflammatory cytokines [4]. This leads to inflammation and the formation of a glial scar around the stroke cavity [4]. Additionally, the BBB prevents the passage of most macromolecules, while allowing the diffusion of hydrophobic molecules and very small polar molecules [113]. There is currently research underway to attempt to bypass the BBB [114, 115]. However, these challenges could be overcome by using local delivery methods such as drug-loaded hydrogels administered directly to the stroke site.

### 2.1.1.2 Decompressive Craniectomy (DC)

Although there is a distinct lack of therapeutic options for stroke treatment, there are options for treating the symptoms and preventing further damage. Both major types of strokes often result in significant brain swelling [23]. The procedure currently used to manage brain swelling is called a decompressive craniectomy (DC), in which the skull is opened at the site of the stroke to allow the pressure to be released [22]. While a DC is an invasive procedure, the benefits have been shown to outweigh the risks as it greatly reduces the probability of disability and death, by reducing the pressure within the skull and preventing further damage to the brain [116, 117, 118, 119, 120]. However, it is important to note that the DC does not reverse any of the damage to the brain caused by the stroke. In a published statement for healthcare professionals Wijdicks *et al.* details the risk-benefit analysis of who should receive a DC given a variety of variables [121].

### 2.2 Protective layers of the brain

During a DC, the integrity of the protective layers around the skull are compromised so that the pressure can be released [121]. The brain has several outer protective layers including the skin and skull. The protective layers under the skull are called the meninges [122]. The meninges, from the outside in, are the dura mater, the arachnoid layer and the pia mater. The outermost layer, the dura mater, lies flush against the skull [122]. It is made of dense and irregular collagen fibers from neural crest cells and is the thickest layer [122]. Its role is to protect the brain [122]. The outer surface of the arachnoid mater is in contact with the dura mater [122]. It is composed of a fine network of collagen and elastin fibers [122]. Its role is to contain the cerebrospinal fluid (CSF) [122]. The role of the CSF is to cushion the brain by

absorbing any shock, as well as circulating nutrients and removing waste products [122]. The pia mater is a very delicate mesh of elastin and collagen fibers bound to the neural tissue [122]. The protective layers around the brain are shown in Figure 2. Since the meninges are compromised during the DC, it is necessary to patch the damaged area to protect the brain and contain the CSF using a duraplasty.

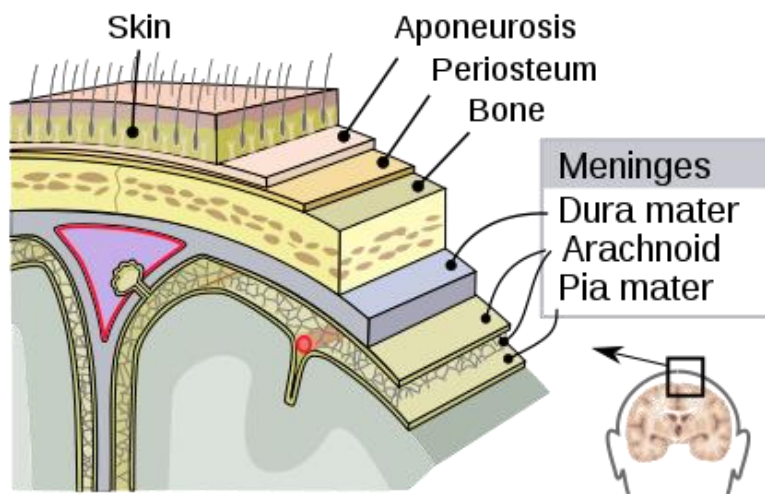


Figure 2. The protective layers around the brain. Reproduced from [123]. License: Public Domain.

### 2.3 Duraplasty

Several types of duraplasty options have been developed for this purpose over the years. An ideal duraplasty material should meet all the following characteristics. First, it must have excellent biocompatibility with no risk of infection [124, 125, 126, 39, 127, 128, 121]. Second, it must have reasonably high mechanical properties, so that it is able to withstand the wear and tear of the implementation surgery and protect the brain tissue, while still maintaining some flexibility and elasticity, so that it is able to conform to the shape of the brain [124, 125, 126, 39, 127, 128, 121]. Third, it must be able to prevent CSF leakage [124, 125, 126, 39, 127, 128,

121]. Fourth, it must be a readily available, cost-effective source material that is easy to produce and store [124, 125, 126, 39, 127, 128, 121].

### 2.3.1 Duraplasty Types

There are four types of material which have been used as duraplasty including: autografts, allografts, xenografts and synthetic materials.

#### 2.3.1.1 Autograft

An autograft involves the use of material that has been taken from the same individual. However, there is often insufficient local material (material available at the site of the original surgery) for replacement, due to the limited size of the surgical site. Therefore, material from other areas of the body are often used [129, 130, 131, 132, 133, 134, 121]. This requires a second surgical site which is a significant disadvantage as it increases patient morbidity [135, 132, 134, 131]. The material often used for dural replacement is the fascia lata, a piece of fibrous tissue deep in the thigh. However, the pericardium, fat, muscle and temporalis fascia have also been used [126, 135, 136, 131, 121]. Autografts have been shown to have a higher rate of CSF fistulas, aseptic meningitis and overall implant failure than non-autologous grafts [137, 138, 121].

#### 2.3.1.2 Allograft

An allograft involves the use of material that has been taken from another individual of the same species. In the past, the material has been removed from cadavers, and while this eliminated the problem autografts suffered from of limited availability, this practice has since been associated with an increased risk of the transmission of viral infections and prion diseases

[139, 129, 131, 140, 141, 142, 121]. Another example of an allograft is a human amniotic membrane [143]. However, this material is limited in quantity and is not easy to obtain because of the ethical issues that surround it, which are similar to those of fetal stem cells [127].

#### 2.3.1.3 Xenograft

A xenograft involves the use of material that has been taken from another species and often collagen obtained from animal tissue is used [141, 144]. Collagen used for this purpose has low mechanical strength as it is re-shaped through solubilization in acetic acid which results in the complete loss of structural organisation from the original collagen matrix [145]. This is problematic because this material has been shown to be susceptible to thinning and hole formation resulting in CSF leakage and subsequent development of pseudomeningocele [146, 147]. In addition, there is the risk of transmitting animal pathogens or viral infections as well as a risk of other immunological problems [148, 149, 150, 151, 152]. However, these grafts can be treated using hydrochloric acid or sodium hydroxide to inactivate prions [153, 132, 133, 134, 140, 141, 154, 155]. A currently commercially available xenograft is the Codman Duraform® Dural Graft made by Johnson & Johnson in New Brunswick, New Jersey [128]. Duraform® is a duraplasty composed of type I collagen tissue harvested from a bovine Achilles tendon [128]. It caused a minimal inflammatory reaction and, because it is absorbable, this reaction decreased over time [128]. It showed manageable handling qualities and was able to prevent CSF leakage [128].

#### 2.3.1.4 Synthetic Duraplasty

Synthetic materials are more versatile as they can be processed easily into a variety of shapes and sizes as required [124]. In addition, they are inert and therefore offer a greatly reduced

possibility of transmitted diseases [131]. Both absorbable and non-absorbable synthetic materials have been developed. Non-absorbable materials are permanent implants, whereas absorbable materials are absorbed by the body over time, which is advantageous as they have a decreased potential of causing chronic inflammation reactions [124]. Examples of synthetic materials used include polytetrafluoroethylene [156, 157, 158], polyester urethane [131], silk fibroin [159, 160] and biosynthesized cellulose [129].

#### 2.3.1.4.1 NeoDura (Medprin Biotech GmbH – Frankfurt, Germany)

This biomimetic patch was primarily composed of biodegradable nonwoven poly (L-lactide acid) (PLLA) fibers [124]. It was shown to have good mechanical strength and biocompatibility [124]. It prevented CSF leakage, caused only low inflammation and fully degraded in 2 years [124]. This patch can help reconstruct the damaged dura mater and thus is an excellent duraplasty option [124].

#### 2.3.1.4.2 Synthecel (DePuy Synthes – Raynham, Massachusetts)

Synthecel is composed of biosynthesized cellulose from *G. xylinus* [129]. The cellulose fibers are non-woven and interconnected to create a mechanical layer which covers and helps repair the dural defect while preventing CSF leakage [129]. It is immunologically inert with a minimal foreign body response [129]. It is reported to have a similar thickness to human dura with good conformation to the brain [161, 162]. It is packaged wet and can be used as an on-lay or sutured. It is shown to be stronger, with a significantly better seal quality than xenografts [129].

Xenografts and synthetics are the two common types of duraplasty currently commercially available [124]. However, they have not been developed to also be used as a drug-delivery system. Therefore, they are not able to treat while performing their role as a duraplasty. This has not been done previously as it is the combination of two research paths: creating synthetic duraplasty for use after a DC and the creation of drug-delivering hydrogels for the promotion of endogenous stem cell therapy.

## 2.4 Hydrogels

The synthetic duraplasty that was previously created by our lab was composed of a hydrogel. Hydrogels are three-dimensional networks of hydrophilic polymers which can absorb a very large amount of water while maintaining their strong mechanical properties [163]. There are many hydrogel materials such as: collagen, gelatin and agarose. Several of those hydrogels have been used previously for tissue engineering and have been shown to be biocompatible. In particular, there are several hydrogels that have been studied for use as potential stroke treatments.

### 2.4.1 Post-Stroke Treatment Using Hydrogels

Hydrogels are a very promising new material to provide local drug delivery. Table 1 summarises some of the injectable hydrogels which are being developed for use as stroke treatment options.

Table 1. Summary of several hydrogels used for stroke treatment

Hydrogel	Results	Delivery Mechanism	References
Porous hyaluronic acid	This hydrogel reduced the initial inflammatory response, increased peri-infarct vascularization, increased neural progenitor cell (NPC) proliferation and migration to the SVZ zone and resulted in NPC migration into the peri-infarct region	Injected using a 30-gauge needle directly into the stroke cavity; needle withdrawn after 5 minutes	[4]
Poly(ethylene glycol)-modified EGF in hyaluronan and methylcellulose (HAMC)	This hydrogel was placed epi-cortically, poly(ethylene glycol) (PEG) was used to modify EGF and successfully decrease EGF degradation by proteases, therefore, there was an increase in protein accumulation at greater tissue depths with increased NPC proliferation and stimulation	Injected into burr hole using a 26-gauge needle directly into the stroke cavity; needle withdrawn after 10 minutes	[164]
HAMC	This hydrogel was placed epi-cortically in mice, it released erythropoietin, reduced the stroke cavity size and the inflammatory response, and increased the number of neurons in the peri-infarct region and migratory neuroblasts in the SVZ, it also decreased apoptosis	Injected into burr hole using a 26-gauge needle directly into the stroke cavity; needle removed after 10 minutes	[165]
Hyaluronic acid	This hydrogel was tested in mice and non-human primates ( <i>Macaca fascicularis</i> ), and it showed that BDNF was delivered for over 3 weeks and promoted substantial motor function recovery	Injected using a 30-gauge needle; injection done at 1 $\mu$ l/min	[166]
Hyaluronan/Heparin sulfate	This hydrogel diminished inflammation and altered the local environment of the infarct to promote survival of NPCs and decrease stress	Injected into burr hole using 30-gauge needle; injection done at 0.7 $\mu$ l/min; needle removed after 5 minutes	[5]
D-block co-polypeptide (K <sub>180</sub> L <sub>20</sub> and E <sub>180</sub> L <sub>20</sub> )	This hydrogel provided sustained delivery of nerve growth factor bioactivity within the BBB	Injected into burr hole using glass micropipettes; injections done at 0.2 $\mu$ l/min	[167]

Acellular extracellular matrix	This hydrogel promoted significant acute endogenous repair	Injected into burr hole using 24-gauge needle; injections made at 10 $\mu$ l/min; needle removed after 5 minutes	[168]
--------------------------------	--	--	-------

## 2.4.2 Cellulose

Cellulose has a three-dimensional structure with hydrogen bonding between the cellulose fibers and it can retain a very large amount of water and is therefore considered a hydrogel. It is the most abundant organic polymer on earth, with a biomass production of around  $1.5 \times 10^{12}$  tons per year [169]. It is a linear homo-polysaccharide consisting of two D-glucose molecules attached via  $\beta$ -1,4-glycosidic linkages as shown in Figure 3. The linear chains join to form elementary sub-fibers which, through hydrogen bonding, join to form microfibrils which crystallize to form cellulose fibers [27, 170].

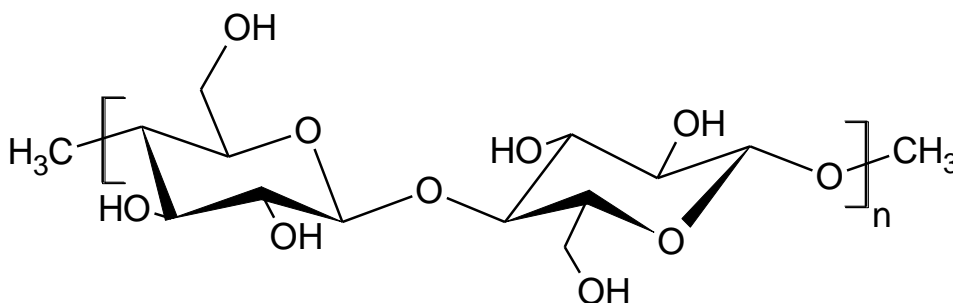


Figure 3. Chemical structure of cellulose [171, 172, 169, 173].

Cellulose is commonly produced from two sources: plants and bacteria. Plants produce cellulose as part of the structure of their cell wall, while certain types of bacteria produce a biofilm layer of cellulose [169]. The cellulose produced by bacteria is referred to by many names, including bacterial cellulose, biosynthesized cellulose, and microbial cellulose [174, 175, 176, 177]. The term biosynthesized cellulose (BC) will be used in this thesis. The bacteria produce cellulose to protect themselves mainly from ultraviolet radiation as well as other chemical and mechanical attacks, such as heavy metal ions and to improve nutrient transport,

because the production of BC keeps the bacteria near the surface of the culture medium where the oxygen content is greatest [175, 178, 179].

BC has the advantage of a higher degree of purity as compared to plant cellulose which requires several chemical treatments to remove the lignin and hemicellulose [169, 180, 181, 35]. BC has several other benefits over plant cellulose, including a 100 times smaller fibril, which allows the overall material to be more porous which has several advantages for tissue engineering including BC's ability to be more absorbent per unit volume than plant cellulose [182, 29, 183]. For example, *Rhizobium leguminosarum* produce cellulose fibers with 5 nm in diameter and up to 10  $\mu\text{m}$  in length [185]. BC has been shown to be able to hold up to 100 times its dry weight in water [183]. Although the cost of producing BC is currently high, there is research being done to increase the production of BC using waste materials to decrease the production cost and be environmentally-friendly [184].

There are several bacteria that produce BC including the gram-negative bacteria *Achromobacter* sp., *Aerobacter* sp., *Agrobacterium* sp., *Alcaligenes* sp., *Enterobacter* sp., *Gluconacetobacter xylinus*, *Psuedomonas* sp., *Rhizobium* sp., *Salmonella* sp. and *Sarcina* sp. [185, 186] and the gram-positive bacterium *Gluconacetobacter hansenii* [187].

#### 2.4.2.1 Properties

BC is chemically pure [24, 25, 182] with variable pore sizes [24, 25]. It has been shown to be biocompatible and this has been attributed to its structural similarities to the extracellular matrix (ECM) [25, 188, 28, 29, 20, 24, 189, 31, 190]. It has a very high water holding capacity [188, 28, 29] and can retain its high tensile strength in a hygroscopic state - while fully

saturated with water [20, 39]. It is highly modifiable, both chemically and physically [190, 32]. For example, altering the container and production method (static, agitated or airlifted) can change the morphology of the membrane, altering the duration of culturing can vary the thickness of the membrane, and altering the contents of the media used can alter the quality of the fibers as well as the homogeneity and density of the membrane [191, 29, 192, 193].

The top and bottom surfaces of BC membranes are different due to the difference between the liquid versus air interactions with cellulose as it is produced. The top of the BC, the side in contact with the air, is more dense than the bottom of the BC, the side in contact with the liquid, which is more gelatinous and porous [194, 195, 196, 197, 198, 183]. This is not ideal for our purposes of a drug-delivering duraplasty and therefore some physical modifications were performed to create a more uniform membrane.

#### 2.4.2.2 Tissue Engineering Applications of BC

The amount of research being done on BC for use in tissue engineering has increased exponentially in recent years [169]. Tissue engineering (TE) uses cells, scaffolds and growth factors to repair and restore the function of damaged tissue. The ideal scaffold must be biocompatible, should have a three-dimensional structure with a well-defined microstructure which consists of an interconnected pore network, and should have mechanical properties like those of the real tissues it is being used to replace [199, 200, 201]. BC has been shown to meet all those requirements and therefore has been used for a variety of different TE applications [202, 203, 195, 35]. Table 2 summarises the major areas of research of TE that are currently employing BC.

Table 2. Summary of several tissue engineering applications of BC

Application	Bacteria	Results	References
Wound dressings	<i>Acetobacter sp. A10</i>	Compared to regular gauze, BC membranes were found to increase the speed of healing of second degree burn injuries on SD rats	[204]
	<i>A. xylinum</i>	Nanocrystalline zinc oxide particles were incorporated into BC and the resulting membranes showed strong antibacterial activity against both gram-positive and gram-negative bacteria	[33]
	<i>A. xylinum</i>	BC coated on cotton gauze significantly increased its water absorbency and wicking ability	[205]
	<i>Obtained BC from Hainan Yida Food Co. Ltd. (China)</i>	The silver sulfadiazine infused BC membranes had significant antimicrobial activity against both gram-positive and gram-negative bacteria	[206]
	<i>A. xylinum</i>	The benzalkonium chloride infused BC film was found to have gained stable antimicrobial properties for at least 24 hours against gram-positive bacteria	[207]
	<i>A. xylinum</i>	Silver nanoparticles were dispersed on BC nanofibers using a reaction between AgNO <sub>3</sub> and NaBH <sub>4</sub> resulting in hybrid nanofibers with strong antimicrobial properties against both gram-positive and gram-negative bacteria	[182]
	<i>G. xylinus</i>	BC was used as both the reducing and stabilizing agent during the hydrothermal synthesis of silver nanoparticles, an environmentally benign process to produce a material which provided a prolonged release of silver and an associate prolonged antibacterial performance against gram-positive bacteria	[208]
	<i>G. xylinus</i>	Silver nanoparticles were imbedded in BC membranes using triethanolamine and the composite membranes were shown to contain only Ag particles (not a mixture of silver oxides) and they displayed strong antimicrobial properties against both gram-positive and gram-negative bacteria	[209]
	<i>A. xylinum</i>	Silver nitrate was incorporated into BC membranes, then sodium borohydride was used to reduce the Ag <sup>+</sup> to Ag <sup>0</sup> (silver nanoparticles) and the membranes exhibited strong antimicrobial activity against both gram-positive and gram-negative bacteria	[176]

	<i>A. xylinum</i>	Dried BC was proposed as a temporary skin substitute	[210]
	Obtained BC from Hainan Yida Food Co. Ltd. (China)	Silver nanoparticles were evenly distributed over BC nanofibers and exhibited significant antibacterial activities against both gram-positive and gram-negative bacteria for over 72 hours while permitting the attachment and growth of epidermal cells in order to promote wound healing	[211]
	<i>A. xylinum</i>	BC membranes were modified with aloe vera gel, which resulted in stronger mechanical strength, higher crystallinity, higher water absorption capacity, higher water vapor permeability, and reduced pore size	[212]
	<i>A. aceti</i>	Hydrolysis was used to incorporate partially deacetylated chitin nanocrystals onto BC nanofibers, which resulted in nanocomposites which showed strong antibacterial activity making this a novel, environmentally friendly way to introduce antimicrobial properties	[213]
	<i>A. xylinum</i>	BC with sodium alginate and silver sulfadiazine were prepared and the composites were shown to have excellent antibacterial activities against both gram-positive and gram-negative bacteria as well as good biocompatibility	[214]
Cardiovascular implants	<i>A. xylinum</i>	An anisotropic PVA-BC nanocomposite was created which had similar mechanical properties to a porcine aorta within the physiological range and even better properties beyond physiological strains	[34]
	<i>A. xylinum</i>	Tubular BC was designed with an inner diameter of 1 mm while retaining the excellent qualities of BC such as high hygroscopic mechanical strength, high water retention capabilities and low roughness of the inner surface making this material very promising as an artificial blood vessel in microsurgery	[194]
	<i>A. xylinum</i>	BC tubes were cross-linked with chitosan/heparin composite to prevent blood clots in its use as a biomimetic scaffold for blood vessel tissues and they were shown to be suitable for cell proliferation and ingrowth	[215]
Cartilage scaffolds	<i>G. xylinus</i>	BC was shown to support growth and proliferation of chondrocytes (cartilage cells) as well as ingrowth into the scaffold	[35]
	<i>G. xylinus</i>	Paraffin beads injected during the fermentation process caused porous BC which offered an optimal environment for chondrocyte seeding and ECM production	[216]

	<i>G. xylinus</i>	BC was shown to have equal mechanical properties to native ear cartilage and other benchmark replacement materials, and it can be uniquely shaped for each patient	[217]
	<i>G. xylinus</i>	BC was compared to collagen and pig meniscus as a potential meniscus implant and was found to have higher mechanical strength than collagen but lower mechanical strength than the pig meniscus, however, it can be produced in the correct shape and it promotes cell migration which makes it an attractive material	[218]
Bone scaffolds	<i>G. xylinus</i>	BC-hydroxyapatite nanocomposite membranes were created by incubation in CaCl <sub>2</sub> followed by Na <sub>2</sub> HPO <sub>4</sub> and were shown to be effective for bone regeneration	[219]
	<i>A. xylinum</i>	BC was found to be a good localized delivery system of bone morphogenetic proteins which induced osteoblast (bone cell) differentiation allowing it to develop more new bone than plain BC scaffolds	[220]
	<i>A. xylinum</i>	Paraffin wax microspheres were incorporated into the fermentation process to create a porous environment which allowed cells to cluster within the pores and form denser mineral deposits than on the surface of BC	[221]
	<i>A. xylinum</i>	Using a biomimetic approach BC was negatively charged using carboxymethyl cellulose to initiate nucleation of calcium-deficient hydroxyapatite, the presence of which on the BC resulted in increased cell attachment, therefore promoting bone healing	[222]
	Obtained BC from Aich Foods Inc. (Japan)	Antibiotics were incorporated into BC, which was then mixed with the bone cement, the mechanical properties of the bone cement were not affected and there were increased levels of antibiotic release than in antibiotic bone cement without cellulose	[223]
	<i>G. hansenii</i>	The skeleton of a sand dollar ((Ca,Mg)CO <sub>3</sub> ), which has an interconnected porosity, was coated by BC, then with calcium phosphate (apatite), a bioactive surface, allowing for cell adhesion while the structure remained conducive to cell migration and vascularization	[224]
	<i>A. aceti</i>	BC was immersed in graphene oxide/hydroxyapatite which supported the adhesion of osteoblast cells with good viability leading to a potentially osteo-inductive material	[225]

	<i>G. hansenii</i>	BC was chemically-modified into dialdehyde BC, making it biodegradable and calcium-deficient hydroxyapatite was attached forming nanocrytallites, giving this material great potential as a synthetic bone graft	[226]
	<i>A. xylinum</i>	A BC-gel/HAp (gelatin/hydroxyapatite) composite was synthesized and it successfully increased the mechanical strength, adhesion, proliferation and differentiation compared to the BC/HAp composite making this new material an ideal bone scaffold	[227]
Dental Treatments	<i>A. hansenii</i>	BC was found to have greater absorption, higher cumulative drug release and better compatibility than paper points (plant cellulose) which are currently used for dental root canal treatment, which makes BC an excellent alternative	[37]
	<i>Acetobacter sp.</i>	BC was synthesized to contain cement (mineral binding powders) and it showed improved features such as setting time and biological properties with the material able to sustain cell survival and promote cell proliferation giving this composite potential for use in endodontics	[228]
Artificial cornea implants	<i>A. xylinum</i>	A BC/PVA composite was developed which had a high percent light transmittance with strong mechanical properties and excellent thermal properties making it a very promising artificial cornea composite material	[38]
Neural implants	<i>G. xylinus</i>	Biocompatible neurotubes were developed which were used as guidance channels to aid in the reconstruction of damaged peripheral nerves by preventing the formation of neuromas while allowing neurotrophic factors to gather and facilitate neural regeneration	[229]
	<i>A. xylinum</i>	BC was used in rabbits as a duraplasty and it was found to be biocompatible and it successfully prevented CSF leakage	[39]
Urinary conduits	<i>A. xylinum</i>	A BC scaffold was generated and seeded with urine-derived stem cells which provided favorable conditions to assist in the development of a TE urinary conduit	[40]
Nutrient delivery	<i>A. xylinum</i>	Microstrands of BC covered with mammalian cells were developed to use as a pathway for nutrition and oxygen to feed the cells in the central region of functional macroscopic tissues	[41]

#### 2.4.2.3 Drug Delivery Applications of BC

While BC has been employed in many TE fields, it is especially interesting for drug delivery applications. Drug release is an important aspect of TE, and BC has been used as a drug delivery platform in a variety of ways. It has been used transdermally to release molecules such as lidocaine, ibuprofen, caffeine and diclofenac [230, 42, 231, 232]. It has also been used as an oral drug-delivery system to provide a more controlled release, from 95 % of drug release in one hour by the commercial tablets, to 80 % of drug released over 20 hours when coated with BC [233, 173]. Hydrogel drug release is based entirely on diffusion [234]. For this thesis, microspheres will be incorporated into the BC to improve the drug delivery profile.

### 2.5 Microspheres

Microspheres are spherical shells on the micro scale composed of protein or a synthetic polymer. For use in TE, a degradable material is often chosen for the formation of microspheres so that they can be filled with a material which will be released as the microsphere degrades. Since they are biodegradable drug-delivery systems, there is no need for device recovery [235].

#### 2.5.1 Types of Microspheres

There are many different materials used to make microspheres, but the most abundantly studied are single polymer microspheres using poly (lactic-*co*-glycolic acid) (PLGA) [235, 236]. This is because the polymers and co-polymers lactic and glycolic acids have been shown to be biodegradable and biocompatible [235, 236]. PLGA degrades due to the hydrolysis of the ester linkages present between the co-polymers to leave lactic acid and glycolic acid which enter the citric acid cycle and are eliminated as carbon dioxide and water [237, 238, 239, 240].

There are several monomer ratios of PLGA commonly available. The chemical structure of PLGA is shown in Figure 4. Other materials used to create microspheres include: chitosan, alginate, PLLA and PLGA with different monomer ratios such as PLGA 50:50 and PLGA 75:25.

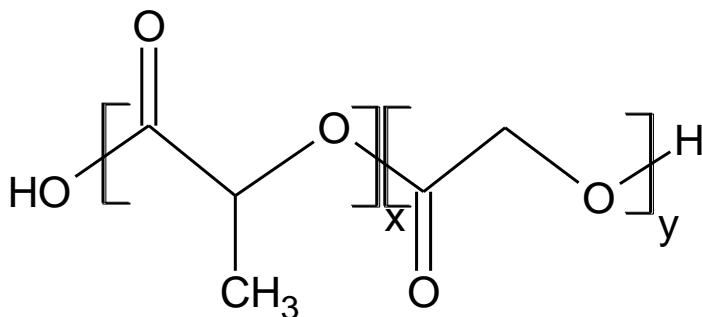


Figure 4. Chemical structure of PLGA where  $x$  refers to the number of units of lactic acid and  $y$  refers to the number of units of glycolic acid [239, 241].

The release profiles of various microspheres have been well documented and used as a method for controlled drug delivery as they have been shown to be able to provide a prolonged release of their contents [235, 239, 242, 243]. They allow for the local release of a high concentration of drugs which circumvents the problems associated with systemic administration [235, 244]. In addition, those release properties can be easily modified by varying the synthesis of the microspheres or their environment during release [245, 246, 247, 56]. Therefore, microspheres have been very successfully used for a variety of drug delivery purposes in TE, specifically for drug delivery to the kidneys, liver, spinal cord, brain and cardiovascular system [44, 45, 46, 47, 48, 49, 50, 51, 52, 53].

### 2.5.1.1 Single-walled microspheres (SWMS)

SWMS are a sphere of polymer encapsulating a protein or drug to be delivered. However, SWMS have some inherent shortcomings to their ability to deliver drugs including a high initial burst and a low encapsulation efficiency. A high initial burst can be harmful, especially if toxic threshold levels are reached [56, 248]. In addition, a low encapsulation efficiency is wasteful and not cost efficient [249, 56].

While there are several different methods for SWMS fabrication, the solvent evaporation method was used here. It is called a solid-in-oil-in water emulsion technique [250, 251, 252]. To create SWMS, the drug is added to a polymer, in our case PLGA 50:50, in solution with an organic solvent. This solution is then emulsified with water containing poly (vinyl alcohol) (PVA) as a surfactant and stirred until the organic solvent has evaporated. The use of a surfactant is to coat the droplets, forming a protective layer, and stabilize the formation of the microspheres to prevent coagulation [253]. Using PVA as a surfactant instead of Tween-20, Span-20 or SDS was shown to result in smaller particles and a smoother surface [254]. Specifically, a 1 % PVA solution was shown to result in more uniform microspheres [255]. As the concentration of polymer increases due to the evaporation of the solvent, the polymer droplets solidify forming microspheres [235].

The release of materials from SWMS is due to a combination of diffusion through the microsphere and degradation of the microsphere [256]. There are three phases to SWMS release. First, there is an initial burst release. Initial burst refers to the amount of drug released within the first 24 hours [56, 248]. Generally, a high encapsulation efficiency is correlated with a high initial burst, which is problematic because a high encapsulation efficiency is

desirable but a high initial burst is not [54, 56, 55]. The encapsulation efficiency is the amount of drug retained by the microsphere compared to the amount loaded. The initial burst is the amount of drug release within the first 24 hours compared to the total amount released. It is postulated that when the encapsulation efficiency is increased in SWMS, the extra drug is in fact located near the surface which causes the high initial burst [54, 56, 55]. Second, there is a slow release phase due to diffusion of the drug through the pores in the microsphere walls [56]. Third, there is a more rapid release phase starting around 20 days when microspheres degradation starts and the pores in the polymer walls increase in size [56, 55, 257]. SWMS have been shown to release for around 80 days, although this varies based on the selected material [239].

#### 2.5.1.2 Double-walled microspheres (DWMS)

DWMS have the potential to be an excellent alternative to SWMS with the ability to provide an improved sustained release for up to several months of release, without the problems associated with SWMS [235, 258, 259, 260, 261]. DWMS have two distinct polymer layers called the core and the shell. The purpose of the double-wall is to ensure that the drug is contained within the core of the DWMS, which provides a larger distance for drug diffusion, alleviating the initial burst [235]. The initial burst has been shown to be decreased to from above 30 % for the SWMS to below 20 % for DWMS [262, 263]. Another group was able to further decrease the initial burst to 4 % using the DWMS [56]. By increasing the diffusion distance and containing the drug located on the surface of the SWMS in the core of the DWMS, the shell acts as a rate-limiting barrier for the drug release [56]. It has also been shown that

DWMS have a higher encapsulation efficiency, above 70 % rather than SWMS of 40 % [56, 260, 262, 264].

In this thesis, PLGA 50:50 was chosen as the core material and poly ( $\text{L}$ -lactic acid) (PLLA) was chosen as the shell material. These materials have previously been shown to be immiscible making them a potential pairing for the double-wall creation [56]. PLLA is a biodegradable polymer with a slower degradation rate than PLGA because it has a higher hydrophilic content. Therefore, it was chosen as a shell to contain the drug for a longer period. DWMS have been successfully used to encapsulate many different molecules including: bovine serum albumin (BSA) [258], doxorubicin [259], piroxicam [265] and gentamicin sulphate [260].

The DWMS were created using the same premise of solvent evaporation as the SWMS. To fabricate the DWMS, the BSA is encapsulated in the PLGA core, then coated with the PLLA shell. This fabrication process is more complicated than the SWMS, and it is called a solid-in-oil-in-oil-in-water emulsion technique [261, 260]. The BSA was dispersed in PLGA 50:50 in solution with an organic solvent, this is the solid-in-oil portion. In this step the drug is dispersed throughout the polymer that will become the core of the double-walled microspheres. Then, that BSA and PLGA polymer mixture was emulsified with a PLLA solution in organic solvent, this is the oil-in-oil portion. The emulsion was then injected into a non-solvent bath of PVA in water, this is the oil-in-water portion. This solution was stirred for a long time allowing for the organic solvent evaporation and therefore an increase in the polymer concentration in the solution. As the polymer concentration increases, there was phase separation between the two immiscible polymers [265, 259, 56, 235, 266]. Based on the spreading coefficient theory, the two polymers are most likely to configure themselves in the

most thermodynamically stable configuration if given enough time (this is dependant on the rate of solvent evaporation) [265, 56]. Spreading coefficient theory is the tendency of a liquid to spread spontaneously across another liquid when they are suspended as emulsified droplets in a solvent and its based on their surface tensions [265]. Therefore, the core and the shell structure of the double-walled microspheres was formed. The spreading coefficient is represented by Equation 1:

$$\lambda_{AB} = \gamma_{BS} - \gamma_{AS} - \gamma_A \quad (1)$$

Where  $\gamma_{AS}$  and  $\gamma_{BS}$  are the interfacial tensions between the solvent and polymer A and B respectfully, and  $\gamma_{AB}$  is the interfacial tension between the two polymers. If the spreading coefficient is positive, polymer A will spontaneously spread on polymer B [265]. The fabrication process took optimization as there are several different possible configurations based on spreading coefficient theory as shown in Figure 5.

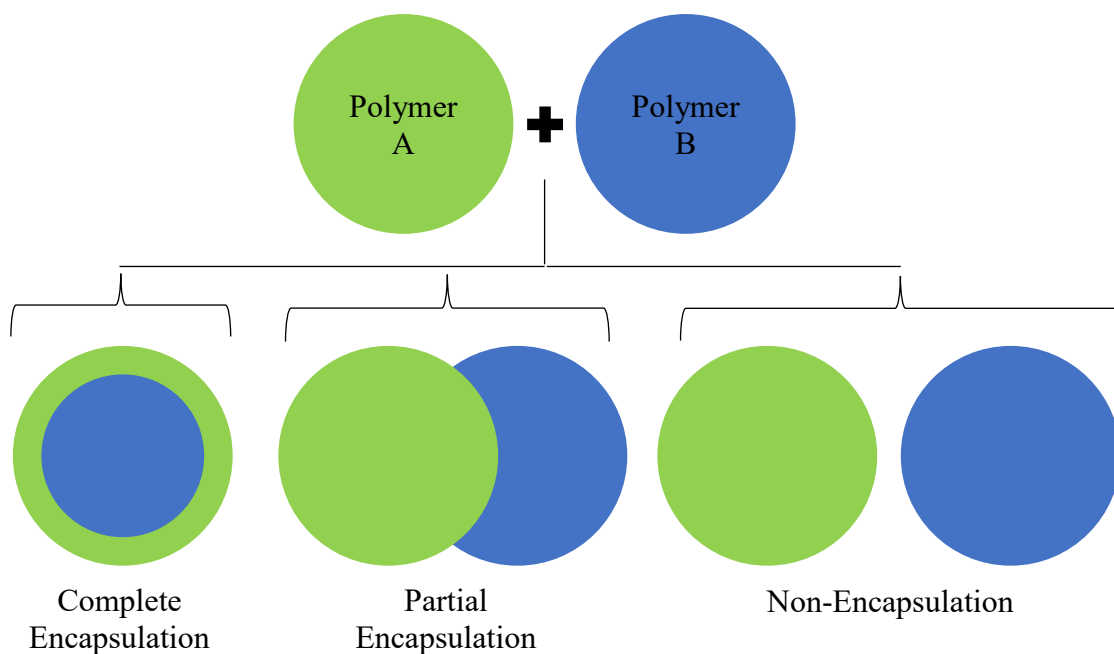


Figure 5. Possible configurations based on spreading coefficient theory; from left to right: complete encapsulation, partial encapsulation and non-encapsulation [265].

DWMS can contain the drug that tends to accumulate on the surface of SWMS and therefore alleviate the issue of initial burst by containing that drug within the core and coating the core with the shell. This not only decreases the amount of drug on the surface of the microsphere, but also increases the distance it must travel to diffuse out of the microsphere. The DWMS have three phases of release. First, there is a lag phase as the shell polymer contains all the drug. Second, there is slow release due to diffusion. Third, there is a more rapid release due to polymer degradation [56, 260].

### 2.5.2 Incorporation into Hydrogels

The incorporation of microspheres into hydrogels has been shown to provide a more controlled drug release than either hydrogels or microspheres alone [202, 267]. The ideal drug release is incremental also called a zero-order release, where the same amount of drug is released each

day over a specific and pre-determined amount of time. Microspheres by themselves are known to have a large initial burst of over 30 %, but they are able to hold a lot of drug and provide a prolonged release of around 80 days or SWMS and up to several months for DWMS [54, 55, 56, 239]. Hydrogel can not hold very much drug as they tend to only release for between 7 to 10 days depending on the hydrogel, but they are an excellent scaffold material [268, 269, 270, 271, 272, 273, 274, 275, 276]. Therefore, the combination of microspheres inside hydrogels will theoretically combine the best of both TE therapies in a duraplasty and achieve an ideal, controlled drug release profile for a prolonged period [202]. Table 3 summarises some of the studies that have incorporated microspheres into hydrogels to improve the resulting drug delivery system.

Table 3. Summary of several microsphere and hydrogel composites.

Hydrogel material	Microsphere material	Encapsulated material	Purpose	Altered TE performance	Reference
Alginate hydrogel	PLGA	Alginate lyase	NPCs were successfully cultured and expanded in this controllably-degradable hydrogel which has a wide variety of potential applications in TE.	The alginate lyase was successfully released from the PLGA microspheres over time allowing for the gradual degradation of the alginate hydrogel. The degrading alginate hydrogel showed an increase in the expansion of the cultured NPCs compared to those cultured in the control, non-degrading alginate hydrogel	[17]
Poly(N-isopropyl acrylamide)-based thermo-responsive hydrogel	PLGA	Anti-VEGFs (ranibizumab or aflibercept)	This material successfully reduced the choroidal neovascularization lesion areas with no adverse effects on retinal cellular function	This composite hydrogel resulted in a greater treatment efficacy for choroidal neovascularization using substantially less drug for posterior segment eye diseases	[57]
Alginate hydrogel	PLGA	Angiogenic factors, such as basic fibroblast growth factor (bFGF)	The scaffold was vascularized with four times more penetrating capillaries due to the controlled release of bFGF due to the increased proliferation of the cardiac fibroblasts, this material therefore has a wide variety of potential uses in TE	The addition of the PLGA microsphere to this hydrogel provided a nearly linear release profile of bFGF, which maintained its bio-activity and the release profile was controlled primarily by the microspheres	[58]

Carboxy methyl chitosan/ Oxidized chondroitin sulfate	Chitosan	Bovine serum albumin (BSA) and bovine articular chondrocytes	This microsphere-containing, injectable hydrogel had strong mechanical properties, good bioactivity, and an appropriate degradation rate showing its great potential as an injectable drug and cell delivery system	The composite hydrogels showed a low protein release rate with a reduced initial burst for 2 weeks which led to higher viability	[18]
Poly(vinyl alcohol)	PLGA	Transforming growth factor- $\beta$ 1	This material promoted chondrocyte adhesion and proliferation in a controlled manner	The composite was able to promote cell adhesion in a statistically significant way in comparison to the blank hydrogels	[59]
Collagen / cellulose	Gelatin	Gentamicin sulfate	This material was used for skin trauma dressing, it was biocompatible with a prolonged release of antibiotic, and it was shown to provide significant inhibition against both gram-positive and gram-negative bacteria	The composite material greatly reduced the initial burst and provided a more controlled and prolonged release	[60]
Oligo(poly(ethylene glycol) fumarate)	Gelatin	Rabbit mesenchymal cells and transforming growth factor- $\beta$ 1	This material held the cells at a specific site and provided a sustained release of bioactive molecules to encourage proliferation, differentiation and matrix production	The composite was able to promote glycosaminoglycan production beyond what the blank hydrogel could attain	[277]
HAMC	PLGA	Cyclosporin A (CsA)	This material allowed for the tunable release of CsA which helps the NPCs survive after transplantation	Incorporating the microspheres into this system more than tripled the length of the release profiles from several days to 3 to 4 weeks	[19]

HAMC	PLGA and PLGA with poly (sebacic acid) coating	Pegylated EGF (EGF-PEG) and erythropoietin	This material held the particles in place and reduced the inflammatory response and provided sequential delivery which lead to tissue repair	The two different types of microspheres integrated into the hydrogel led to the successful creation of a dual-phase release	[62]
PEG-diamine	PLGA	Transforming growth factor- $\beta$ 1	The lung cell growth inhibition was constant throughout the study period	The composite was able to eliminate the initial burst and provide zero-order release	[45]
Silk fibroin	Alginate	Nerve growth factor (NGF)	NGF was loaded and released from the composite scaffold and it enhanced the sparing of spinal cord tissue and increased the number of surviving neurons	The rats treated with the composite hydrogel showed improved motor function when compared to the control group after 8 weeks	[63]
PVA, chitosan and gelatin	PCL	bFGF	The composite was created to be able to delivery bFGF, used to promote fibroblast proliferation and migration, without the loss of bioactivity that occurs when it is directly administered	The composite demonstrated a zero-order release without affecting the viscoelastic properties of the hydrogel and managed to accelerate wound regeneration to 50% closure in only 4 days	[278]
HAMC	PLGA	CsA	The composite was designed to provide local delivery of CsA to stimulate endogenous stem cells while providing tissue protection in the CNS	The composite was shown to provide sustained release for 14 days, and there was a marked improvement when compared to systemic delivery	[21]

## 2.6 Purpose

### 2.6.1 Motivation

The motivation behind this project was to address the serious current lack of effective stroke treatments. The plan to accomplish that was to combine several areas currently undergoing research as treatment options for stroke, including synthetic duraplasty development, drug-delivery systems and endogenous stem cell therapies. Since duraplasty are frequently used as part of the treatment plan for strokes, the plan was to develop a duraplasty that was simultaneously a drug-delivery system. The drugs to be delivered, specifically growth factors, would induce endogenous stem cell therapy to promote neural regeneration.

In this work, we hypothesized that the blended biosynthesized cellulose (BBC) duraplasty membranes with incorporated, drug-loaded microspheres would provide a sustained drug release profile suitable for stimulating endogenous regeneration for stroke treatment.

### 2.6.2 Objectives

The following were the objectives for this thesis.

Aim 1: Fabricate the blended biosynthesized cellulose (BBC) membranes, the SWMS and the DWMS.

Aim 2: Characterize the SWMS and DWMS including size distribution, physical characterization using scanning electron microscope (SEM) images and encapsulation efficiency. The physical characterization for the DWMS will also include layer analysis.

Aim 3: Fabricate the SWMS composite membranes and the DWMS composite membranes.

Aim 4: Characterize the composite membranes including the microsphere retention, physical characterization using SEM images and thickness, swelling ratio and mechanical testing.

Aim 5: Evaluate the drug release profiles of the SWMS, DWMS, SWMS composite membranes and DWMS composite membranes.

The purpose of this study was to fabricate and characterize a composite membrane with the potential to be a drug-releasing duraplasty. The characterization of the composite membranes was done to ensure that the addition of the microspheres did not damaged the properties of the duraplasty that was previously developed and to compare to a commercially available duraplasty, Duraform®. Both SWMS and DWMS will be incorporated in the duraplasty to create SWMS composite membranes and DWMS composite membranes to improve the drug delivery profile. For the material development, BSA was used as a test drug. The novel aspect of this thesis lies in the improvement of the length of the potential therapeutic effect of the new drug-delivering composite membranes which are an innovative option for stroke treatment.

### 3. Materials and Methodology

#### 3.1 Materials

##### 3.1.1 Microspheres

PLLA (inherent viscosity: 0.90-1.20 dL/g) and PLGA 50:50 (inherent viscosity: 0.76-0.94 dL/g) were purchased from Durect Corporation (Cupertino, CA). BSA (66.3 kDA) was purchased from MP Biomaterials, Inc (Solon, OH). PVA (mw: 44.053 g\* $\text{mol}^{-1}$ ) was purchased from Sigma-Aldrich (Burlington, MA). Analytical grade chloroform (mw: 119.38 g\* $\text{mol}^{-1}$ ) was purchased from OmniSolv® (Etobicoke, ON).

##### 3.1.2 Membranes

*Gluconacetobacter hansenii* was obtained from American Type Culture Collection (ATCC®, Manassasm VA). DWK Life Sciences Kimble™ KIMAX™ Buchner Kimflow™ fritted disc filters with coarse porosity (60 mL borosilicate glass) were obtained from Fisher Scientific Company L.L.C. (Ottawa, ON) for the filtering process. Phosphate buffer saline (PBS) used for *in vitro* release study was obtained from VWR (Mississauga, ON) containing 137 mM NaCl, 2.7 mM KCl and 10 mM phosphate buffer. 0.02 % (w/v) analytical grade sodium azide ( $\text{NaN}_3$ , mw: 65.01 g\* $\text{mol}^{-1}$ ) was added to the PBS, obtained from BDH Chemicals (Mississauga, ON).

All other materials and solvents used were of analytical grade. All materials and solvents were used without modification unless otherwise indicated.

## 3.2 Methodology

### 3.2.1 Microsphere Protocol

#### 3.2.1.1 Preparation of Single-Walled Microspheres (SWMS)

The SWMS were created using a double emulsion evaporation technique called solid-in-oil-in-water, following the protocol developed by Cao and Shoichet [279]. In brief, 0.2 g of BSA were added to 4 mL of 25 % (w/v) solution of PLGA 50:50 in chloroform. Subsequently, 20 mL of 1 % PVA solution were added to the dispersion and it was emulsified for 90 seconds at 7500 rpm using a homogenizer (Power Gen 500 from Fisher Scientific, Loughborough, Leicestershire). The emulsion was then added to 300 mL of 0.1 % PVA and mixed for 3 hours at room temperature using a mixer at 300 rpm. The resulting microspheres were extensively washed and then lyophilized for 2 days. This process is shown in Figure 6. For blank SWMS, the same methodology described above was used with no addition of BSA.

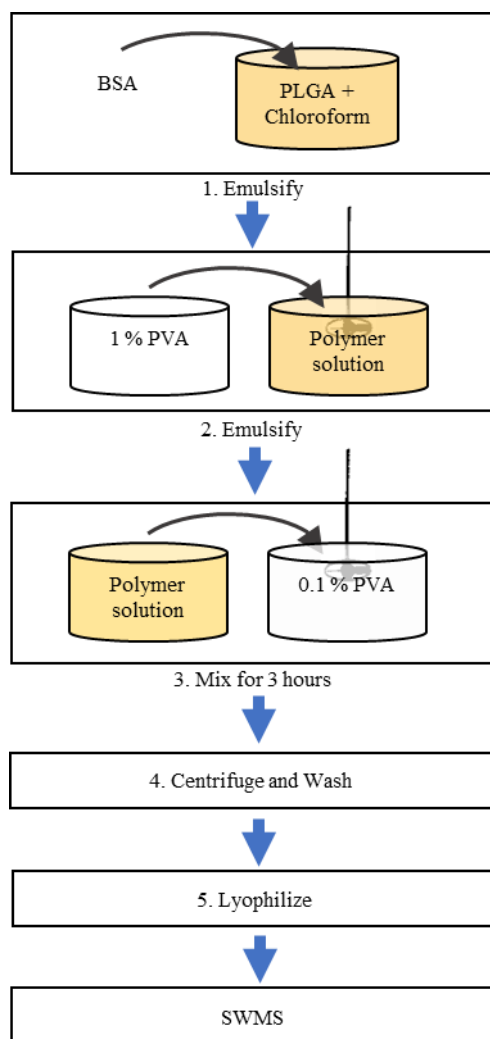


Figure 6. Schematic of SWMS fabrication.

### 3.2.1.2 Preparation of Double-Walled Microspheres (DWMS)

The DWMS were created using a solid-in-oil-in-oil-in-water solvent evaporation methodology, following the protocol developed by Tan, Lin and Wang [280]. In brief, 0.02 g of BSA were added to 1 mL of 20 % (w/v) solution of PLGA 50:50 in dichloromethane (DCM) and emulsified for 30 seconds at 7500 rpm using a homogenizer (Power Gen 500 from Fisher Scientific, Loughborough, Leicestershire). Subsequently, 1 mL of 20 % or 40 % (w/v) solution of PLLA in DCM was added to the PLGA/BSA solution and emulsified for a further 120

seconds. When 20 % was used, the polymer ratio in the resulting microspheres was 1:1, and when 40 % was used, the polymer ratio in the resulting microspheres was 2:1, with twice as much PLLA as PLGA 50:50. The emulsion was then injected slowly into 200 mL of 0.5 % PVA using a 3 mL syringe and mixed for 4 hours at room temperature using a mixer at 500 rpm. The resulting microspheres were extensively washed and then lyophilized for 2 days. This process is shown in Figure 7. For blank DWMS, the same methodology described above was used with no addition of BSA.

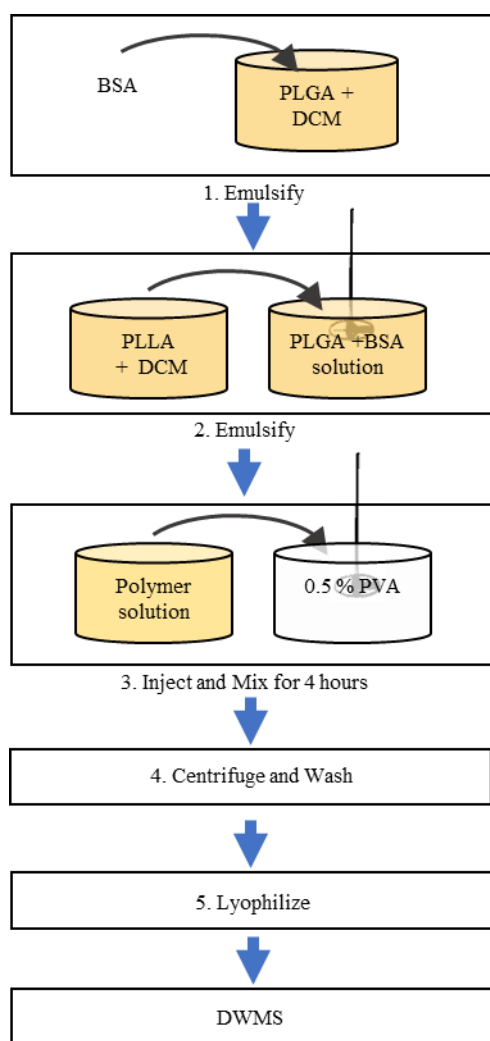


Figure 7. Schematic of DWMS formation.

### 3.2.2 Encapsulation Efficiency

The encapsulation efficiency (EE) of the microspheres was calculated to determine the amount of drug per gram of microspheres. Specifically, 0.1 g of microspheres created from a single batch were added to 1.5 mL of 0.5 M NaOH and incubated for 48 hours at 37 °C. The resulting reactants were then centrifuged, and the supernatant was collected to determine the BSA content. The EE was calculated using Equation 2. The encapsulation efficiencies of both

SWMS and DWMS were evaluated. Experiments were conducted in triplicate for three different batches of each SWMS and DWMS.

$$EE (\%) = \frac{\text{actual BSA content}}{\text{theoretical BSA content}} * 100 \% \quad (2)$$

### 3.2.3 Microsphere Size Analysis

To characterize the size distribution of the SMWS and DWMS, a scanning electron microscope (SEM, Phenom Pro, Phoenix, AZ) was used. The size analysis was performed to compare the BSA-loaded and blank microspheres to ensure their similarity and to be able to predict based on the literature the estimated length of release. Using 40 SEM images of five batches of microspheres, the size of all the imaged microspheres were determined. ImageJ was used to determine the diameter of the microspheres [281].

### 3.2.4 DWMS Polymer Layer Characterization

To characterize the layers of the DWMS, the microspheres were cryo-sectioned and then loaded directly onto SEM mounts. The cross-sectioned DWMS were imaged, then rinsed with 10 mL of ethyl acetate. Once dry, the cross-sectioned DWMS were imaged again.

### 3.2.5 Composite Blended Biosynthesized Cellulose (BBC) Membrane Production Protocol

The BC membranes were produced by *Gluconacetobacter hansenii*, with an inoculum concentration of  $1.3 * 10^5$  CFU\*mL<sup>-1</sup>, in a culture medium containing 20 g/L glucose, 5 g/L peptone, 5 g/L yeast extract, 2.7 g/L Na<sub>2</sub>HPO<sub>4</sub> and 1.5 g/L citric acid for 7 days at 26 °C. The BC membranes were purified by immersing them in 0.1 M NaOH at 50 °C for 24 hours and then rinsing them with distilled water until a neutral pH was reached. The purified BC membranes were subsequently mixed with water in a blender to create a BBC pulp as shown

in Figure 8. Both high and low BBC pulp concentrations were used to create the BBC membranes. For the high pulp concentration, a pulp concentration of 0.00318 g cellulose / mL water was used, while for the low pulp concentration, a pulp concentration of 0.00158 g cellulose / mL water was used.

70 mL of BBC pulp and varying amounts of dried microspheres (0.1 g, 0.05 g, 0.025 g or 0 g) were added to two 50 mL centrifuge tubes and well mixed using a vortex. The pulp mixture was then vacuum filtered to remove most of the water content. Both centrifuge tubes were rinsed to ensure minimal loss of product in the transfer. The filtration continued until the water stopped dripping which took approximately 1 hour per membrane. The BBC membrane was then delicately removed from the filter and then lyophilized for 1 day. This process is shown in Figure 8.

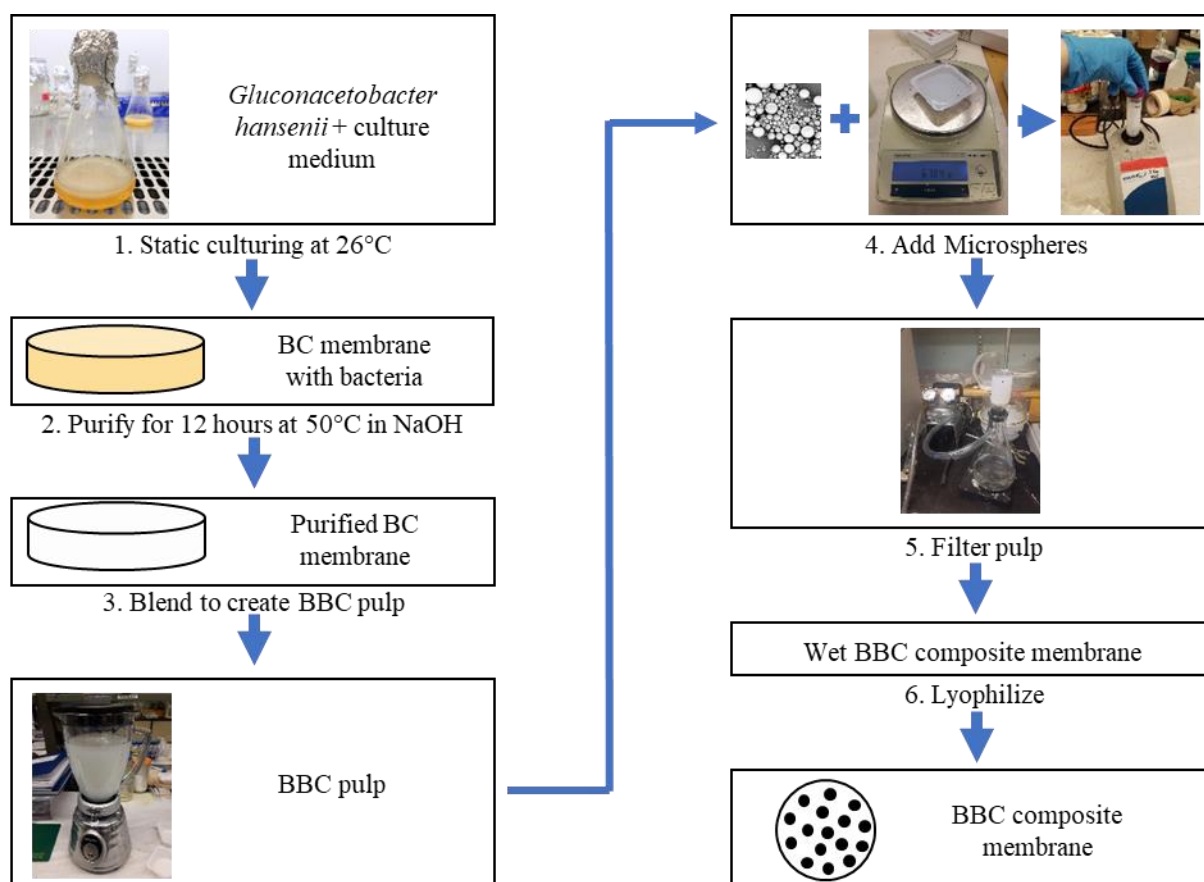


Figure 8. Schematic of BBC composite membrane fabrication.

### 3.2.6 Microsphere Retention

The microsphere retention (MR) into the composite membranes was calculated by using the difference in mass between the control and composite membranes. The only change in the fabrication protocol between the control and composite membranes was the addition of the microspheres and therefore the additional mass in the composite membrane was as a result of the microspheres. Large batches of pulp were made to ensure uniformity in the amount of BC between all membranes. Equation 3 was then used to calculate microsphere retention.

$$MR (\%) = \frac{(\text{composite membrane mass} - \text{control membrane mass})}{\text{mass of microspheres added}} * 100 \% \quad (3)$$

### 3.2.7 Swelling Ratio Protocol

Each membrane was submerged in 15 mL of distilled water. At predetermined times points, the membranes were retrieved from the water and weighed. Equation 4 was used to calculate the swelling ratio of the membranes.

$$SR (\%) = \frac{(W_{swo} - W_{dry})}{W_{dry}} * 100 \% \quad (4)$$

Where SR was the swelling ratio,  $W_{swo}$  was the weight of the swollen membrane at each time point and  $W_{dry}$  was the initial dry weight of the membrane.

### 3.2.8 Mechanical Test Protocol

Fully rehydrated samples were cut into 10 mm by 30 mm rectangles [282]. The thickness of each sample was measured immediately prior to each test to obtain the cross-sectional area of each sample. Filter paper was used between the grips of the mechanical tester and the sample, on both ends of the sample to prevent slippage. 7.5 mm of the sample were gripped by the clamps on both ends of the sample. An Instron 3000 tensile (Norwood, MA) testing machine was used with a cross-head speed of 5 mm/min to take all the samples to failure. Samples where fracture occurred at clamp edge were discarded. Load-extension curves were recorded using the Instron Bluehill 2 software (Norwood, MA) and used to measure Young's modulus, ultimate tensile strength and elongation-at-break.

### 3.2.9 Drug Release

The (0.1 g, 0.05 g, 0.025 g and 0 g) SWMS and DWMS composite membranes and the (0.1 g, 0.05 g, 0.025 g and 0 g) SWMS and DWMS alone were submerged into 15 mL and 2 mL of PBS with 0.02 % (w/v) NaN<sub>2</sub>, respectively. All the samples were sealed and placed in a 37 °C incubator. At predetermined time points, 0.32 mL of PBS were removed from each sample and the same amount of fresh PBS was added back into the sample. The microsphere samples were centrifuged prior to PBS removal and vortexed after fresh PBS addition. All the collected samples were tested for the presence of BSA using a micro bicinchoninic acid (BCA) kit following the vendor's protocol. Equation 5 was used to calculate the cumulative amount of BSA released.

$$R = (c_n * v_o) + \sum_{i=1}^{n-1}(c_i * v_i) \quad (5)$$

Where R was the cumulative amount of BSA released at each time point,  $c_n$  was the measured concentration from the BCA assay,  $v_o$  was the total volume of the sample at that time point,  $c_i$  were all the previously measured concentrations from the BCA assay, and  $v_i$  were the aliquot volumes which were removed from the sample at each time point.

The initial burst release (BR) was calculated at the 24 hours time point using Equation 6.

$$BR = \frac{\text{Cumulative amount released after 24 hours}}{\text{Total cumulative amount released}} * 100 \% \quad (6)$$

### 3.2.10 Statistical Analysis

The results are presented as mean  $\pm$  standard deviation. All the data were treated statistically using a one-way and two-way analysis of variance (ANOVA). A statistically significant

difference was considered at  $p < 0.05$ . Statistical analysis was performed using GraphPad Prism 6 Data (Graphpad Software, La Jolla, CA).

## 4. Results and Discussion

### 4.1 Preparation and Characterization of Microspheres

The first aim of this thesis was to produce the microspheres to improve the drug-delivery properties of the duraplasty developed by our lab. The SWMS were successfully produced and characterized before incorporation into the composite membranes. It was important to determine the size of the microspheres because it had been shown previously that the size directly affected the drug release profile [283, 284, 285]. The surface area to volume ratio was shown to impact the speed of the microsphere degradation; the higher the ratio the faster the degradation [283, 284, 285]. The degradation rate has been directly correlated to the diffusion rate of the drug out of the pores in the microspheres and therefore the microsphere release profile [283, 284, 285].

For the SWMS, there was no statistically significant difference between the size of the BSA-loaded and blank microspheres ( $p > 0.05$ ) as shown in Figure 9A. Therefore, the blank microspheres were used for characterization purposes and the BSA-loaded microspheres were used for the release studies. The BSA-loaded and blank SWMS had a narrow size distribution (Figure 9A), with most of the microspheres falling between 10 and 15  $\mu\text{m}$ . The SEM images shown in Figure 9B and 9C are representative images showing blank and BSA-loaded SWMS with an average size of  $16 \pm 5 \mu\text{m}$  and  $16 \pm 4 \mu\text{m}$  in diameter, respectively. The average SWMS size obtained here was similar to many other papers [286, 287, 288, 289]. For example, Cao and Shoichet showed a SWMS composed of PLGA 50:50 with a diameter of around 16  $\mu\text{m}$  [279] and Determan *et al.* prepared a SWMS composed of poly sebacic anhydride and

poly(1,6-bis-p-carboxyphenoxy)hexane using a similar water/oil/water methodology and obtained microspheres with an average diameter of 20  $\mu\text{m}$  [286]. In the future, it would be useful to sieve the microspheres to obtain a more monodisperse sample since size is of such vital importance for predicting drug release. The blank and BSA-loaded SWMS were both spherical with a smooth surface (Figure 9B and C).

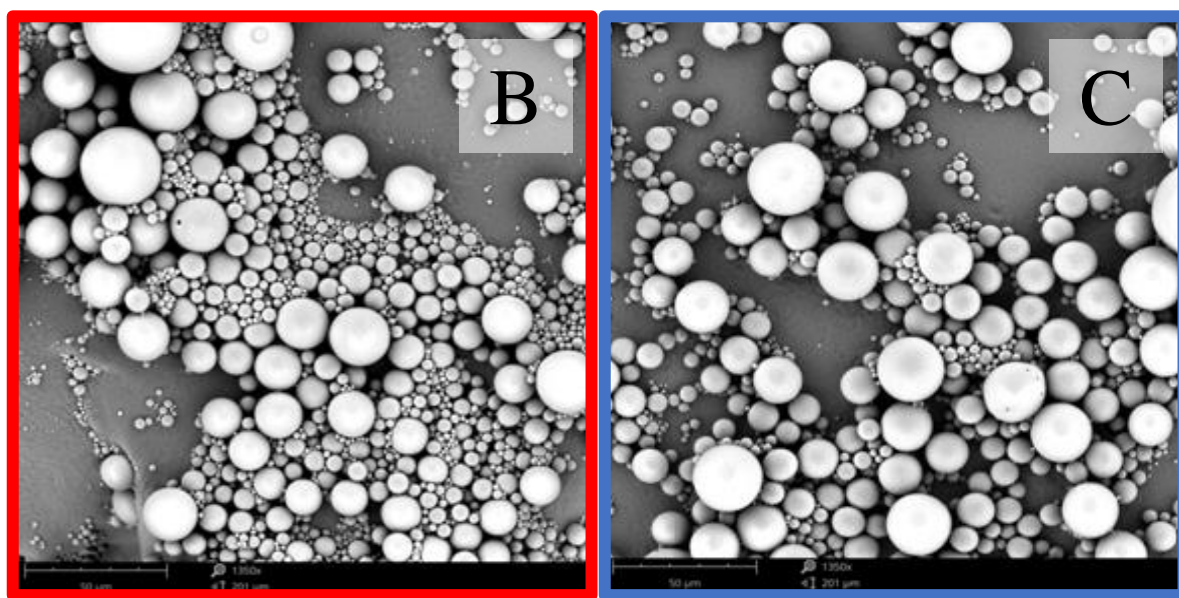
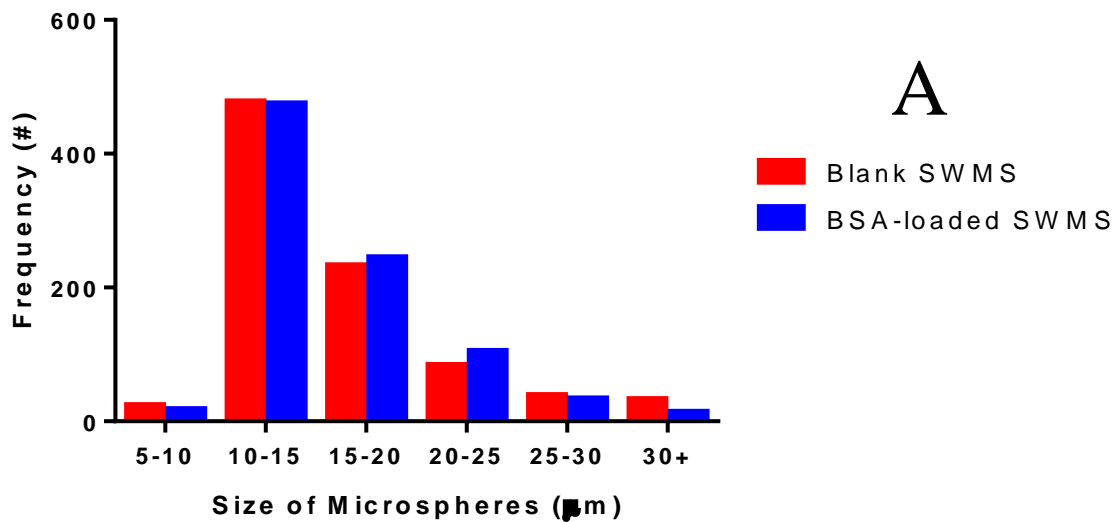
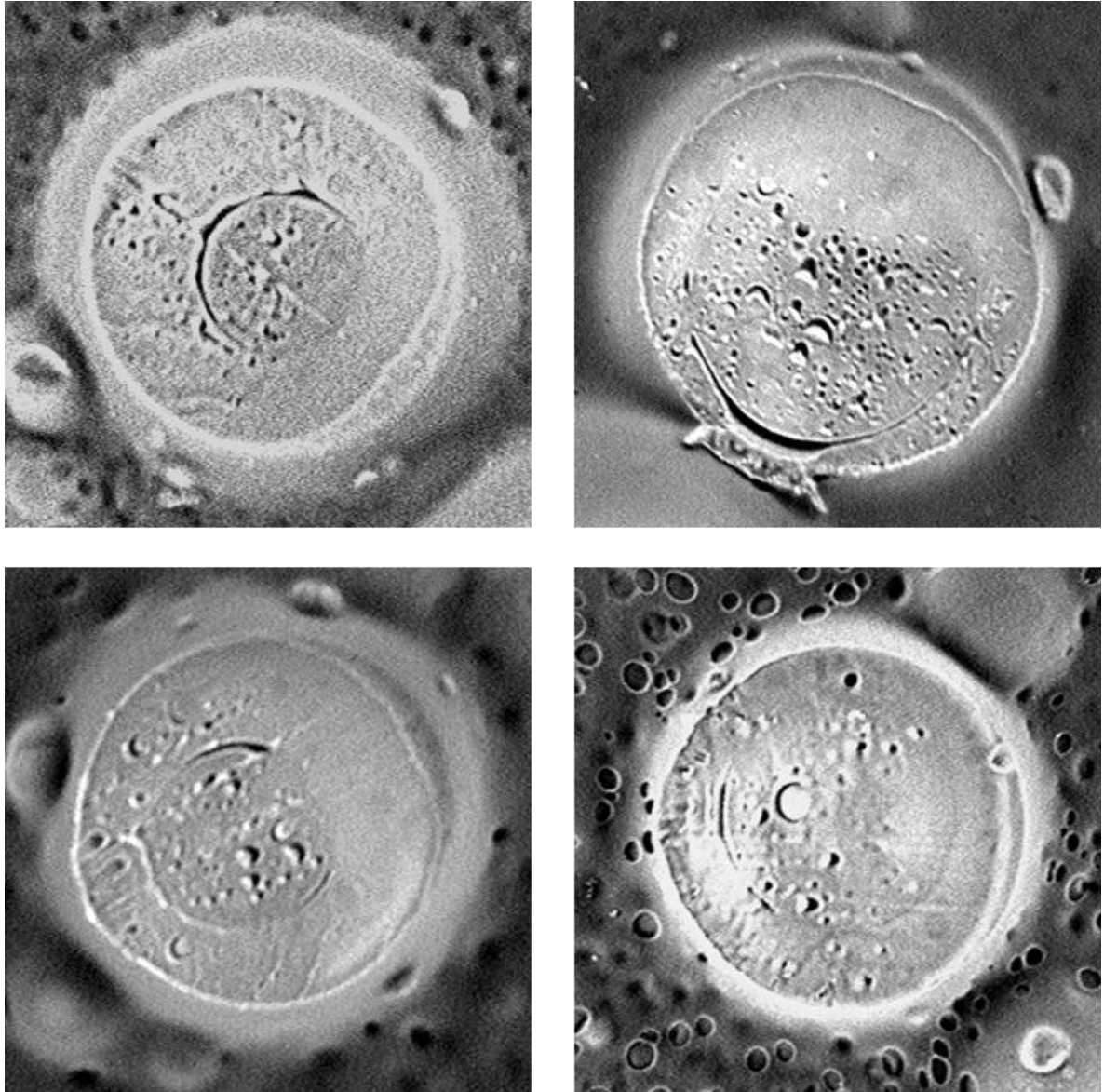


Figure 9. Morphological characterization of the SWMS. A. Histogram of the size distribution of the blank and BSA-loaded SWMS; B. A representative SEM image of blank SWMS; C. A representative SEM image of BSA-loaded SWMS.

The DWMS were produced and characterized before incorporation into the composite membranes. The DWMS were intended to further improve the potential drug-delivery properties from the SWMS. The DWMS had been previously shown to have a significantly

reduced initial burst and a higher encapsulation efficiency than the SWMS [56, 260, 262, 264, 263]. The DWMS have only been produced successfully by a few research groups using the double-emulsion technique as it is a difficult chemical procedure to optimize [56, 290]. The double-wall was successfully fabricated, and the two distinct polymer layers are visible in the cross-sectioned DWMS shown in the representative SEM images shown in Figure 10.



*Figure 10. Representative SEM images of cross-sectioned DWMS showing the two distinct polymer layers.*

Characterizing the size of the DWMS was important for the same reasons as for the SWMS. For the DWMS, there was a statistically significant difference in diameter between the blank and BSA-loaded microspheres ( $p < 0.05$ ) as shown in Figure 11A. Therefore, the BSA-loaded DWMS were used for all the subsequent characterization. The SEM images shown in Figure

11B and 11C are representative images showing blank and BSA-loaded DWMS with an average size of  $560 \pm 90 \mu\text{m}$  and  $760 \pm 100 \mu\text{m}$  in diameter, respectively. The average BSA-loaded DWMS size obtained was similar to other papers [56, 260, 261]. For example, Lee *et al.* prepared DWMS using the same ratio of polymers and obtained an average size of  $432.3 \pm 179.2 \mu\text{m}$  [261] and Zheng prepared PLGA 80:20 and PLGA 75:25 2:1 DWMS which resulted in an average size of  $775.0 \pm 156.6 \mu\text{m}$  [56].

The size of blank microspheres was not reported in the literature on DWMS. Therefore, it is unknown if they observed the same increase in size of the BSA-loaded DWMS when compared to the blank DWMS. The 30 additional seconds during the fabrication of the BSA-loaded DWMS when the BSA was homogenized with the PLLA could have caused additional DCM evaporation when compared to the blank DWMS. This could have increased the viscosity of the mixture which could have reduced the stirring efficiency. This has previously been shown to create larger emulsified droplets and therefore result in larger microspheres [291].

The narrow size distribution achieved for both the BSA-loaded and blank DWMS (Figure 11A) was excellent when compared to Tan and Ye who prepared PLLA and PLGA 50:50 DWMS with a large size distribution from 50 to 700  $\mu\text{m}$  and an average diameter of 276.25  $\mu\text{m}$  [260]. However, a smaller size of microspheres would likely be better for our application as the release would be more evenly distributed across the surface of the membrane. The microspheres are added to the composite membranes based on mass. 0.1 g of microspheres with a large diameter would result in fewer microspheres than 0.1 g of microspheres with a

small diameter. A larger number of microspheres spread throughout the composite membrane would allow for a more uniform release across the entire membrane surface. It has been shown that a higher mixing speed will result in smaller microspheres, therefore further testing should be done to optimise the effects of this variable [292]. Once again, sieving the microspheres to create a more monodisperse sample may be of use to be able to better predict the drug release.

As shown in Figure 11B and C the blank and BSA-loaded DWMS were spherical. They also both show dimples on their surface where small droplets of the core polymer were trapped in the shell. This phenomenon was previously seen by several other researchers who fabricated DWMS.

When comparing the sizes of the SWMS and the DWMS, the DWMS are significantly larger ( $p < 0.05$ ). However, neither average size that we have synthesized here is optimal for our drug release application. The smaller SWMS have a very larger surface area to volume ratio, which is likely to increase their initial burst when compared to SWMS of a larger size. The DWMS are so large that in the quantities that we added them to the membranes, they are not able to coat the whole membrane, so there is not an even release across the entire surface of the membrane. An optimal size has not been established; however, it likely falls somewhere between the sizes of the synthesized SWMS and DWMS.

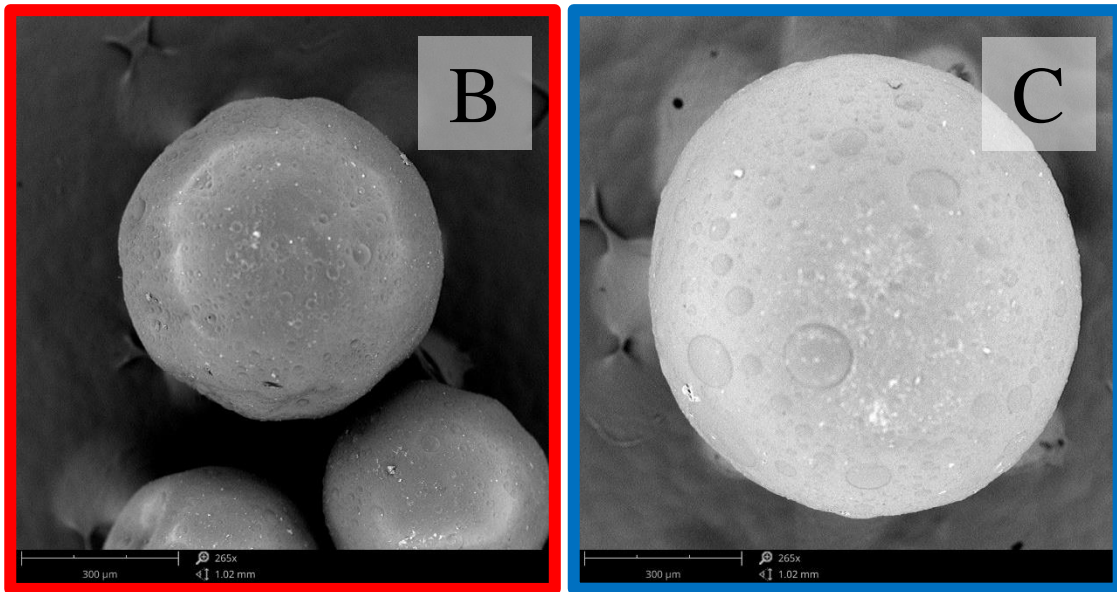
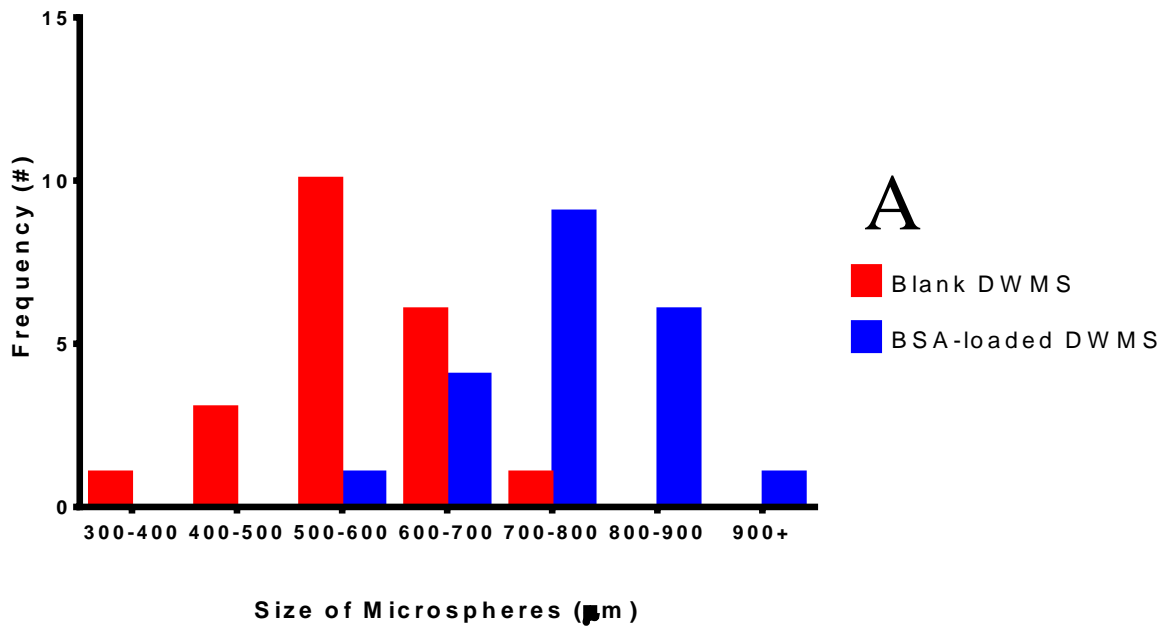
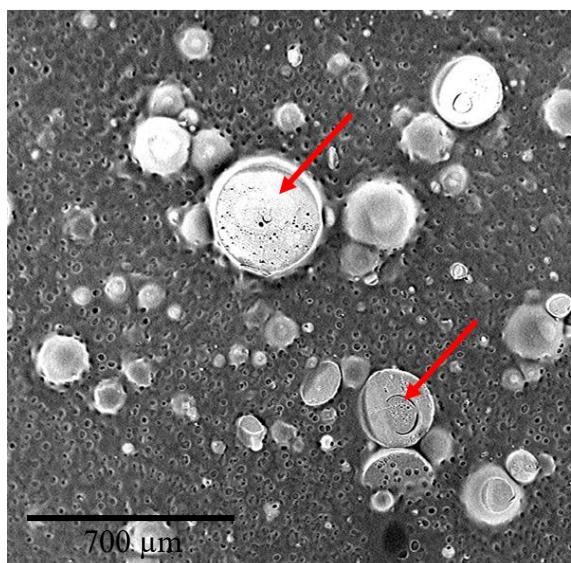


Figure 11. Morphological characterization of the DWMS. A. Histogram of the size distribution of the blank and BSA-loaded DWMS; B. A representative SEM image of blank DWMS; C. A representative SEM image of BSA-loaded DWMS.

Layer analysis was done on the cross-sectioned DWMS to determine which layer was composed of which polymer. It was determined that PLGA 50:50 was the core material and PLLA was the shell material. After washing with ethyl acetate (EA), which only dissolves

PLGA 50:50, the core was gone while the shell remained intact as shown in the before and after images in Figure 12. This was the expected result based on the literature [293, 294, 235]. This was also the desired result because PLGA 50:50 has a faster degradation rate than PLLA under physiological conditions, because it is more hydrophilic [235]. Therefore, the shell will remain intact longer than the core. This will provide a reduced initial burst by containing the drug for longer by increasing the distance over which it needs to diffuse.

DWMS before washing with EA



DWMS after washing with EA

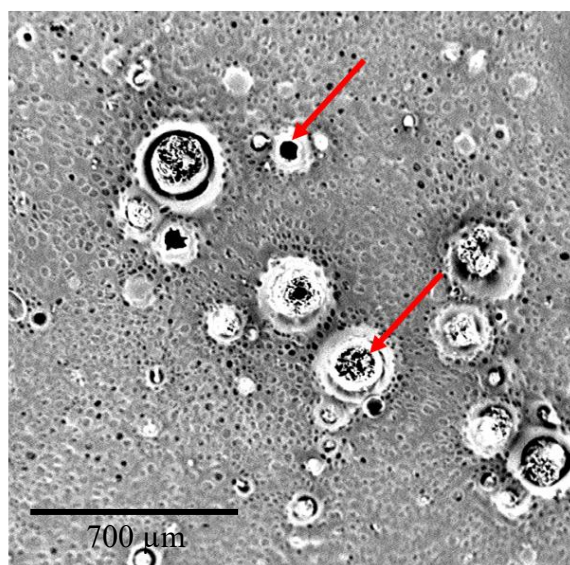
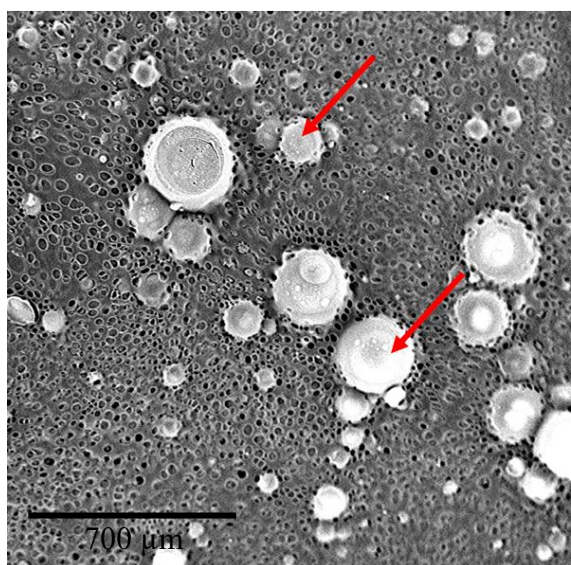
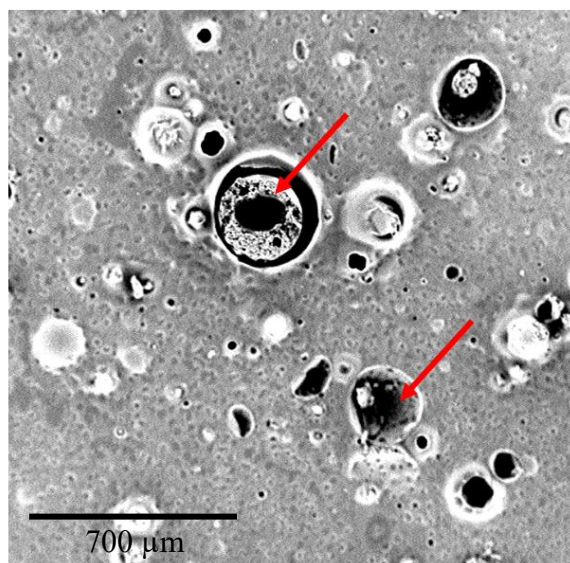


Figure 12. Representative cross-sectioned SEM images of DWMS before and after washing with ethyl acetate (EA) where the arrows indicate the core of the DWMS.

## 4.2 Preparation and Characterization of Composite Membranes

The next aim of this thesis was the incorporation of the synthesized SWMS and DWMS into the BBC membranes to fabricate SWMS composite membranes and DWMS composite membranes, respectively.

To start, the blank blended BC (BBC) membranes were successfully re-created. The purpose of creating the BBC membrane was to eliminate the porosity difference seen in the native BC between the top and bottom sides of the membranes as they are formed, thereby allowing more consistency in the swelling ratio, mechanical characteristics and release profile [295, 296]. Figure 13 shows representative SEM photos of the top and bottom sides of the BBC membranes. They are very similar, therefore, the blending protocol appears to have effectively created a more uniform composite membrane when compared to the native BC, as was previously shown by our lab [43]. The blending protocol also allowed for the addition of the microspheres to the BBC membranes, which cannot be incorporated into the native BC membrane.

High and low cellulose content control membranes were fabricated and compared to the commercially available Duraform®. As demonstrated in the SEM images in Figure 13, there were no visible differences in the porosity between to high and low cellulose content control membranes. However, the porosity of Duraform® was not uniform, the bottom was more porous than the top (Figure 13). Duraform® was designed that way. It was not designed as a drug delivery system but was optimised as a duraplasty. The varied porosity between the sides allowed it to better perform its sole function of retaining the CSF [128]. Therefore, the high

and low cellulose content control membranes are better suited as a drug-delivery duraplasty than the commercially available Duraform®.

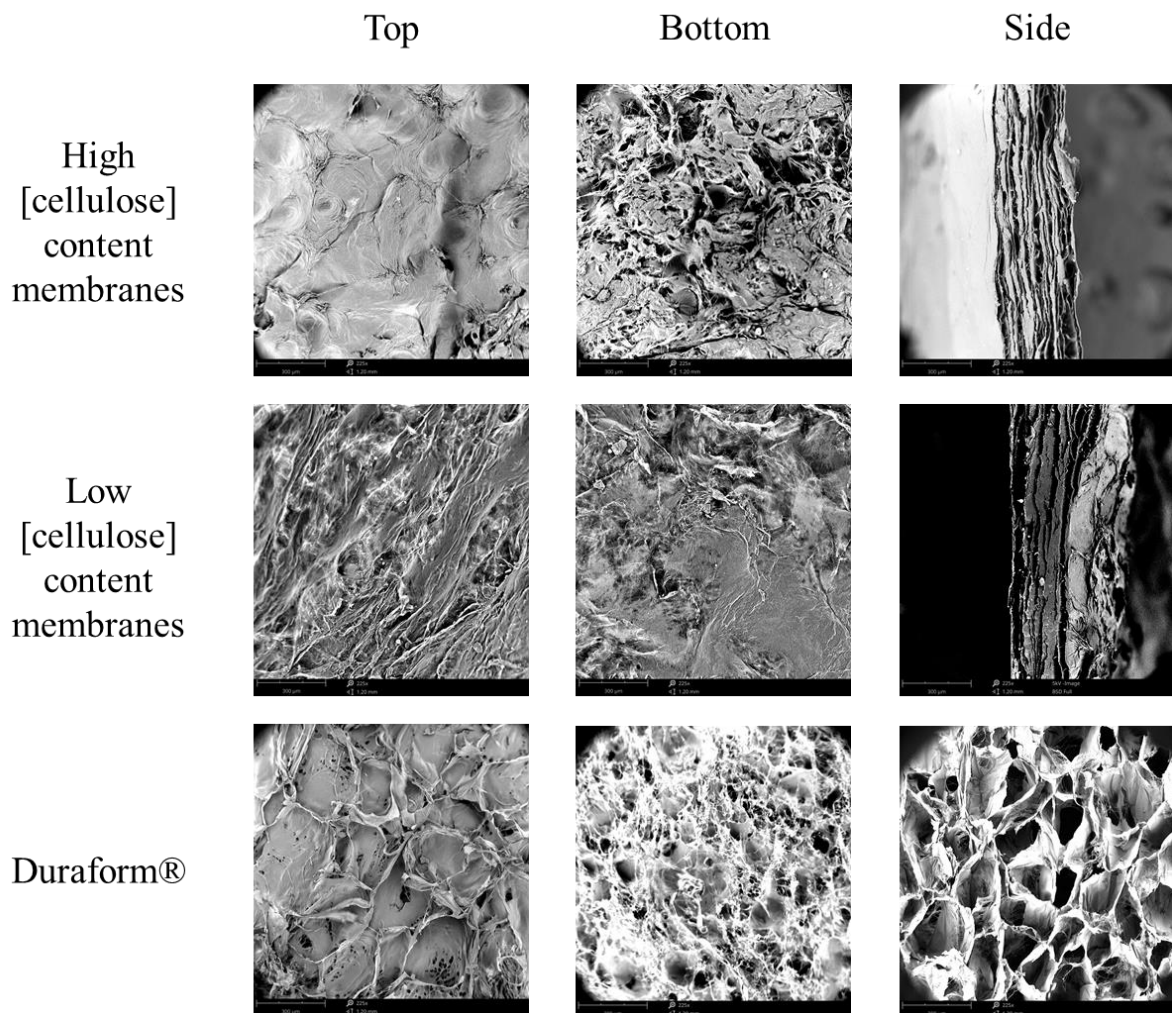
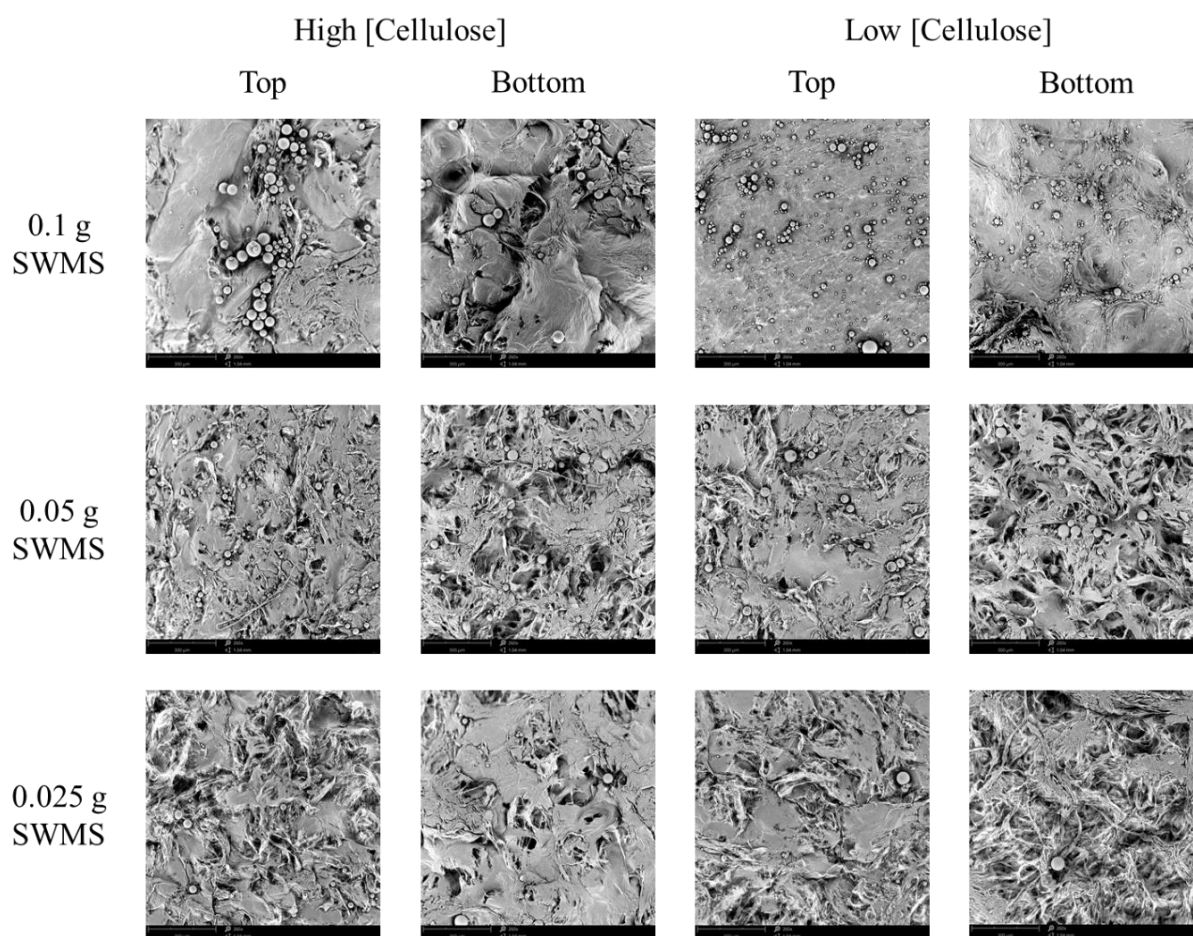


Figure 13. Representative SEM images of high and low cellulose content control membranes and the commercially available Duraform®. All the above SEM images are at 225 x magnification.

The physical characterization of the composite membranes was done as a visual verification that the microsphere incorporation was successful. The SWMS were successfully incorporated into the BBC membranes to produce the SWMS composite membranes. SEM images were

taken of the SWMS composite membranes made with varying amounts of SWMS, as shown in Figure 14. When comparing the 0.025 g SWMS composite membranes to the 0.05 g SWMS composite membranes in Figure 14, more microspheres are clearly visible on the surface of the membranes. The same holds true when comparing the 0.05 g SWMS composite membranes to the 0.1 g SWMS composite membranes (Figure 14). The representative top and bottom SEM images of the composite membranes show a similar number of visible microspheres (Figure 14). The mixing of the microspheres with the BBC pulp before the filtration process allowed the microspheres to be distributed throughout the membranes. This is clear since the microspheres are visible on both surfaces of the membrane. There was no visible difference visible between the high and the low cellulose content composite membranes (Figure 14).



*Figure 14. Representative SEM images of top and bottom of the SWMS composite membranes with varying amount of SWMS (0.1 g, 0.05 g and 0.025 g) and high and low cellulose concentrations. All the above SEM images are at 260 x magnification.*

The DWMS were successfully incorporated into the membranes to produce the DWMS composite membranes. The DWMS composite membranes were only created using the higher cellulose content. The porosity of the composite membranes played a large role in their properties. Therefore, this variable should be quantified to increase our understanding of this material.

The swelling ratio (SR) of the composite membranes was tested because the SR has been shown to have a large impact on the release behaviour of hydrogels [297, 298, 299]. The more a hydrogel swells and allows liquid into the matrix, the faster a drug can diffuse out [300]. The SR of a hydrogel depends primarily on its porosity and the hydrogen bonds it can form with water molecules [29, 301]. As shown in Figure 15, the control and the composite membranes quickly absorbed water and swelled before levelling off and reaching equilibrium at 24 hours. Both the high and low cellulose content membranes had a significantly lower SR than the commercially available Duraform® ( $p < 0.05$ , Figure 15A). The increased cellulose content significantly decreased the SR ( $p < 0.05$ , Figure 15A). This is due to the increased number of hydrogen bonds formed by the extra cellulose molecules within the membrane. In addition, the increased cellulose content decreased the porosity of the membrane resulting in membranes which were denser and thus they had a lower influx of water. The SR results for the control membranes suggest that the higher cellulose content membranes would allow drugs to diffuse out of them more slowly since they have a lower SR. This could help decrease the initial burst of the drug which would be beneficial for the application. Therefore, only the high cellulose content composite membrane SR results are shown in Figure 15B and C.

Figure 15B and C show the SR of the SWMS composite membranes and DWMS composite membranes over time. As more microspheres were added to the composite membranes the SR significantly decreased for both the SWMS and DWMS composite membranes ( $p < 0.05$ , Figure 15B and C). This suggests that the addition of the microspheres decreased the porosity of the membranes and therefore they were able to retain less water. Fan *et al.* saw the same trend in composite injectable hydrogels which were able to retain less water as more

microspheres were added [18]. In Figure 15B, the 0.1 g SWMS composite membrane had the lowest SR of  $500 \pm 20$  %. In Figure 15C, the 0.1 g DWMS composite membrane had the lowest SR of  $480 \pm 30$  %. When comparing the DWMS composite membranes to the SWMS composite membranes, the 0.1 g DWMS composite membrane showed the lowest overall SR. Therefore, the 0.1 g DWMS composite membrane retained the least amount of water suggesting it would demonstrate the lowest initial burst making it the best composite membrane for the drug release application.

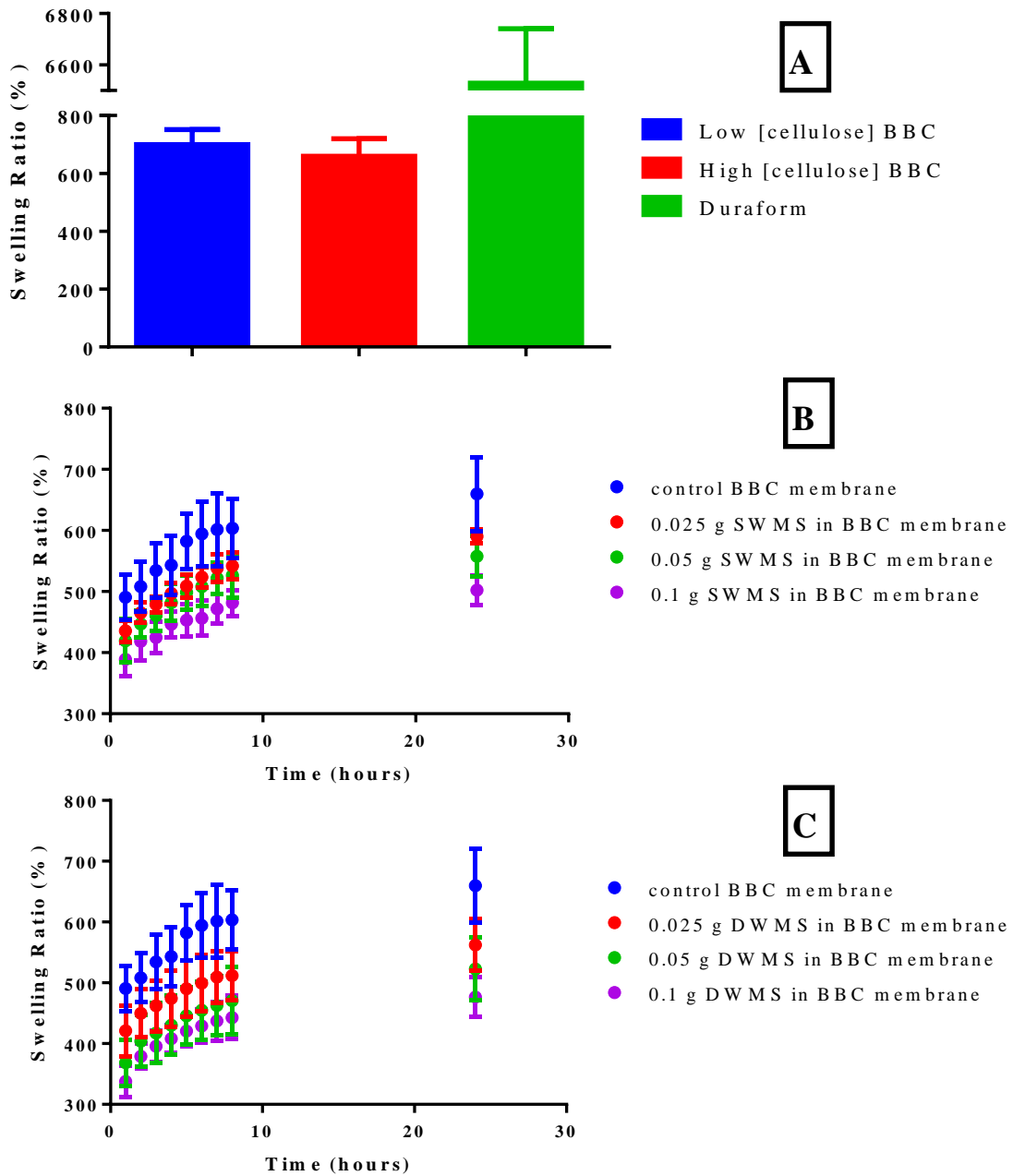


Figure 15. Swelling ratio of the composite membranes, control BBC membranes and Duraform® (N=8); A: SR at 24 hours of control BBC membranes and Duraform®; B: SR over time of high cellulose concentration membranes containing various amounts of SWMS; C: SR over time of high cellulose concentration membranes containing various amounts of DWMS.

The thickness of the membranes was tested when they were fully saturated to ensure that the composite membranes were a suitable thickness for use as a duraplasty. The duraplasty is placed into the brain post DC, therefore it is important that it cause no further harm to an already damaged area. The thickness must not cause increased pressure in the area. As shown in Table 4, the control and composite membranes are all significantly less thick than the commercially available Duraform® ( $p < 0.05$ ) when fully saturated. They are also within the range of human dura mater, 0.35 to 0.58 mm [161, 162]. Therefore, the thickness of the composite membranes should not cause any problems when the duraplasty is implanted regardless of the variations between the different samples.

Table 4. Average thickness of the control and composite membranes as well as the commercially available Duraform® when fully saturated with water (N=10).

	<b>Average membrane thickness when fully saturated (mm)</b>
<b>Duraform®</b>	4.02 ± 0.07
<b>BBC control membrane</b>	0.35 ± 0.07
<b>0.1 g SWMS composite membrane</b>	0.59 ± 0.09
<b>0.05 g SWMS composite membrane</b>	0.5 ± 0.1
<b>0.025 g SWMS composite membrane</b>	0.46 ± 0.05
<b>0.1 g DWMS composite membrane</b>	0.51 ± 0.07
<b>0.05 g DWMS composite membrane</b>	0.43 ± 0.05
<b>0.025 g DWMS composite membrane</b>	0.38 ± 0.04

The mechanical properties of the composite membranes were tested, specifically their strength and elasticity, to show that they can perform as a duraplasty and withstand the manipulation of the implantation procedure and conform to the desired brain shape. The samples were tested when fully hydrated, as they will be wet upon implantation. Materials generally lose strength when they are wet, because they swell which reduces their physical entanglement and hydrogen bonding thereby increasing their mobility [302]. For the strength and elasticity of the duraplasty, we were looking to approximate or improve from the properties of the commercially available duraplasty, Duraform®.

As shown in Figure 16A, all the control and composite membranes were significantly stronger than Duraform® ( $p < 0.05$ ), which presented an ultimate tensile strength (UTS) of  $0.020 \pm 0.003$  MPa. Therefore, all the composite membranes will easily be able to withstand the implementation procedure and they were easy to handle. The high cellulose content membranes were all significantly higher than the corresponding low cellulose content membranes ( $p < 0.05$ , Figure 16A). The high cellulose content control membrane presented an UTS of  $1.6 \pm 0.3$  MPa. The increased strength was due to the increased number of hydrogen bonds formed by the extra cellulose molecules within the high cellulose content membranes. The SWMS disrupted these hydrogen bonds and caused a significant decrease in the UTS regardless of cellulose content ( $p < 0.05$ , Figure 16A). As more microspheres were added to the composite membranes the UTS decreased, for both the SWMS and the DWMS ( $p < 0.05$ , Figure 16A). The strongest SWMS composite membrane was the 0.025 g SWMS composite membrane with an UTS of  $0.8 \pm 0.1$  MPa. The initial addition of the DWMS to the membranes showed the opposite effect as the SWMS, they in fact caused a significant increase in the strength of the material when compared to the control membrane ( $p < 0.05$ , Figure 16A). There was therefore clearly some sort of interaction between the PLLA shell of the DWMS and the cellulose which increased the strength of the DWMS composite membrane. However, as more microspheres were added, the strength decreased. This could also be due to the disrupted hydrogen bonds as with the SWMS. The strongest DWMS composite membranes was the 0.025 g DWMS composite membrane with an UTS of  $10 \pm 2$  MPa.

The Young's modulus and elongation-at-break both speak to the elasticity of the material. A small Young's modulus and high elongation-at-break demonstrate a high elasticity, which is

beneficial for the implementation procedure and the conformity of the duraplasty to the brain's surface. As shown in Figure 16B and C, Duraform® is significantly more elastic than all the control and composite membranes with a Young's modulus of  $0.06 \pm 0.01$  MPa and an elongation-at-break of  $44 \pm 3$  %. The low cellulose content membranes were significantly more elastic than the high cellulose content membranes ( $p < 0.05$ , Figure 16B and C). The low cellulose control membranes showed a Young's modulus of  $40 \pm 10$  MPa and an elongation-at-break of  $3.9 \pm 0.6$  %. It follows that the elasticity increased as the cellulose content decreased, since fewer cellulose fibrils decreased the number of hydrogen bonds in the membrane [27, 170]. The SWMS increased the elasticity of the composite membranes and the DWMS decreased the elasticity of the composite membranes ( $p < 0.05$ , Figure 16B and C). As more microspheres were added to the composite membranes the elasticity increased, for both the SWMS and the DWMS ( $p < 0.05$ , Figure 16B). The most elastic SWMS composite membrane was the low cellulose content 0.1 g SWMS composite membrane with a Young's modulus of  $5.5 \pm 0.9$  MPa and an elongation-at-break of  $3.6 \pm 0.6$  %. The most elastic DWMS composite membrane was the high cellulose content 0.1 g DWMS composite membrane with a Young's modulus of  $190 \pm 30$  MPa and an elongation-at-break of  $2.6 \pm 0.6$  %. While the composite membranes are less elastic than the Duraform®, they are still malleable enough to be able to conform to the shape of the brain. In addition, their ability to retain their structure may be beneficial to the implementation procedure. However, the difference in this variable for the composite membranes when compared to the commercially available Duraform® many present some unknown negative effects, and this should be further evaluated.

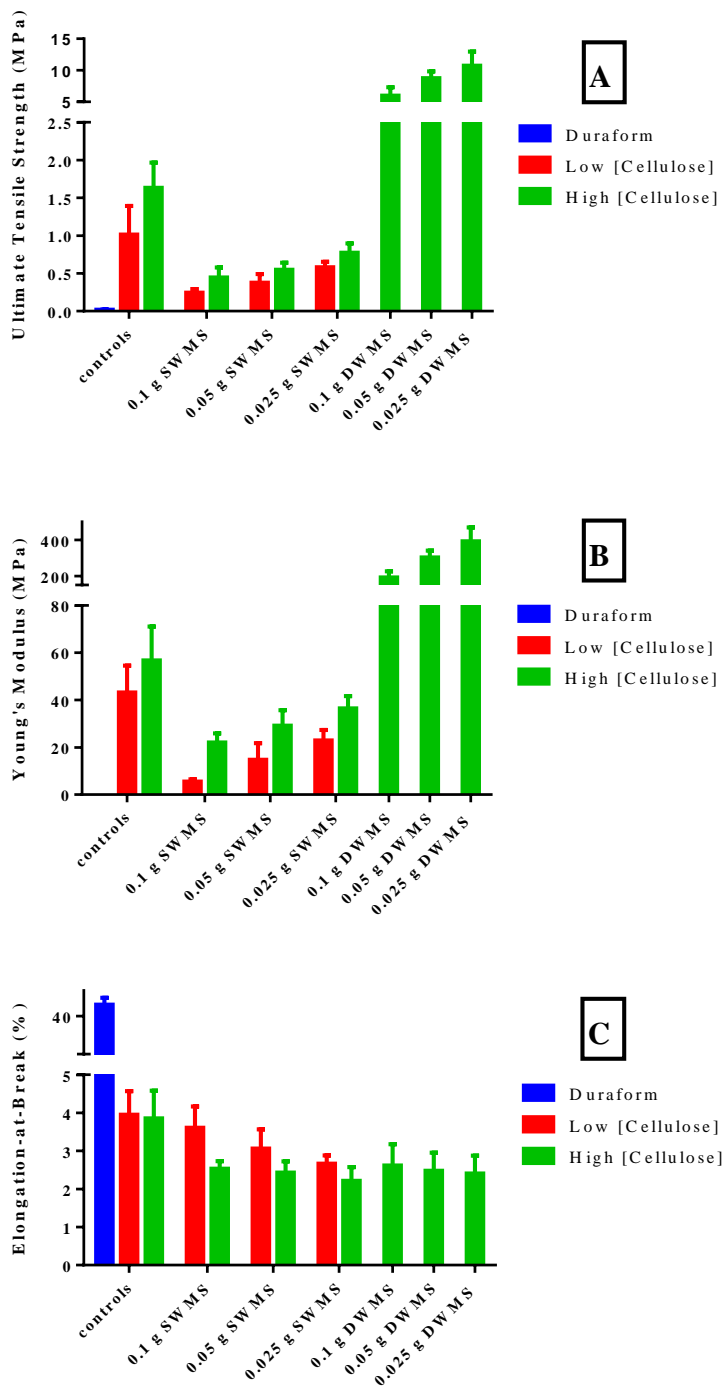


Figure 16. The mechanical testing of the composite and control membranes and the commercially available Duraform® (N=8); A: The average ultimate tensile strength; B: The average Young's modulus; C: The average elongation-at-break.

Taking all the physical characterisation, the SR and the mechanical testing results together, the most promising composite membrane for the application of a drug-releasing duraplasty for post-stroke treatment was the high cellulose content 0.05 g DWMS composite membrane. It displayed the second-best SR, was the optimal thickness, was the second strongest membrane and still maintained some elasticity.

#### 4.3 Drug Retention and Release

The final aim of this thesis was to determine the drug retention and release of the composite membranes to determine whether they have the potential to be used as a drug-releasing duraplasty for stroke treatment. Achieving a high encapsulation efficiency (EE) of the drug within the microspheres was important to optimise the method for industrial processing. In addition, waste reduction was important to reduce environmental impact and cost. The DWMS nearly doubled the EE from the SWMS while maintaining consistency within the batch as shown in Table 5. The reason the EE for the DWMS was significantly higher than that of the SWMS was due to the shell of the DWMS. As the organic solvent slowly evaporates from the emulsified polymer droplets to solidify the polymer and form a microsphere, the drug can diffuse out of the SWMS into the surrounding PVA [262]. However, for the DWMS, the emulsified droplet already contains two polymer layers and as the microsphere solidifies, the shell prevents the drug diffusion that occurs for the SWMS [262].

Unfortunately, the EE obtained here was lower than that described by other authors. Tan and Ye were able to attain an EE of 42.01 % for their SWMS and increased that to 70.57 % using a 2:1 ratio of PLLA and PLGA 50:50 [260]; that is an increase of nearly 30 %. Xu *et al.* attained an EE of  $80.0 \pm 2.6$  % using a 2:1 ratio of PLLA and PLGA 50:50 [293]. However, it

has been previously observed that when more drug was loaded it decreased the EE, so that is a variable to optimise in the future to increase the EE [303, 54, 304].

*Table 5. Average encapsulation efficiency percentage (EE %) of both SWMS and DWMS.*

	<b>EE (%)</b> <b>(Average ± SD of 3 batches)</b>	<b>EE (%)</b> <b>(Average ± SD of 3 samples from 1 batch)</b>
<b>SWMS</b>	16 ± 4	20.4 ± 0.1
<b>DWMS</b>	26 ± 6	24.9 ± 0.4

The microsphere retention into the membranes was tested to minimize drug loss. As shown in Figure 17, the retention of the microspheres into the membranes was nearly 100 % regardless of the mass or type of microspheres added ( $p > 0.05$ ). The lower cellulose concentration reduced the SWMS retention in a statistically significant way ( $p < 0.05$ ). This implies an interaction between the microspheres and the cellulose; however, it is not practically significant since the retention of all the samples is so close to 100%. However, taking together the retention, strength and SR, the higher cellulose content membranes were the only ones used moving forward with the release testing.

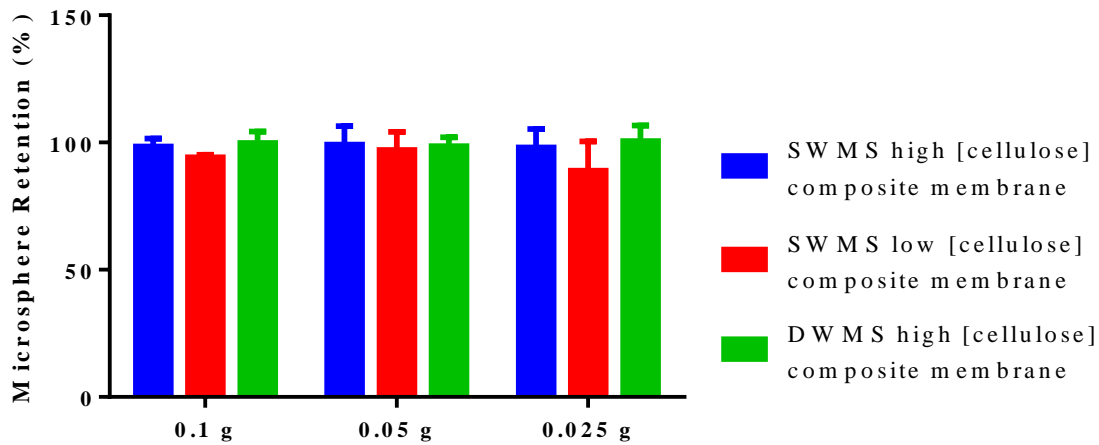


Figure 17. The retention percentage of the varying amounts of SWMS and DWMS into the high and low cellulose content composite membranes (N=8).

The drug release assessment was performed using BSA as a model drug. The BSA release was tested from varying amounts of the SWMS and DWMS alone as well as from varying amount of the microspheres in the SWMS composite membranes and DWMS composite membranes.

There is a shortcoming to the methodology used to test the drug release. Samples must be collected to detect the amount of BSA and to avoid the use of a large initial volume which would make small amounts of BSA difficult to detect, a small volume of PBS was used and replaced with fresh PBS after each sample was collected. This very likely affected the release kinetics as it reduced the concentration of BSA outside of the microspheres, which promoted more BSA to leave the microspheres than might have done if they were left alone [307]. However, biologically some of the drug would be absorbed by the brain as it performed its therapeutic function and therefore this methodology best reflects what will be happening *in vivo* [308].

Another potential shortcoming of the methodology for testing the release stems from the different PBS volumes for the microspheres and composite membranes due to the difference in size of the samples. Since the composite membranes were in a larger volume it could have been theorized that they would be drawn to release more since the release of the same amount of BSA would have resulted in a lower concentration in the PBS than for the microspheres. However, as shown by both types of microspheres, the microspheres alone released more than the composite membranes (Figures 18 and 19), so this did not impact the results in a significant way.

The SWMS on their own have a significant initial burst, but it was drastically reduced when they were incorporated into the SWMS composite membranes as shown in Figure 18. This could be due to the additional processing of the microspheres which were loaded into the composite membranes. To further understand the affect of this process the microspheres should undergo the same processes without the BBC for comparison purposes prior to testing their release. As of 72 days, 0.1 g of SWMS alone showed a cumulative release of  $110 \pm 15$   $\mu\text{g}$  of BSA. As of 72 days, the 0.1 g SWMS composite membrane showed a cumulative release of  $77 \pm 4$   $\mu\text{g}$  of BSA. For the microspheres alone, the amount released was reduced as half as many microspheres were used. Figure 188 shows that despite the same amount of microspheres and therefore drug being loaded, the microspheres alone release more than the composite membranes. A possible explanation for this is the degradation of BSA over time, which should be evaluated in the future to determine its exact effect.

There was an anomaly in the data which showed that the 0.025 g SWMS composite membranes appeared to be able to release more than the 0.025 g SWMS alone. This can be

attributed to the variation between the batches of SWMS and slight variations between the amount of microspheres used in the experiments.

The SWMS alone stopped releasing in a statistically significant way after 14 days, whereas the composite membranes continued to show release up to 40 days. The SWMS composite membranes were able to release for significantly longer than the microsphere-free BBC membranes, which released for less than 7 days as previously tested by our lab [43]. It would be interesting to see how the presence of the microspheres affected the release of drug that was loaded onto the top of composite membranes. This would be very relevant in the future for the creation of a dual-phase release where one drug would be released from the membrane first, followed by a second drug being released from the microspheres within the membrane. These composite membranes have the potential to be tuned to drastically improve stroke outcomes. The drug release from the duraplasty could be designed to promote maximal healing post-stroke. Since most of the healing after a stroke occurs within the first three months, several months of release, as shown by the SWMS composite membranes, would provide a significant amount of support to promote healing [305]. Therefore, this material is promising for the stroke treatment application.

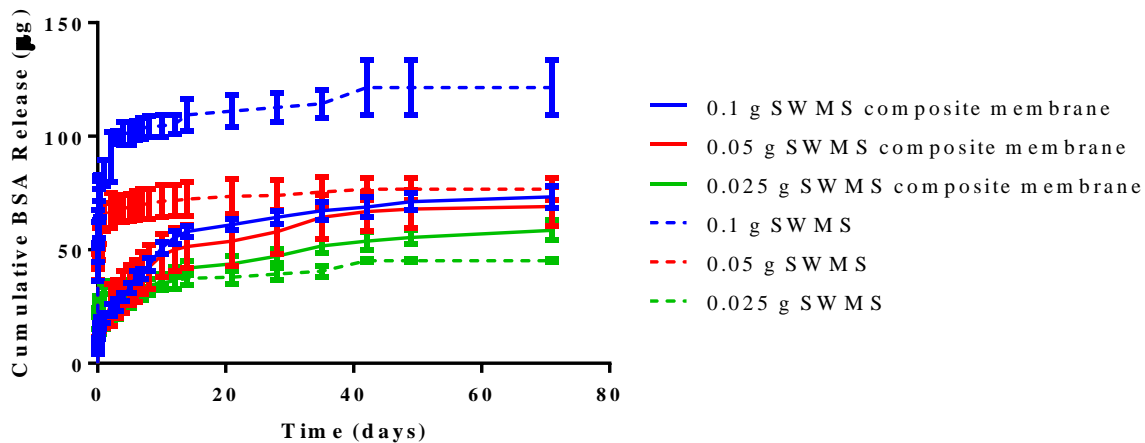


Figure 18. Cumulative BSA released from the various amounts of SWMS alone and incorporated into the SWMS composite membranes (N=6).

An initial experiment was done to obtain preliminary results for the DWMS release profile using a 1:1 ratio of the two polymers. The 1:1 DWMS demonstrated a high initial burst and did not display the release profile that was seen by many other papers that generated the DWMS, which demonstrated a delay followed by a prolonged near zero-order release [290, 261, 262, 293, 56]. It is likely that the double-wall was not successfully created in all the tested microspheres and that there was some incomplete and non-encapsulation. Based on those results, it was decided to increase the amount of polymer in the shell and create a 2:1 polymer ratio to decrease the initial burst.

As shown in Figure 19, the release profile of the 2:1 DWMS were tested. As of 72 days, 0.1 g of the DWMS alone showed a cumulative release of  $460 \pm 84 \mu\text{g}$  and the 0.1 g DWMS composite membranes showed a cumulative release of  $190 \pm 30 \mu\text{g}$ . For the DWMS less drug was released as half as many microspheres were used. The same trend is seen as with the

SWMS where less drug is released from the microspheres embedded within the membranes. Once again a thorough study to examine the degradation of BSA over time should be performed. Many papers achieved a similar or slightly longer release than this. For example, Devrim and Bozkir achieved release for over 63 days using 2:1 PLLA and PLGA 50:50 DWMS [303], Ansary *et al.* achieved release for over 90 days using slightly different DWMS (Glu-PLGA and PLGA) [290], Xu *et al.* achieved release for over 125 days using 2:1 PLLA and PLGA 50:50 DWMS [293] and Rahman and Mathiowitz achieved a release of 240 days using 2:1 PLLA and PLGA 50:50 DWMS [259]. Therefore, further tuning of the DWMS has the potential to further elongate the release profile if that is desirable.

While the 2:1 DWMS release profile still did not perfectly replicate other papers where there was a clear lag phase followed by near zero order release, the release profile was still a major improvement when compared to the SWMS and the initial results from the 1:1 DWMS. The increased shell size of the DWMS, from a 1:1 polymer ratio to a 2:1 polymer ratio, successfully improved the release profile. This improvement was likely due to a combination of improvements in the manufacturing techniques as well as the increased size of the shell. The improved fabrication likely resulted in a higher percentage of the microspheres with the double-wall.

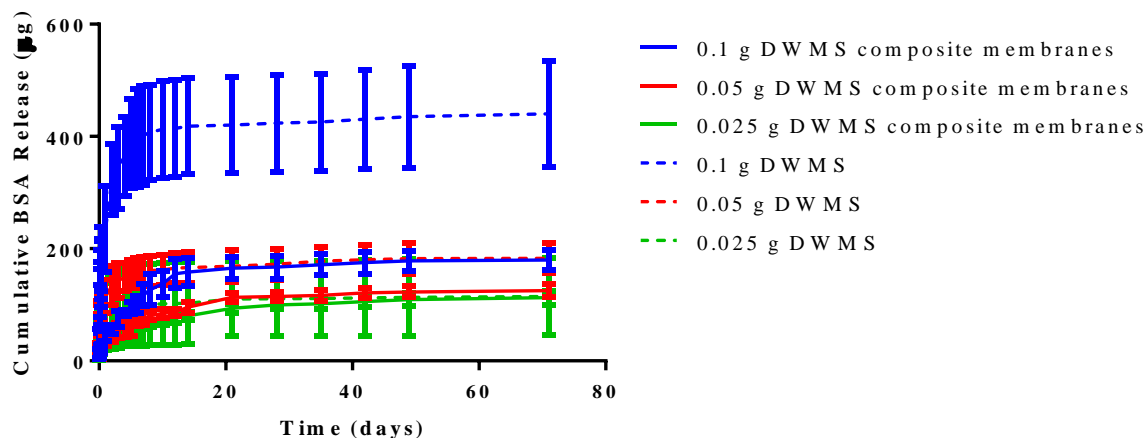


Figure 19. Cumulative released BSA amount from various amounts of DWMS and DWMS composite membranes (N=6).

The SWMS composite membrane and DWMS composite membrane release profiles are alternatively shown as percent cumulative release in the Appendix.

As shown in Table 6, the DWMS show a significantly reduced initial burst when compared to the SWMS ( $p < 0.05$ ). This was expected based on the literature. For example, Devrim and Bozkir achieved an initial burst of  $10.36 \pm 1.01$  using 2:1 PLLA and PLGA 50:50 DWMS [303] and Navaei *et al.* achieved an initial burst of  $17.43 \pm 1.39$  for their PLGA 75:25 and PLGA 50:50 DWMS [262]. Given the lower DWMS initial burst seen in literature, there is still optimisation to be done to further improve the DWMS.

Table 6. Initial burst release after 24 hours.

Sample	Initial burst release (%)
SWMS composite membrane	$28 \pm 3$
DWMS composite membrane	$19 \pm 3$

Having seen the SWMS and DWMS composite membrane release profiles, moving forward the best drug-releasing duraplasty was the high cellulose content 0.05 g DWMS composite membrane.

BBC is not a biodegradable material and therefore it remains intact in solution. However, the microspheres are biodegradable [235]. After the SWMS and initial testing of the SWMS composite membrane release studies had run for 42 days, the samples were lyophilized and imaged to be able to visualize their degradation. It is clear from Figure 20 that the microspheres degraded since the pores are clearly visible, while the cellulose membrane remained intact as was expected. Although this suggests biodegradation of the microspheres, a detailed degradation study would generate useful information regarding the degradation rate. This would increase our understanding of the release profiles for the composite membranes.

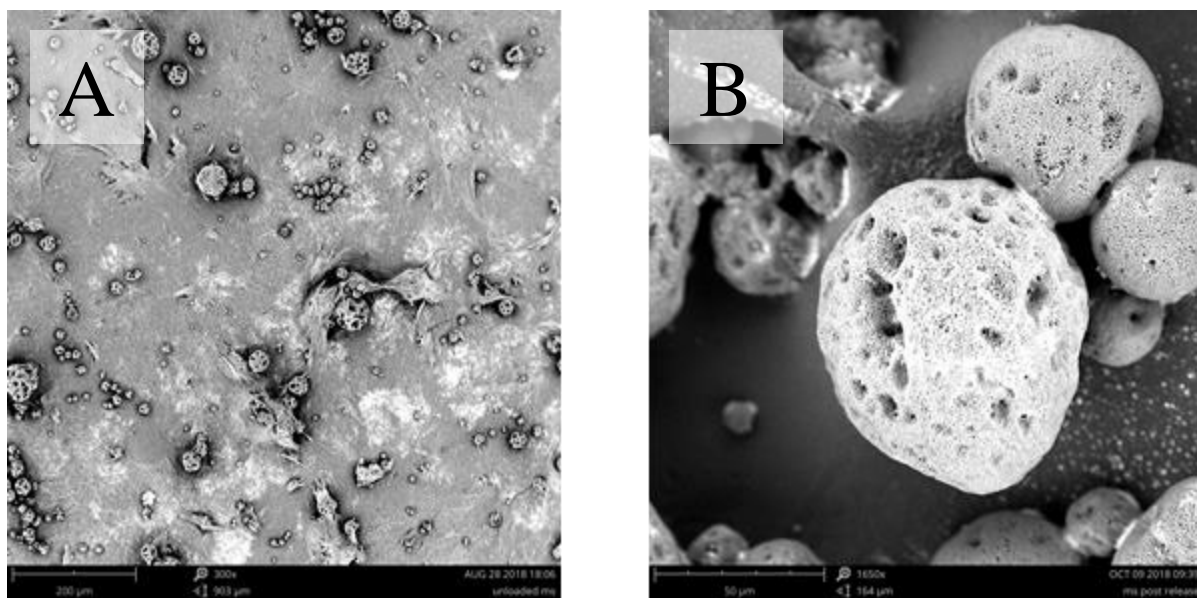


Figure 20. Representative SEM images after 42 days of release testing to demonstrate degradation; A: SWMS composite membrane; B: SWMS alone.

## 5. Conclusions

The purpose of this thesis was to take the BBC duraplasty developed by our lab and improve its drug releasing capabilities by incorporating microspheres. First, the SWMS and DWMS were successfully fabricated and their morphologies were characterized. Further to that, the composition of the DWMS was characterized to determine that the core was PLGA 50:50 and the shell was PLLA. Second, the BBC control membranes were successfully re-created. Third, the SWMS and DWMS were incorporated into the cellulose to create composite membranes. They were then characterized using SEM imaging and there are clearly more microspheres visible on the surface of the composite membrane as more microspheres were added. The swelling ratio was tested to determine which composite membrane retained the least amount of water and would therefore allow the lowest initial burst. The thickness was determined when the membranes were fully saturated to ensure that all the membranes were close in thickness to human dura mater. The mechanical testing was done to determine the strongest composite membrane while also ensuring that it retained some elasticity. This would allow the duraplasty to withstand the implantation procedure and conform to the shape of the brain. Overall, the results showed that the high cellulose content DWMS composite membranes were the best composite membranes. Furthermore, all the composite membranes showed improved results when compared to the commercially available Duraform®. Fourth, the drug incorporation in the composite membranes was tested through encapsulation efficiency of the drug within the microspheres and the microsphere retention within the composite membranes. The DWMS had a significantly higher EE than the SWMS and the microspheres were incorporated with nearly 100 % retention in the membranes. Fifth, the drug release profile of

the microspheres and the composite membranes were tested and compared. The DWMS were shown to be a marked improvement over the SWMS. Furthermore, the DWMS composite membrane showed a closer to zero-order release in comparison to the SWMS composite membrane. Taken together all the results show that the high cellulose content 0.05 g DWMS composite membranes were the best option for moving forwards. In conclusion, this thesis demonstrated the potential for using DWMS composite BBC membranes as a long-term drug-delivering duraplasty for stroke treatment.

The next step will be to incorporate growth factors into the composite membranes. However, there are several steps required before that can be achieved. First, the growth factors need to be incorporated into the microspheres and drug activity needs to be tested. To be suitable for any further *in vitro* and *in vivo* testing, the composite membranes need to be fabricated in a completely sterile environment using sterilized BBC pulp and the biocompatibility of the material needs to be tested. Then, the drug release profiles of the growth factors need to be evaluated using an enzyme-linked immunosorbent assay (ELISA).

## 6. References

- [1] W. H. Organization, "Global Health Estimates," 2015. [Online]. Available: [http://www.who.int/healthinfo/global\\_burden\\_disease/estimates/en/](http://www.who.int/healthinfo/global_burden_disease/estimates/en/).
- [2] B. Ovbiagele and M. Nguyen-Huynh, "Stroke epidemiology: Advancing our understanding of disease mechanism and therapy," *Neurotherapeutics*, vol. 8, no. 3, pp. 319-329, 2011.
- [3] L. Nih, S. Carmichael and T. Segura, "Hydrogels for brain repair after stroke: an emerging treatment option," *Current Opinion in Biotechnology*, vol. 40, pp. 155-163, 2016.
- [4] L. Nih, E. Sideris, S. Carmichael and T. Segura, "Injection of microporous annealing particle (MAP) hydrogels in the stroke cavity reduced gliosis and inflammation and promotes NPC migration to the lesion," *Adv. Mater.*, vol. 29, p. 1606471, 2017.
- [5] J. Zhong, A. Chan, L. Morad, H. Kornblum, G. Fan and S. Carmichael, "Hydrogel matrix to support stem cell survival after brain transplantation in stroke," *Neurorehabilitation and Neural Repair*, vol. 24, no. 7, pp. 636-644, 2010.
- [6] O. Bang, J. Lee, P. Lee and G. Lee, "Autologous mesenchymal stem cell transplantation in stroke patients," *Annals of Neurology*, vol. 57, no. 6, pp. 874-882, 2005.
- [7] G. Fonarow, E. Smith, J. Saver, M. Reeves, D. Bhatt, M. Grau-Sepulveda and e. al, "Timeliness of tissue-type plasminogen activator therapy in acute ischemic stroke: patient characteristics, hospital factors, and outcomes associated with door-to needle times within 60 minutes," *Circulation*, vol. 123, no. 7, pp. 750-758, 2011.
- [8] A. Yoo, B. Pulli and R. Gonzalez, "Imaging-based treatment selection for intravenous and intra-arterial stroke therapies: a comprehensive review," *Expert Rev Cardiovasc Ther*, vol. 9, no. 7, pp. 857-876, 2011.
- [9] M. Fisher and G. Albers, "Advanced imaging to extend the therapeutic time window of acute ischemic stroke," *Ann Neurol*, vol. 73, no. 1, pp. 4-9, 2013.
- [10] E. Duffis, Z. Al-Qudah, C. Prestigiacomo and C. Gandhi, "Advanced neuroimaging in acute ischemic stroke: extending the time window for treatment," *Neurosurg Focus*, vol. 30, no. 6, p. E5, 2011.
- [11] G. Sandhu and J. Sunshine, "Advanced neuroimaging to guide acute stroke therapy," *Curr Cardiol Rep*, vol. 14, no. 6, pp. 741-753, 2012.
- [12] K. Lees, E. Bluhmki, R. von Kummer, T. Brott, D. Toni, J. Grotta, G. Albers, M. Kaste, J. Marler and S. e. a. Hamilton, "Time to treatment with intravenous alteplase and outcome in stroke: an updated pooled analysis of ECASS, ATLANTIS, NINDS, and EPITHET trials," *Lancet*, vol. 375, no. 9727, pp. 1695-1703, 2010.
- [13] C. Meltzer and e. al, "Serial [18F]fluorodeoxyglucose position emission tomography after human neuronal implantation for stroke," *Neurosurgery*, vol. 49, pp. 586-591, 2001.

- [14] D. Kondziolka, L. Wechsler, S. Goldstein, C. Meltzer, K. Thulborn, J. Gebel, P. Jannetta, S. DeCesare, E. Elder, M. McGrogan, M. Retiman and L. Bynum, "Transplantation of cultured human neuronal cells for patients with stroke," *Neurology*, vol. 55, no. 4, pp. 565-569, 2000.
- [15] P. Nelson and e. al, "Clonal human (hNT) neuron grafts for stroke therapy: neuropathology in patient 27 months after implantation," *Am J Pathol*, vol. 160, pp. 1201-1206, 2002.
- [16] Y. Li, J. Chen, X. Chen, L. Wang, S. Gautan, Y. Xu, M. Katakowski, L. Zhang, M. Lu, N. Janakiraman and M. Chopp, "Human marrow stromal cell therapy for stroke in rat neurotrophins and functional recovery," *Neurology*, vol. 59, no. 4, 2002.
- [17] R. Ashton, A. Banerjee, S. Punyani, D. Schaffer and R. Kane, "Scaffolds based on degradable alginate hydrogels and poly(lactide-co-glycolide) microspheres for stem cell culture," *Biomaterials*, vol. 28, pp. 5518-5525, 2007.
- [18] M. Fan, Y. Ma, H. Tan, Y. Jia, S. Zou, S. Guo, M. Zhao, H. Huang, Z. Ling, Y. Chen and X. Hu, "Covalent and injectable chiton-chondroitin sulfate hydrogels embedded with chitosan microspheres for drug delivery and tissue engineering," *Materials Science and Engineering C*, vol. 71, pp. 67-74, 2017.
- [19] M. Caicco, M. Cooke, Y. Wang, A. Tuladhar, C. Morshead and M. Shoichet, "A hydrogel composite system for sustained epi-cortical delivery of Cyclosporin A to the brain for treatment of stroke," *Journal of Controlled Release*, vol. 166, pp. 197-202, 2013.
- [20] Y. Wan, Y. Huang, C. Yuan, S. Raman, Y. Zhu, H. Jiang, F. He and C. Gao, "Biomimetic synthesis of hydroxyapatite/bacterial cellulose nanocomposites for biomedical applications," *Mater Sci Eng C*, vol. 27, pp. 855-864, 2007.
- [21] A. Tuladhar, C. Morshead and M. Shoichet, "Circumventing the blood-brain barrier: local delivery of cyclosporin A stimulates stem cells in stroke-injured rat brain," *Journal of Controlled Release*, vol. 215, pp. 1-11, 2015.
- [22] J. Broderick and e. al, "Guidelines for the management of spontaneous intracerebral hemorrhage in adults," American Heart Association/American Stroke Association, stroke coucil, high blood pressure research coucil and the quality of care and outcomes in research interdisciplinary working group, 2007.
- [23] S. Shah and W. Kimberly, "The modern appraoch to treating brain swelling in the neuro ICU," *Semin Neurol*, vol. 36, no. 6, pp. 502-507, 2016.
- [24] A. Doerfler, M. Forsting, W. Reith, C. Staff, S. Heiland, W.-R. Scharitz, R. von Kummer, W. Hacke and K. Sartor, "Decompressive craniectomy in a rat model of "malignant" cerebral hemispheric stroke: experimental support for an aggressive therapeutic approach," *J Neurosurg*, vol. 85, p. 853:859, 1996.
- [25] J. Murthy, G. Chowdary, T. Murthy, P. Bhasha and T. Naryanan, "Decompressive craniectomy with clot evacuation in large hemispheric hypertensive intracerebral hemorrhage," *Neurocritical Care*, vol. 2, pp. 258-262, 2005.

- [26] E. Juttler, A. Enterberg, J. Woitzik, J. Bosel, H. Amiri, O. Sakowitz, M. Gondan, P. Schiller, R. Limprecht, S. Luntz, H. Schneider, T. Pinzer, C. Hobohm, J. Meixensberger and W. Hacke, "Hemicraniectomy in older patients with extensive middle-cerebral-artery stroke," *The New England Journal of Medicine*, vol. 370, no. 12, pp. 1091-1100, 2014.
- [27] S. Harscher, R. Reichart, C. Terborg, G. Hagermann, R. Kalff and O. Witte, "Outcome after decompressive craniectomy in patients with severe ischemic stroke," *Acta Neurochir*, vol. 148, pp. 31-37, 2006.
- [28] K. Vahedi, E. Vicault, J. Mateo, A. Kurtz, M. Orabi, J.-P. Guichard, C. Boutron, G. Couvreur, F. Rouanet, E. Touze, B. Guillon, A. Carpentier, A. Yelnik, B. George, D. Payen and M.-G. Bousser, "Sequential-Design, multicenter, randomized, controlled trial of early decompressive craniectomy in malignant middle cerebral artery infarction (DECIMAL Trial)," *Stroke*, vol. 38, pp. 2506-2517, 2007.
- [29] A. Sokolnicki, R. Fisher, T. Harrah and D. Kaplan, "Permeability of bacterial cellulose membranes," *J Membrane Sci*, vol. 272, pp. 15-27, 2006.
- [30] A. Marzieh Moosavi-Nasab, "Investigation of physiochemical properties of the bacterial cellulose produced by *Gluconacetobacter xylinus* from date syrup," *World Academy of Science, Engineering and Technology*, pp. 1248-1253, 2010.
- [31] H. Barud, C. Ribeiro, J. Capela, M. Crespi, S. Ribeiro and Y. Messadeq, "Kinetic parameters for thermal decomposition of microcrystalline, vegetal, and bacterial cellulose," *J Therm Anal Calorim*, vol. 105, pp. 421-426, 2011.
- [32] S.-P. Lin, I. Loira Calvar, J. Catchmark, J.-R. Liu, A. Demirci and K.-C. Cheng, "Biosynthesis, production and applications of bacterial cellulose," *Cellulose*, vol. 20, pp. 2191-2219, 2013.
- [33] C. Choi, H. Song, M. Kim, M. Chang and S. Kim, "Properties of bacterial cellulose produced in a pilot-scale spherical type bubble column bioreactor," *Korean J Chem Eng*, vol. 26, pp. 136-140, 2009.
- [34] M. Ul-Islam, T. Khan and J. Park, "Water holding and release properties of bacterial cellulose obtained by in situ and ex situ modification," *Carbohydr Polym*, vol. 88, pp. 596-603, 2012.
- [35] Y. Wan, C. Gao, M. Han, H. Liang, K. Ren, Y. Wang and H. Luo, "Preparation and characterization of bacterial cellulose/heparin hybrid nanofiber for potential vascular tissue engineering scaffolds," *Polym Advan Technol*, vol. 22, pp. 2643-2648, 2011.
- [36] G. Xiong, H. Luo, F. Gu, J. Zhang and Y. Wan, "A novel in vitro three-dimensional macroporous scaffolds from bacterial cellulose for culture of breast cancer cells," *Journal of Biomaterials and Nanobiotechnology*, vol. 4, pp. 316-326, 2013.
- [37] W. Hu, S. Chen, J. Yang, Z. Li and H. Wang, "Functionalized bacterial cellulose derivatives and nanocomposites," *Carbohydr Polym*, vol. 101, pp. 1043-1060, 2014.
- [38] C. Katepetch, R. Rujiravanit and H. Tamura, "Formation of nanocrystalline ZnO particles into bacterial cellulose pellicle by ultrasonic-assisted in situ synthesis," *Cellulose*, vol. 20, pp. 1275-1292, 2013.

- [39] L. Millon, G. Guhadós and W. Wan, "Anisotropic polyvinyl alcohol-bacterial cellulose nanocomposite for biomedical applications," *J Biomed Mater Res B Appl Biomater*, vol. 86, pp. 444-452, 2008.
- [40] A. Svensson, E. Nicklasson, T. Harrah, B. Panilaitis, D. Kaplan, M. Brittberg and P. Gatenholm, "Bacterial cellulose as a potential scaffold for tissue engineering of cartilage," *Biomaterials*, vol. 26, pp. 419-431, 2005.
- [41] S. Saska, R. Scarel-Caminaga, L. Teixeira, L. Franchi, R. dos Santos, A. Gaspar, P. de Oliveira, A. Rosa, C. Takahashi, Y. Messaddeq, S. Ribeiro and R. Marchetto, "Characterization and in vitro evaluation of bacterial cellulose membranes functionalized with osteogenic growth peptide for bone tissue engineering," *J Mater Sci-Mater M*, vol. 23, pp. 2253-2266, 2012.
- [42] A. Yoshino, M. Tabuchi, M. Uo, H. Tatsumi, K. Hideshima, S. Kondo and J. Sekine, "Application of bacterial cellulose as an alternative to paper points in endodontic treatment," *Acta Biomater*, vol. 9, pp. 6116-6122, 2013.
- [43] J. Wang, C. Gao, Y. Zhang and Y. Wan, "Preparation and in vitro characterization of BC/PVA hydrogel composite for its potential use as artificial cornea biomaterial," *Mat Sci Eng C-Mater*, vol. 30, pp. 214-218, 2010.
- [44] C. Xu, X. Ma, S. Chen, M. Tao, L. Yuan and Y. Jing, "Bacterial cellulose membranes used as artificial substitutes for dural deflection in rabbits," *Int J Mol Sci*, vol. 15, pp. 10855-10867, 2014.
- [45] A. Bodin, S. Bharadwaj, S. Wu, P. Gatenholm, A. Atala and Y. Zhang, "Tissue-engineered conduit using urine-derived stem cells seeded bacterial cellulose polymer in urinary reconstruction and diversion," *Biomaterials*, vol. 31, pp. 8889-8901, 2010.
- [46] K. Hirayama, T. Okitsu, H. Teramae, D. Kiriva, H. Onoe and S. Takeuchi, "Cellular building unit integrated with microstrand-shaped bacterial cellulose," *Biomaterials*, vol. 34, no. 10, pp. 2421-2427, 2013.
- [47] E. Trovatti, C. Freire, P. Pinto and e. al, "Bacterial cellulose membranes applied in topical and transdermal delivery of lidocaine hydrochloride and ibuprofen: in vitro diffusion studies," *Int J Pharm*, vol. 435, no. 1, pp. 83-87, 2012.
- [48] T. Stumpf, R. Sandarage, P. Fournier, T. Li, E. Tsai and X. Cao, "Design and evaluation of a novel drug delivery system to repair post-stroke neural injury," in *68th Canadian Chemical Engineering Conference*, Toronto, 2018.
- [49] A. Kelmendi-Doko, P. Rubin, K. Klett, C. Mahoney, S. Wang and K. Marra, "Controlled dexamethasone delivery via double-walled microspheres to enhance long-term adipose tissue retention," *Journal of Tissue Engineering*, vol. 8, pp. 1-10, 2017.
- [50] A. DeFail, C. Chu, N. Izzo and K. Marra, "Controlled release of bioactive TGF-beta 1 from microspheres embedded within biodegradable hydrogels," *Biomaterials*, vol. 27, pp. 1579-1585, 2006.
- [51] A. DeFail, H. Edington, S. Malthews, W.-C. Lee and K. Marra, "Controlled release of bioactive doxorubicin from microspheres embedded within gelatin scaffolds," *Journal of Biomedical Materials Research Part A*, pp. 954-962, 2006.

- [52] F. Han, K. Thurecht, A. Whittaker and M. Smith, "Bioerodable PLGA-based microparticles for producing sustained-release drug formulations and strategies for improving drug loading," *Frontiers in Pharmacology*, vol. 7, p. 185, 2016.
- [53] L. Brannon-Peppas, "Recent advances on the use of biodegradable microparticles and nanoparticles in controlled drug delivery," *International Journal of Pharmaceutics*, vol. 116, pp. 1-9, 1995.
- [54] K. Soppimath, A. Kulkarni, Aminabhavi and T, "Development of hollow microspheres as floating controlled-release systems for cardiovascular drugs: preparation and release characteristics," *Drug Development and Industrial Pharmacy*, vol. 27, no. 6, pp. 507-515, 2001.
- [55] K. Santhosh, A. Alizadeh and S. Karimi-Abdolrezaee, "Design and optimization of PLGA microparticle for controlled and local delivery of Neuregulin-1 in traumatic spinal cord injury," *Journal of Controlled Release*, vol. 261, pp. 147-162, 2017.
- [56] B. Bailey, K.-G. Desai, L. Ochyl, S. Ciotti, J. Moon and S. Schwendeman, "Self-encapsulating poly(lactic-co-glycolic acid) (PLGA) microspheres for intranasal vaccine delivery," *Molecular Pharmaceutics*, vol. 14, pp. 3228-3237, 2017.
- [57] N. Teekamp, F. Van Dijk, A. Broesder, M. Evers, J. Zuidema, R. Steendam, E. Post, J. Hillebrands, H. Frijlink, K. Poelstra, L. Beljaars, P. Olinga and W. Hinrichs, "Polymeric microspheres for the sustained release of a protein-based drug carrier targeting the PDGF beta-receptor in the fibrotic kidney," *International Journal of Pharmaceutics*, vol. 534, pp. 229-236, 2017.
- [58] W. Wang, Y. Lei, H. Sui, W. Zhang, R. Zhu, J. Feng and H. Wang, "Fabrication and evaluation of nanoparticle-assembled BSA microparticles for enhanced liver delivery of glycyrrhetic acid," *Artificial Cells, Nanomedicine, and Biotechnology*, vol. 45, no. 4, pp. 740-747, 2017.
- [59] Y. Yeo and K. Park, "Control of encapsulation efficiency and initial burst in polymeric microparticle systems," *Arch Pharm Res*, vol. 27, pp. 1-12, 2004.
- [60] O. Corrigan and X. Li, "Quantifying drug release from PLGA nanoparticulates," *European Journal of Pharmaceutical Sciences*, vol. 37, pp. 477-485, 2009.
- [61] W. Zheng, "A water-in-oil-in-water (W/O/O/W) method for producing drug-releasing double-walled microspheres," *International Journal of Pharmaceutics*, vol. 374, pp. 90-95, 2009.
- [62] C. Osswald, M. Guthrie, A. Avila, J. Valio, W. Mieler and J. Kang-Mieler, "In vivo efficacy of an injectable microsphere-hydrogel ocular drug delivery system," *Current Eye Research*, vol. 42, no. 9, pp. 1293-1301, 2017.
- [63] A. Perets, Y. Baruch, F. Weisbuch, G. Shoshany, G. Meufeld and S. Cohen, "Enhancing the vascularization of three-dimensional porous alginate scaffolds by incorporating controlled release basic fibroblast growth factor microspheres," *J Biomed Mater Res*, vol. 65A, pp. 489-497, 2003.
- [64] L. Nie, G. Zhang, R. Hou, H. Xu, Y. Li and J. Fu, "Controllable promotion of chondrocyte adhesion and growth on PVA hydrogels by controlled release of TGF- $\beta$ 1

- from porous PLGA microspheres," *Colloids and Surfaces B: Biointerfaces*, vol. 125, pp. 51-57, 2015.
- [65] Q. Zhu, J. Teng, X. Liu, Y. Lan and R. Guo, "Preparation and characterization of gentamycin sulfate-impregnated gelatin microspheres/collagen-cellulose/nanocrystal scaffolds," *Polym Bull*, vol. 75, pp. 77-91, 2018.
- [66] J. Park, H.-J. Lim, S. Yi and K.-H. Park, "Stem cell differentiation-related protein-loaded PLGA microspheres as a novel platform micro-typed scaffold for chondrogenesis," *Biomedical Materials*, vol. 11, 2016.
- [67] Y. Wang, M. Cooke, N. Sachewsky, C. Morshead and M. Shoichet, "Bioengineered sequential growth factor delivery stimulates brain tissue regeneration after stroke," *Journal of Controlled Release*, vol. 172, no. 1, pp. 1-11, 2013.
- [68] G. Jiao, Y. Pan, C. Wang, Z. Li, Z. Li and R. Guo, "A bridging SF/Alg composite scaffold loaded NGF for spinal cord injury repair," *Materials Science and Engineering C*, vol. 76, pp. 81-87, 2017.
- [69] S. Haas, N. Weidner and J. Winkler, "Adult stem cell therapy in stroke," *Current Opinion in Neurology*, vol. 18, no. 1, pp. 59-64, 2005.
- [70] G. Parker, "Stem cell therapy for stroke," *Journal of Pediatric Neurology*, vol. 8, no. 3, pp. 333-341, 2010.
- [71] J. Lam, W. Lowry, T. Carmichael and T. Segura, "Delivery of iPS-NPCs to the stroke cavity within a hyaluronic acid matrix promotes the differentiation of transplanted cells," *Adv. Fund. Mater.*, vol. 24, pp. 7053-7062, 2014.
- [72] S. Bhaskar, P. Stanwell, D. Cordato, J. Attia and C. Levi, "Reperfusion therapy in acute ischemic stroke: dawn of a new era," *BMC Neurol*, vol. 18, p. 8, 2018.
- [73] R. von Kummer, K. Allen, R. Holle, L. Bozzao, S. Bastianello, C. Manelfe, E. Bluhmki, P. Ringleb, D. Meier and W. Hacke, "Acute stroke: usefulness of early CT findings before thrombolytic therapy," *Radiology*, vol. 205, no. 2, pp. 327-333, 1997.
- [74] W. Hacke, G. Donnan, C. Fieschi, M. Kaste, R. von Kummer, J. Broderick, T. Brott, M. Frankel, J. Grotta, E. J. Haley and e. al, "Association of outcome with early stroke treatment: pooled analysis of ATLANTIS, ECASS and NINDS rt-PA stroke trials," *Lancet*, vol. 363, no. 9411, pp. 768-774, 2004.
- [75] T. Kwiatkowski, R. Libman, M. Frankel, B. Tilley, L. Mogenstern, M. Lu, J. Broderick, C. Lewandowski, J. Marler, S. Levine and e. al, "Effects of tissue plasminogen activator for acute ischemic stroke at one year. National Institute of Neurological Disorders and Stroke recombinant tissue Plasminogen activator stroke study group," *N Engl J Med*, vol. 340, no. 23, pp. 1781-1787, 1999.
- [76] A. Frew, "Different Strokes: Recovery triumphs and challenges at any age," Heart and Stroke Foundation of Canada, 2017.
- [77] O. Lindvall, Z. Kokaia and A. Martinez-Serrano, "Stem cell therapy for human neurodegenerative disorders - how to make it work," *Nature Medicine*, vol. 10, pp. S42-S50, 2004.

- [78] P. Meyers and e. al, "Current status of endovascular stroke treatment," *New Drugs and Technologies*, vol. 123, pp. 2591-2601, 2011.
- [79] S. Kelly, T. Bliss, A. Shah, G. Sun, M. Ma, W. oo, J. Masel, M. Yenari, I. Weissman, N. Uchida, T. Palmer and G. Steinberg, "Transplanted human fetal neural stem cels survive, migrate, and differentiate in ischemic rat cerebral crotex," *Proc Netl Acad Sci USA*, vol. 101, pp. 11839-11844, 2004.
- [80] S. Farber, S. Onifer, Y. Kaseda, S. Murphy, D. Wells, B. Vietje, J. Wells and W. Low, "Neural transplantation of horseradish peroxidase-labeled hippocampal cell suspensions in an experimental model of cerebral ischemia," *Progress in Brain Research*, vol. 78, pp. 103-107, 1988.
- [81] N. Aihara, K. Mizukawa, K. Koide, H. Mabe and H. Nishino, "Striatl grafts in infarct striatopallidum increase GABA release, reorganize GABAA receptor and improve water-maze learning in the rat," *Brain Res Bull*, vol. 33, no. 5, pp. 483-488, 1994.
- [82] B. Mattsson, J. Sorensen, J. Zimmer and B. Johansson, "Neural grafting to experimental neocortical infarcts improves behavioural outcome and reduces thalamic atrophy in rats housed in enriched but not in standard environments," *Stroke*, vol. 28, no. 6, pp. 1225-31, 1997.
- [83] Z. Zhang, Q. Jiang, R. Zhang, L. Zhang, L. Wang, L. Zhang, P. H. K. Arniego and M. Chopp, "Magnetic resonance imaging and neurosphere therapy of stroke in rat," *Ann Neurol*, vol. 53, no. 2, pp. 259-63, 2003.
- [84] H. Nishino and C. Borlongan, "Restoration of function by neural transplantation in the ischemic brain," *Prog Brain Res*, vol. 127, pp. 461-76, 2000.
- [85] J. Parent, Z. Vexler, C. Gong and e. al, "Rat forebrain neurogenesis and striatal neuron replacement after focal stroke," *Ann Neurol*, vol. 52, pp. 802-813, 2002.
- [86] A. Arvidsson, T. Collin, D. Kirik, Z. Kokaia and O. Lindvall, "Neuronal replacement from endogeneous precursors in the adult brain after stroke," *Nat Med*, vol. 8, pp. 963-970, 2002.
- [87] K. Jin and e. al, "Directed migration of neuronal precursors into the ischemic cerecral cortex and striatum," *Mol Cell Neurosci*, vol. 24, pp. 171-189, 2003.
- [88] H. Kuhn, H. Dickinson-Anson and F. Gage, "Neurogenesis in the dentate gyrus of the adult rat: age-related decrease of neuronal progenitor proliferation," *J Neurosci*, vol. 16, pp. 2027-2033, 1996.
- [89] P. Eriksson, E. Perfilieva, T. Bjork-Eriksson and e. al, "Neurogenesis in the adult human hippocampus," *Nat Med*, vol. 4, pp. 1313-1317, 1998.
- [90] K. Naoko, E. Kako and K. Sawamoto, "Prospects and limitations of using endogenous neural stem cells for brain regeneration," *Genes*, vol. 2, no. 1, pp. 107-130, 2011.
- [91] L. Wright, K. Prowse, K. Wallace and e. al, "Human progentior cells isolated from the developing cortex undergo decreased neurogenesis and eventual senescence following expansion in vitro," *Exp Cell Res*, vol. 312, pp. 2107-2120, 2006.

- [92] C. Svendson, D. Clarke, A. Rosse and S. Dunnett, "Survival and differentiation of rat and human epidermal growth factor-responsive precursor cells following grafting into the lesioned adult central nervous system," *Exp Neurol*, vol. 137, pp. 376-388, 1996.
- [93] M. Kaplan and D. Bell, "Mitotic neuroblasts in the 9-day-old and 11-month-old rodent hippocampus," *J Neurosci*, vol. 4, pp. 1429-1441, 1984.
- [94] J. Altman and G. Das, "Autoradiographic and histological evidence of postnatal hippocampal neurogenesis in rates," *J Comp Neurol*, vol. 124, pp. 319-335, 1965.
- [95] N. Sanai and e. al, "Unique astrocyte ribbon in adult human brain contains neural stem cells but lacks chain migration," *Nature*, vol. 427, pp. 740-744, 2004.
- [96] R. Zhang, Z. Zhang, L. Wang and e. al, "Activated neural stem cells contribute to stroke-induced neurogenesis and neuroblast migration toward the infarct boundary in adult rats," *J Cereb Blood Flow Metab*, vol. 24, pp. 441-448, 2004.
- [97] R. Zhang, Z. Zhang, C. Zhang and e. al, "Stroke transiently increases subventricular zone cell division from asymmetric to symmetric and increases neuronal differentiation in the adult rat," *J Neurosci*, vol. 24, pp. 5810-5815, 2004.
- [98] A. Arvidsson, Z. Kokaia and O. Lindvall, "N-methyl-D-aspartate receptor-mediated increase of neurogenesis in adult rat dentate gyrus following stroke," *Eur J Neurosci*, vol. 14, pp. 10-18, 2001.
- [99] A. Rice, A. Khaldi, H. Harvery and e. al, "Proliferation and neuronal differentiation of mitotically active cells following traumatic brain injury," *Exp Neurol*, vol. 183, pp. 406-417, 2003.
- [100] Y. Sun, K. Jin, L. Xie and e. al, "VEGF-induced neuroprotection, neurogenesis and angiogenesis after focal cerebral ischemia," *J Clin Invest*, vol. 111, pp. 1843-1851, 2003.
- [101] W. Jiang, W. Gu, T. Brannstrom and e. al, "Cortical neurogenesis in adult rats after transient middle cerebral artery occlusion," *Stroke*, vol. 32, pp. 1201-1207, 2001.
- [102] H. Kuhn, J. Winkler, G. Kempermann and e. al, "Epidermal growth factor and fibroblast growth factor-2 have different effects on neural progenitors in the adult rat brain," *J Neurosci*, vol. 17, pp. 5820-5829, 1997.
- [103] K. Jin, X. Mao, Y. Sun, L. Xie and D. Greenberg, "Stem cell factor stimulated neurogenesis in vitro and in vivo," *J Clin Invest*, vol. 110, pp. 311-319, 2002.
- [104] S. Yoshimura and e. al, "FGF-2 regulation of neurogenesis in adult hippocampus after brain injury," *Proc Natl Acad Sci USA*, vol. 98, pp. 5874-5879, 2001.
- [105] K. Jin, Y. Zhu, Y. Sun and e. al, "Vascular endothelial growth factor (VEGF) stimulates neurogenesis in vitro and in vivo," *Proc Natl Acad Sci USA*, vol. 99, pp. 11946-11950, 2002.
- [106] A. Schanzer, F. Wachs, D. Wilhelm and e. al, "Direct stimulation of adult neural stem cells in vitro and neurogenesis in vivo by vascular endothelial growth factor," *Brain Pathol*, vol. 14, pp. 237-248, 2004.

- [107] E. Gustafsson, G. Andsberg, V. Darsalia and e. al, "Anterograde delivery of brain-derived neurotrophic factor to stratu via nigral transduction of recombinant adeno-associated virus increases neuronal death but promoted neurogenic response following stroke," *Eur J Neurosci*, vol. 17, pp. 2667-2678, 2003.
- [108] E. Chmielnicki, A. Benraiss, A. Economides and e. al, "Adenovirally expressed noggin and brain-derived neurotrophic factor cooperate to induce new meedium spiny neurons from resident progenitor cells in the adult striatal ventricular zone," *J Neurosci*, vol. 24, pp. 2133-2142, 2004.
- [109] T. Shingo, S. Sorokan, T. Shimazaki and S. Weiss, "Erythropoietin regulated the in vitro and in vivo production of neuronal progenitors by mammalian forebrain neural stem cells," *J Neurosci*, vol. 21, pp. 9733-9743, 2001.
- [110] T. Teramoto, J. Qiu, J. Plumier and M. Moskowitz, "EGF amplifies the replacement of parvalbumin-expressing striatal interneurons after ischemia," *J Clin Invest*, vol. 111, pp. 1125-1132, 2003.
- [111] C. Ekdahl and e. al, "Caspase-mediated death of newly formed neurons in the adult rat dentate gyrus following status epilepticus," *Eur J Neurosci*, vol. 16, pp. 1463-1471, 2002.
- [112] C. Ekdahl, J. Claasen, S. Bonde, Z. Kokaia and O. Lindvall, "Inflammation is detrimental for neurogenesis in adult brain," *Proc Natl Acad Sci USA*, vol. 203, pp. 13632-13627, 2003.
- [113] M. Monje, H. Toda and T. Palmer, "Inflammatory blockade restores adult hippocampal neurogenesis," *Science*, vol. 302, pp. 1760-1765, 2003.
- [114] H. Zhang, L. Vutskits, M. Pepper and J. Kiss, "VEGF is a chemoattractant for FGF-2-stimulated neural progenitors," *J Cell Biol*, vol. 163, pp. 1375-1385, 2003.
- [115] H. Nakatomi, T. Kuriu, S. Okabe and e. al, "Regeneration of hippocampal pyrimidal neurons after ischemic brain injury by recruitment of endogenous neural progenitors," *Cell*, vol. 110, pp. 429-441, 2002.
- [116] L. Wang, Z. Zhang, Y. Wang and e. al, "Treatment of stroke with erythropoietin enhances neurogenesis and angiogenesis and improves neurological function in rats," *Stroke*, vol. 35, pp. 1732-1737, 2004.
- [117] H. Ehrenreich, M. Hasselblatt, C. Dembowski and e. al, "Erythropoietin therapy for acute stroke is both safe and beneficial," *Mol Med*, vol. 8, pp. 495-505, 2002.
- [118] N. Abbott, A. Patabendige, D. Dolman, S. Yusof and D. Begley, "Structure and function of the blood-brain barrier," *Neurobiology of Disease*, vol. 37, no. 1, pp. 13-25, 2010.
- [119] X. Dong, "Current strategies for brain drug delivery," *Theranostics*, vol. 8, no. 6, pp. 1481-1493, 2018.
- [120] D. Begley, "Delivery of therapeutic agents to the ventral nervous system: the problem and the possibilities," *Pharmacol Ther*, vol. 104, no. 1, pp. 29-45, 2004.
- [121] E. Wijdicks, K. Sheth, B. Carter, D. Greer, S. Kasner, T. Kimberly, S. Schwab, E. Smith, R. Tamargo and M. Wintermark, "Recommendations for the Management of

- Cerebral and Cerebella Infarction With Swelling," *Stroke*, vol. 45, pp. 1222-1238, 2014.
- [122] D. Azzam, P. Romiyo, T. Nguyen, J. Sheppard, Y. Alkhalid, C. Lagman, G. Preashant and I. Yang, "Dural repair in cranial surgery is associated with moderate rates of complications with both autologous and nonautologous dural substitutes," *World Neurosurgery*, vol. 113, pp. 244-248, 2018.
- [123] F. Martini, J. Nath and E. Bartholomew, *Fundamentals of Anatomy and Physiology*, 10th ed., Glenview: Pearson Education Inc, 2015.
- [124] "Wikipedia," [Online]. Available: <http://en.wikipedia.org/wiki/File:Meninges-en.svg>.
- [125] Z. Shi, T. Xu, Y. Yuan, K. Deng, M. Liu, Y. Ke, C. Luo, T. Yuan and A. Ayyad, "A new absorbable synthetic substitute with biomimetic design for dural tissue repair," *Artificial Organs*, vol. 40, no. 4, pp. 403-413, 2016.
- [126] P. Narotam, K. Reddy, D. Fewer, F. Qiao and N. Nathoo, "Collagen matrix duraplasty for cranial and spinal surgery: a clinical and imaging study," *J Neurosurg*, vol. 106, pp. 45-51, 2007.
- [127] K. Yamada, S. Miyamoto, I. Nagata, H. Kikuchi, Y. Ikada, H. Iwata and K. Yamamoto, "Development of a dural substitute from synthetic bioabsorbable polymers," *J Neurosurg*, vol. 86, pp. 1012-1017, 1997.
- [128] G. Brzezicki, R. Jankowski, T. Blok, J. Szymas, J. Huber, A. Szukala, S. Nowak and M. Borejsza-Wysocki, "Evaluation of epidural scar formation in lumbar spine after TachoComb application - An experimental study," *Neurol Neurochir Pol*, vol. 42, pp. 223-230, 2008.
- [129] B. Sommerich, A. Barnick, M. Barakat and M. Ward, "In vivo tissue reaction, resorption, safety, and efficacy of a collagen dural substitute in an animal model," Codman and Shurtleff, Inc, Raynham, MA, 2005.
- [130] C. Rosen, G. Steinberg, F. DeMonte, J. J. Delashaw, S. Lewis, M. Shaffrey, K. Aziz, J. Hantel and F. Marciano, "Results of the prospective, randomized, multicenter clinical trial evaluating a biosynthesized cellulose graft for repair of dural defects," *Neurosurgery*, vol. 69, no. 5, pp. 1093-1104, 2011.
- [131] E. Caroli, G. Rocchi, M. Salcati and R. Delfini, "Duraplasty: our current experience," *Surg Neurol*, vol. 61, pp. 55-59, 2004.
- [132] M. Malliti, P. Page, C. Gury, E. Chomette, F. Nataf and F. Roux, "Comparison of deep wound infection rates using a synthetic dural substitute (Neuro-Patch) or pericranium graft for dural closure: a clinical review of 1 year," *Neurosurgery*, vol. 54, no. 3, pp. 599-603, 2004.
- [133] A. Laquerriere, J. Yun, J. Tiollier, J. Hemet and M. Tadie, "Experimental evaluation of bilayered human collagen as a dural substitute," *J Neurosurg*, vol. 78, no. 3, pp. 487-491, 1993.
- [134] T. McCall, D. Fults and R. Schmidt, "Use of resorbable collagen dural substitutes in the presence of cranial and spinal infections - report of 3 cases," *Surg Neurol*, vol. 70, pp. 92-97, 2008.

- [135] E. Tachibana, K. Saito, K. Fukuta and J. Yoshida, "Evaluation of the healing process after dural reconstruction achieved using a free fascial graft," *J Neurosurg*, vol. 96, no. 2, pp. 280-286, 2002.
- [136] D. Hoover and A. Mahmood, "Ossification of autologous pericranium used in duraplasty. Case Report," *J Neurosurg*, vol. 95, no. 2, pp. 350-352, 2001.
- [137] J. Keller, S. Dunsker, J. McWhorter, C. Ongkiko, M. Saunders and F. Mayfield, "The fate of autogenous grafts to the spinal dura: an experimental study," *J Neurosurg*, vol. 49, pp. 412-418, 1978.
- [138] F. Lam and E. Kasper, "Augmented autologous pericranium duraplasty in 100 posterior fossa surgeries - a retrospective case series," *Neurosurgery*, vol. 71, p. suppl 2, 2012.
- [139] A. Abla, T. Link, D. Fusco, D. Wilson and V. Sonntag, "Comparison of dural grafts in Chiari decompression surgery: review of the literature," *J Craniovert Junction Spine*, vol. 1, pp. 29-37, 2010.
- [140] M. MacFarlane and L. Symon, "Lyophilised dura mater: experimental implantation and extended clinical neurosurgical use," *J Neurol Neurosurg Psychiatry*, vol. 42, pp. 854-858, 1979.
- [141] J. Campbell, C. Bassett and J. Robertson, "Clinical use of freeze-dried human dura mater," *J Neurosurg*, vol. 15, pp. 207-214, 1958.
- [142] P. Narotam, J. van Dellen and K. Bhoola, "A clinicalpathological study of collagen sponge as a dural graft in neurosurgery," *J Neurosurg*, vol. 82, pp. 406-412, 1995.
- [143] K. Von Wild, "Examination of the safety and efficacy of an absorbable dura mater substitute (Dura Patch) in normal applications in neurosurgery," *Surg Neurol*, vol. 52, pp. 418-425, 1999.
- [144] T. Tomita, N. Hayashi, M. Okabe, T. Yoshida, H. Hamada, S. Endo and T. Nikaido, "New dried human amniotic membrane is useful as a substitute for dural repair after skull base surgery," *J Neurol Surg B Skull Base*, vol. 73, pp. 302-307, 2012.
- [145] G. Bejjani and J. Zabramski, "Safety and efficacy of the porcine small intestine submucosa dural substitute: results of a prospective multicenter study and literature review," *J Neurosurg*, vol. 106, no. 6, pp. 1028-1033, 2007.
- [146] M. Achilli and D. Mantovani, "Tailoring mechanical properties of collagen-based scaffolds for vascular tissue engineering: the effects of pH, temperature and ionic strength on gelation," *Polymers*, vol. 2, pp. 664-680, 2010.
- [147] S. Moskowitz, J. Liu and A. Krishnaney, "Postoperative complications associated with dural substitutes in suboccipital craniotomies," *Neurosurgery*, vol. 64, pp. 28-33, 2009.
- [148] C. Bowers, C. Brimley, C. Cole, W. Gluf and R. Schmidt, "Alloderm for duraplasty in Chiari malformation: superior outcomes," *Acta Neurochir*, vol. 157, pp. 507-511, 2015.
- [149] G. Bejjani and J. Zabramski, "Safety and efficacy of the porcine small intestinal submucosa dural substitute: results of a prospective multicenter study and literature review," *J Neurosurg*, vol. 106, pp. 1028-1033, 2007.

- [150] J. Martinez-Lage, M. Perez-Espeio, J. Palazon, F. Lopez Hernandez and P. Puerta, "Autologous tissues for dural grafting in children: a report of 56 cases," *Childs Nerv Syst*, vol. 22, pp. 139-144, 2006.
- [151] J. Martinez-Lage, A. Rabano, J. Bermejo and e. al, "Creutzfeldt-Jakob disease acquired via a dural graft: failure of therapy with quinacrine and chlorpromazine," *Surg Neurol*, vol. 64, no. discussion 545, pp. 542-545, 2005.
- [152] A. Montinaro, C. Gianfreda and P. Proto, "Equine pericardium for dural grafts: clinical results in 200 patients," *J Neurosurg Sci*, vol. 51, pp. 17-19, 2007.
- [153] A. Foy, C. Giannini and C. Raffel, "Allergic reaction to a bovine dura substitute following spinal cord untethering," *J Neurosurg Pediatr*, vol. 1, pp. 167-169, 2008.
- [154] F. Esposito, P. Cappabianca, M. Fusco and e. al, "Collagen-only biomatrix as a novel dural substitute: examination of the efficacy, safety and outcome clinical experince on a series of 208 patients," *Clin Neural Neurosurg*, vol. 110, pp. 343-351, 2008.
- [155] R. Collins, D. Christiansen, G. Zazanis and F. Silver, "Use of collagen film as a dural substitute: preliminary animal studies," *J Biomed Mater Res*, vol. 25, pp. 267-276, 1991.
- [156] F. San-Galli, C. Deminiere, J. Guerin and M. Rabaud, "Use of a biodegradable elastin-fibrin material, Neuroplast, as a dural substitute," *Biomaterials*, vol. 17, pp. 1081-1085, 1996.
- [157] J. Sherman, N. Pouratian, D. Okonkwo, J. J. Jane and E. Laws, "Reconstruction of the sellar dura in transphenoidal surgery using an expanded polytetrafluoroethylene dural substitute," *Surg Neurol*, vol. 69, pp. 73-76, 2008.
- [158] T. Kawaguchi, K. Hosoda, Y. Shibata and J. Koyama, "Expand polytetrafluoroethylene membrane for prevention of adhesions in patients undergoing external decompression and subsequesnt cranioplasty," *Neurol Med Chir*, vol. 43, pp. 320-323, 2003.
- [159] A. Vakis, D. Koutentakis, D. Karabetsos and G. Kalostos, "Use of polytetrafluorotheylene dural substitute as adhesion preventive material during craniectomies," *Clin Neurol Neurosurg*, vol. 108, pp. 798-802, 2006.
- [160] B. Kundu, R. Rajkhowa, S. Kundu and X. Wang, "Silk fibroin biomaterials for tissue regenerations," *Advanced Drug Delivery Reviews*, vol. 65, no. 4, pp. 457-470, 2013.
- [161] D. Kim, W. Eum, S. Jang, J. Park, D.-H. Heo, S.-H. Sheen, H.-R. Lee, H. Kweon, S.-W. Kang, K.-G. Lee, S.-Y. Cho, H.-J. Jin, Y.-J. Cho and S. Choi, "A transparent artificial dura mater made of silk fibroin as an inhibitor of inflammation in craniotomized rats," *J Neurosurg*, vol. 114, pp. 485-490, 2011.
- [162] S. Otano, M. Sacks and T. Malinin, "Mechanical behavior of human dura mater," *Transcripts from the BED Bioeng Conf ASME*, vol. 29, pp. 329-330, 1995.
- [163] M. Sacks, M. Jimenez Hamann, S. Otano-Lata and T. Malinin, "Local mechanical anisotrophy in human cranial dura mater allografts," *J Biomech Eng*, vol. 120, pp. 541-544, 1998.
- [164] E. Ahmed, "Hydrogel: preparation, characterization and applications: a review," *Journal of Advanced Research*, vol. 6, no. 2, pp. 105-121, 2015.

- [165] M. Cooke, Y. Wang, C. Morshead and M. Shoichet, "Controlled epi-cortical delivery of epidermal growth factor for the stimulation of endogenous neural stem cell proliferation in stroke-injured brain," *Biomaterials*, vol. 32, no. 24, pp. 5688-5697, 2011.
- [166] Y. Wang, M. Cooke, C. Morshead and M. Shoichet, "Hydrogel delivery of erythropoietin to the brain for endogenous stem cell stimulation after stroke injury," *Biomaterials*, vol. 33, pp. 2681-2692, 2012.
- [167] D. Cook, C. Nguyen, H. Chun, I. Llorento, A. Chiu, M. Machnicki, T. Zarembinski and S. Carmichael, "Hydrogel-delivered brain-derived neurotrophic factor promotes tissue repair and recovery after stroke," *Journal of Cerebral Blood Flow and Metabolism*, vol. 37, no. 3, pp. 1030-1045, 2017.
- [168] B. Song, J. Song, S. Zhang, M. Anderson, Y. Ao, C.-Y. Yang, T. Deming and M. Sofroniew, "Sustained local delivery of bioactive nerve growth factor in the central nervous system via tunable diblock copolypeptide hydrogel depots," *Biomaterials*, vol. 33, no. 35, pp. 9105-9116, 2012.
- [169] H. Ghuman, A. Massensini, J. Donnelly, S.-M. Kim, C. Medberry, S. Badylak and M. Modo, "ECM hydrogel for the treatment of stroke: characterization of the host cell infiltrate," *Biomaterials*, vol. 91, pp. 166-181, 2016.
- [170] D. Klemm, B. Heublein, H. Fink and A. Bohn, "Cellulose: Fascinating biopolymer and sustainable raw material," *Angew Chem Int Edit*, vol. 44, pp. 3358-3393, 2005.
- [171] M. Koyama, W. Helbert, T. Imai, J. Sugiyama and B. Henrissar, "Parallel-up structure evidences the molecular directionality during biosynthesis of bacterial cellulose," *Proc Natl Acad Sci*, vol. 94, pp. 9091-9095, 1997.
- [172] K. Pandey, "A study of chemical structure of soft and hardwood and wood polymers by FTIR spectroscopy," *Journal of Applied Polymer Science*, vol. 71, no. 12, pp. 1969-1975, 1999.
- [173] R. Dudley, C. S. P. Fyfe, Y. Deslandes, G. Hamer and R. Marchessault, "High-resolution  $^{13}\text{C}$  CP/MAS NMR spectra of solid oligomers and the structure of cellulose II," *J Am Chem Soc*, vol. 105, no. 8, pp. 2469-2472, 1983.
- [174] L. Huang, X. Chen, T. Nguyen and e. al, "Nano-cellulose 3D-networks as controlled-release drug carriers," *J Mater Chem B*, vol. 23, no. 1, pp. 2976-2984, 2013.
- [175] Y. Yang, S. Park, J. Hwang, Y. Pyun and Y. Kim, "Cellulose production by *Acetobacter xylinum* BRC5 under agitated condition," *Journal of Fermentation and Bioengineering*, vol. 85, no. 3, pp. 312-317, 1998.
- [176] M. Iguchi, S. Yamanaka and A. Budhiono, "Bacterial cellulose - a masterpiece of nature's arts," *J Mater Sci*, vol. 35, pp. 261-270, 2000.
- [177] T. Maneerung, S. Tokura and R. Rujiravanit, "Impregnation of silver nanoparticles into bacterial cellulose for antimicrobial wound dressing," *Carbohydrate Polymers*, vol. 72, pp. 43-51, 2008.

- [178] L. Fu, J. Zhang and G. Yang, "Present status and applications for bacterial cellulose-based materials for skin tissue repair," *Carbohydrate Polymers*, vol. 92, no. 2, pp. 1432-1442, 2013.
- [179] P. Ross, R. Mayer and M. Benziman, "Regulation of cellulose synthesis in acetobacter-xylinum by cyclic diguanylic acid," *Nature*, vol. 325, pp. 279-281, 1987.
- [180] A. Silvestre, C. Freire and C. Nero, "Do bacterial cellulose membranes have potential in drug-delivery systems?," *Expert Opin Drug Deliv*, vol. 11, no. 7, pp. 1113-1124, 2014.
- [181] K. Keegstra, "Plant cell walls," *Plant Physiol*, vol. 154, pp. 483-486, 2010.
- [182] H. Barud, J. Souza, D. Santos, M. Crespi, C. Ribeiro, Y. Messaddeq and S. Ribeira, "Bacterial cellulose/poly(3-hydroxybutyrate) composite membranes," *Carbohydr Polym*, vol. 83, pp. 1279-1284, 2011.
- [183] J. Yang, X. Liu, L. Huang and D. Sun, "Antibacterial properties of novel bacteria cellulose nanofiber containing silver nanoparticles," *Chinese Journal of Chemical Engineering*, vol. 21, no. 12, pp. 1419-1424, 2013.
- [184] W. Czaja, D. Young, M. Kawecki and R. J. Brown, "The future prospects of microbial cellulose in biomedical applications," *Biomacromolecules*, vol. 8, no. 1, 2007.
- [185] G. Smit, J. Kijne and B. Lugtenberg, "Correlation between extracellular fibrils and attachment of *Rhizobium leguminosarum* to pea root hair tips," *J Bacteriol*, vol. 168, pp. 821-827, 1986.
- [186] M. Islam, M. Ullah, S. Khan, N. Shah and J. Park, "Strategies of cost-effective and enhanced production of bacterial cellulose," *Int J Biol Macromol*, pp. 1166-1173, 2017.
- [187] H. El-Saied, A. Basta and R. Gobran, "Research progress in friendly environmental technology for the production of cellulose products (bacterial cellulose and its application)," *Polym-Plast Technol*, vol. 43, pp. 797-820, 2004.
- [188] A. Jozala, R. Pertile, C. dos Cantos, V. Santos-Ebinuma, M. Seckler, F. Gama, P. Jr and A., "Bacterial cellulose production by *Gluconacetobacter xylinus* by employing alternative culture media," *Appl Microbial Biotechnol*, vol. 99, pp. 1181-1190, 2015.
- [189] K. Ji, W. Wang, B. Zeng, S. Chen, Q. Zhao, Y. Chen, G. Li and T. Ma, "Bacterial cellulose synthesis mechanism of facultative anaerobe *Enterobacter* sp. FY-07," *Scientific Reports*, vol. 6, p. 21063, 2016.
- [190] S. Lin, C. Hsu, L. Chen and H. Chen, "Adding enzymatically modified gelatin to enhance the rehydration abilities and mechanical properties of bacterial cellulose," *Food Hydrocolloid*, vol. 23, pp. 2195-2203, 2009.
- [191] Z. Yan, S. Chen, H. Wang, B. Wang, C. Wang and J. Jiang, "Cellulose synthesized by *Acetobacter xylinum* in the presence of multi-walled carbon nanotubes," *Carbohydr Res*, vol. 343, pp. 73-80, 2008.
- [192] N. Shah, M. Ul-Islam, W. Khatkhat and J. Park, "Overview of bacterial cellulose composites: a multipurpose advanced material," *Carbohydr Polym*, vol. 98, pp. 1585-1598, 2013.

- [193] D. Recouvreux, C. Rambo, F. Berti, C. Carminatti, R. Antonio and L. Porto, "Novel three-dimensional cocoon-like hydrogels for soft tissue regeneration," *Mat Sci Eng C-Mater*, vol. 31, pp. 151-157, 2011.
- [194] K. Cheng, J. Catchmark and A. Demirci, "Effect of different additives on bacterial cellulose production by *Acetobacter xylinum* and analysis of material property," *Cellulose*, vol. 16, pp. 1033-1045, 2009.
- [195] O. Shezad, S. Khan, T. Khan and J. Park, "Physicochemical and mechanical characterization of bacterial cellulose produced with an excellent productivity in static conditions using a simple fed-batch cultivation strategy," *Carbohydrate Polymers*, vol. 82, pp. 173-180, 2010.
- [196] D. Klemm, D. Schumann, U. Udhardt and S. Marsch, "Bacterial synthesized cellulose - artificial blood vessels for microsurgery," *Prog Polym Sci*, vol. 26, pp. 1561-1603, 2001.
- [197] H. Backdahl, G. Helenius, A. Bodin, U. Nannmark, B. Johansson, B. Risberg and P. Gatenholm, "Mechanical properties of bacterial cellulose and interactions with smooth muscle cells," *Biomaterials*, vol. 27, pp. 2141-2149, 2006.
- [198] J. Camarero, B. Hackel, J. de Yoreo and A. Mitchell, "A new method for the preparation of peptide C-terminal alpha-thioesters compatible with Fmoc-solid-phase peptide synthesis," *Peptide Revolution: Genomics, Proteomics and Therapeutics*, pp. 111-112, 2004.
- [199] P. White, R. Steinauer, S. Barthelemy and B. Dorner, "Pseudoproline dipeptides in Fmoc-solid phase peptide synthesis," *J Pept Sci*, vol. 10, p. 151, 2004.
- [200] F. Berti, C. Rambo, P. Dias and L. Porto, "Nanofiber density determines endothelial cell behaviour on hydrogel matrix," *Materials Science and Engineering: C*, vol. 33, pp. 4684-4691, 2013.
- [201] X. Liu, Q. Sun, H. Wang, L. Zhang and J. Wang, "Microspheres of corn protein, zein, for an ivermectin drug delivery system," *Biomaterials*, vol. 26, pp. 109-115, 2005.
- [202] D. Yu, X. Li, X. Wang, J. Yang, S. Annie Bligh and G. Williams, "Nanofibers fabricated using triaxial electrospinning as zero order drug delivery systems," *Applied Materials and Interfaces*, vol. 7, pp. 18891-18897, 2015.
- [203] Y. Perrie and T. Rades, "Controlling drug delivery," in *FASTTrack: Pharmaceuticals - Drug Delivery and Targeting*, Pharmaceutical Press, 2012, pp. 1-24.
- [204] M. Biondi, F. Ungaro, F. Quaglia and P. Netti, "Controlled drug delivery in tissue engineering," *Advanced Drug Delivery Reviews*, vol. 60, pp. 229-242, 2008.
- [205] S. Yamanaka, K. Watanabe, N. Kitamura, M. Iguchi, S. Mitsunashi, Y. Nishi and M. Uryu, "The structure and mechanical properties of sheets prepared from bacterial cellulose," *Journal of Materials Science*, vol. 24, no. 9, pp. 3141-3145, 1989.
- [206] M. Kwak, J. Kim, J. Go, E. Koh, S. Song, H. Son, H. Kim, T. Yun, Y. Jung and D. Hwang, "Bacterial cellulose membrane produced by *Acetobacter* sp A10 for burn wound dressing applications," *Carbohyd Polym*, vol. 122, pp. 387-398, 2015.

- [207] A. Meftahi, R. Khajavi, A. Rashidi, M. Sattari, M. Yazdanshenas and M. Torabi, "The effects of cotton gauze coating with microbial cellulose," *Cellulose*, vol. 17, pp. 199-204, 2010.
- [208] J. Luan, J. Wu, Y. Zheng, W. Song, G. Wang, J. Guo and X. Ding, "Impregnation of silver sulfadiazine into bacterial cellulose for antimicrobial and biocompatible wound dressing," *Biomed Mater*, vol. 7, 2012.
- [209] B. Wei, G. Yang and F. Hong, "Preparation and evaluation of a kind of bacterial cellulose dry films with antimicrobial properties," *Carbohydr Polym*, vol. 84, pp. 533-538, 2011.
- [210] G. Yang, J. Xie, Y. Deng, Y. Bian and F. Hong, "Hydrothermal synthesis of bacterial cellulose/AgNPs composite: A "green" route for antibacterial application," *Carbohydrate Polymers*, vol. 87, pp. 2482-2487, 2012.
- [211] H. Barud, T. Regiani, R. Marques, W. Lustrri, Y. Messaddeq and S. Ribeiro, "Antimicrobial bacterial cellulose-silver nanoparticles composite membranes," *Journal of Nanomaterials*, pp. 1-8, 2011.
- [212] J. Fontant, A. Desouza, C. Fontana, I. Torriani, J. Moreschi, B. Gallotti, S. Desouza, G. Narcisco, J. Bichara and L. Farah, "Acetobacter cellulose pellicle as a temporary skin substitute," *Appl Biochem Biotech*, Vols. 24-5, pp. 253-264, 1990.
- [213] J. Wu, Y. Zheng, W. Song, J. Luan, X. Wen, Z. Wu, X. Chen, Q. Wang and S. Guo, "In situ synthesis of silver-nanoparticles/bacterial cellulose composites for slow-release antimicrobial wound dressing," *Carbohydrate Polymers*, vol. 102, pp. 762-771, 2014.
- [214] O. Saibuatong and M. Phisalaphong, "Novo aloe vera-bacterial cellulose composite film from biosynthesis," *Carbohydr Polym*, vol. 79, pp. 455-460, 2010.
- [215] N. Butchosa, C. Brown, P. Larsson, L. Berglund, V. Bulone and Q. Zhou, "Nanocomposites of bacterial cellulose nanofibers and chitin nanocrystals: fabrication, characterization and bacterial activity," *Green Chem*, vol. 15, pp. 3404-3413, 2013.
- [216] W. Shao, H. Liu, X. Liu, S. Wang, J. Wu, R. Zhang, H. Min and M. Huang, "Development of silver sulfadiazine loaded bacterial cellulose/sodium alginate composite films with enhanced antibacterial property," *Carbohydr Polym*, vol. 132, pp. 351-358, 2015.
- [217] J. Wang, Y. Wan and Y. Huang, "Immobilisation of heparin on bacterial cellulose-chitosan nano-fibres surfaces via the cross-linking technique," *Int Nanobiotechnol*, vol. 6, pp. 52-57, 2012.
- [218] E. Feldmann, J. Sundberg, B. Bobbili, S. Schwarz, P. Gatenholm and N. Rotter, "Description of a novel approach to engineer cartilage with porous bacterial nanocellulose for reconstruction of a human auricle," *Journal of Biomaterials Applications*, vol. 28, pp. 626-640, 2013.
- [219] L. Nimeskern, H. Avila, J. Sundberg and e. al, "Mechanical evaluation of bacterial nanocellulose as an implant material for ear cartilage replacement," *J Mech Behav Biomed Mater*, vol. 22, pp. 12-21, 2013.

- [220] A. Bodin, S. Concaro, M. Brittberg and P. Gatenholm, "Bacterial cellulose as a potential meniscus implant," *J Tissue Eng Regen M*, vol. 1, pp. 406-408, 2007.
- [221] S. Saska, H. Barud, A. Gaspar, R. Marchetto and S. M. Y. Ribeiro, "Bacterial cellulose-hydroxyapatite nanocomposites for bone regeneration," *IntJ Biomater*, vol. 2011, p. 175362, 2011.
- [222] Q. Shi, Y. Li, J. Sun, H. Zhang, L. Chen, B. Chen, H. Yang and Z. Wang, "The osteogenesis of bacterial cellulose scaffold loaded with bone morphogenetic protein-2," *Biomaterials*, vol. 33, pp. 6644-6649, 2012.
- [223] M. Zaborowska, A. Bodin, H. Backdahl, J. Popp, A. Golstein and P. Gatenholm, "Microporous bacterial cellulose as a potential scaffold for bone regeneration," *Acta Biomater*, vol. 6, pp. 2540-2547, 2010.
- [224] K. Zimmermann, J. LeBlanc, K. Sheets, R. Fox and P. Gatenholm, "Biomimetic design of a bacterial cellulose/hydroxyapatite nanocomposite for bone healing applications," *Mat Sci Eng C Mater*, vol. 31, pp. 43-49, 2011.
- [225] R. Mori, T. Nakai, K. Enomoto, Y. Uchio and K. Yoshino, "Increased antibiotic release from a bone cement containing bacterial cellulose," *Clinical Orthopaedics and Related Research*, vol. 469, pp. 600-606, 2011.
- [226] A. Barreiro, D. Recouvreux, D. Hotza, L. Porto and C. Rambo, "Sand dollar skeleton as templates for bacterial cellulose coating and apatite precipitation," *J Mater Sci*, vol. 45, pp. 5252-5256, 2010.
- [227] D. Ramani and T. Sastry, "Bacterial cellulose-reinforced hydroxyapatite functionalized graphene oxide: a potential osteoinductive composite," *Cellulose*, vol. 21, pp. 3585-3595, 2014.
- [228] S. Hutchens, R. Benson, B. Evans, C. Rawn and H. O'Neill, "A resorbable calcium-deficient hydroxyapatite hydrogel composite for osseous regeneration," *Cellulose*, vol. 16, pp. 887-898, 2009.
- [229] J. Ran, P. Jiang, S. Liu, G. Sun, P. Yan, X. Chen and H. Tong, "Constructing multi-component organic/inorganic composite bacterial cellulose-gelatin/hydroxyapatite double-network scaffold platform for stem cell-mediated bone tissue engineering," *Materials Science and Engineering C*, vol. 78, pp. 130-140, 2017.
- [230] G. Voicu, S.-I. Jinga, B.-G. Drosu and C. Busuioc, "Improvement of silicate cement properties with bacterial cellulose powder addition for applications in dentistry," *Carbohydrate Polymers*, vol. 174, pp. 160-170, 2017.
- [231] K. Kowalska-Ludwicka, J. Cala, B. Grobelski, D. Sygut, D. Jesionek-Kupnicka, M. Kolodziejczyk, S. Bielecki and Z. Pasiaka, "Modified bacterial cellulose tubes for regeneration of damaged peripheral nerves," *Arch Med Sci*, vol. 9, pp. 527-534, 2013.
- [232] E. Trovatti, N. Silva and I. e. a. Duarte, "Biocellulose membranes as supports for dermal release of lidocaine," *Biomacromolecules*, vol. 12, pp. 4162-4168, 2011.
- [233] N. Silva, I. Drumond, I. Almeida and e. al, "Topical caffeine delivery using biocellulose membranes: a potential innovative system for cellulite treatment," *Cellulose*, vol. 21, pp. 665-674, 2014.

- [234] N. Silva, A. Rodrigues, I. Almeida and e. al, "Bacterial cellulose membranes as transdermal delivery sytems for diclofenac: in vitro dissolution and permeation studies," *Carbohydr Polym*, vol. 106, pp. 264-269, 2014.
- [235] M. Amin, A. Abadi, N. Ahmad and e. al, "Bacterial cellulose film coating as drug delivery system: physiological, thermal and drug release properties," *Sains Malaysiana*, vol. 41, no. 5, pp. 561-568, 2012.
- [236] C. Lin and A. Metters, "Hydrogels in controlled release formulations: network design and mathematic modeling," *Advanced Drug Delivery Reviews*, vol. 58, pp. 1379-1408, 2006.
- [237] L. Kokai, H. Tan, S. Jhunjhunwala, S. Little, J. Frank and K. Marra, "Protein bioactivity and polymer orientation is affected by stabilizer incorporation for double-walled microspheres," *Journal of Control Release*, vol. 141, pp. 168-176, 2010.
- [238] R. Jain, N. Shah, A. Malick and C. Rhodes, "Controlled drug delivery by biodegradable poly(ester) devices: different preparative approaches," *Drug Development and Industrial Pharmacy*, vol. 24, no. 8, pp. 703-727, 1998.
- [239] T. Farahani, A. Entezami, H. Mobedi and M. Abtahi, "Degradation of poly(D,L-lactide-co-glycolide) 50:50 implant in aqueous medium," *Iranian Polymer Journal*, vol. 14, no. 8, pp. 753-763, 2005.
- [240] G. Crotts and T. Park, "Protein delivery from poly (lactic-co-glycolic acid) biodegradable microspheres: release kinetics and stability issues," *J Microencapsul*, vol. 15, pp. 699-713, 1998.
- [241] H. Makadia and S. Siegel, "Poly lactic-co-glycolic acid (PLGA) as biodegradable controlled drug delivery carrier," *Polymers (Basel)*, vol. 3, no. 3, pp. 1377-1397, 2012.
- [242] X. Ma, S. Oyamada, T. Wu, M. Robich, H. Wu, X. Wang, B. Buchholz, S. McCarthy, C. Bianchi, F. Sellke and R. Laham, "In vitro and in vivo degradation of poly(D,L-lactide-co-glycolide)/amorphous calcium phosphate copolymer coated on metal stents," *J Biomed Mater Res A*, vol. 96, no. 4, pp. 632-638, 2012.
- [243] R. Ansary and M. R. M. Awang, "Biodegradable Poly(D,L-lactic-co-glycolic acid)-based micro/nanoparticles for sustained release of protein drugs - a review," *Tropical Journal of Pharmaceutical Research*, vol. 13, no. 7, pp. 1179-1190, 2014.
- [244] E. Fournier, C. Passirani, C. Mntero-Menei and J. Benoit, "Biocompatibility of implantable synthetic polymeric drug carriers: focus on brain biocompatibility," *Biomaterials*, vol. 24, pp. 3311-3331, 2003.
- [245] S. Fredenberg, M. Wahlgren, M. Reslow and A. Axelsson, "The mechanisms of grud release in poly(lactic-co-glycolic acid) - based drug delivery systems - a review," *Int J Pharm*, vol. 415, no. 1-2, pp. 34-52, 2011.
- [246] M. van de Weert, W. Hennink and W. Jiskoot, "Protein instability in poly(lactic-co-glycolic acid) microparticles," *Pharmaceutical Research*, vol. 17, no. 10, pp. 1159-1167, 2000.

- [247] G. Jiang, B. Thanoo and P. DeLuca, "Effect of osmotic pressure in the solvent extraction phase on BSA release profile from PLGA microspheres," *Pharmaceutical development and technology*, vol. 7, no. 4, pp. 391-399, 2002.
- [248] S. Cohen, T. Yoshioka, M. Lucarelli, L. Hwang and R. Langer, "Controlled delivery systems for proteins based on poly(lactic/glycolic acid) microspheres," *Pharmaceutical Research*, vol. 8, no. 6, pp. 713-720, 1991.
- [249] J. Wu, X. Xie, Z. Zheng, G. Li, X. Wang and Y. Wang, "Effect of pH on polyethylene glycol (PEG)-induced silk microsphere formation for drug delivery," *Materials Science and Engineering C*, vol. 80, pp. 549-557, 2017.
- [250] R. Mehta, B. Thanoo and P. DeLuca, "Peptide containing microspheres from low molecular weight and hydrophilic poly(D,L-lactide-co-glycolide)," *J Control Release*, vol. 41, pp. 249-257, 1996.
- [251] X. Huang and C. Brazel, "On the importance and mechanisms of burst release in matrix controlled drug delivery systems," *Journal of Controlled Release*, vol. 73, pp. 121-136, 2001.
- [252] T. Morita, Y. Sakamura, Y. Horikiri, T. Suzuki and H. Yoshino, "Protein encapsulation into biodegradable microspheres by a novel S/O/W emulsion method using poly(ethylene glycol) as a protein micrization adjuvant," *Journal of Controlled Release*, vol. 69, no. 3, pp. 435-444, 2000.
- [253] A. Paillard-Giteau, V. Tran, O. Thomas, X. Garric, J. Coudane, S. Marchal, I. Chourpa, J. Benoit, C. Montero-Menei and M. Venier-Julienne, "Effect of various additives and polymers on lysozyme release from PLGA microspheres prepared by an s/o/w emulsion technique," *European Journal of Pharmaceutics and Biopharmaceutics*, vol. 75, no. 2, pp. 128-136, 2010.
- [254] R. Mundargi, S. Srirangarajan, S. Agnihotri, S. Patil, S. Ravindra, S. Setty and T. Aminabhavi, "Development and evaluation of novel biodegradable microspheres based on poly(D,L-lactide-co-glycolide) and poly(E-caprolactone) for controlled delivery of doxycycline in the treatment of human periodontal pocket: in vitro and in vivo studies," *Journal of Controlled Release*, vol. 119, no. 1, pp. 59-68, 2007.
- [255] H. Zhao, J. Gagnon and U. Hafeli, "Process and formulation variables in the preparation of injectable and biodegradable magnetic microspheres," *Biomgn Res Technol*, vol. 5, p. 2, 2007.
- [256] D. Novindri, I. Jaswir, M. Taher, F. Mohamed, H. Salleh, I. Noorbacha, F. Octavianti, W. Lestari, R. Hendri, H. Ahmad, K. Miyashita and A. Abdullah, "Fabrication of fucoxanthin-loaded microsphere (F-LM) by two steps double-emulsion solvent evaporation method and characterization of fucoxanthin before and after microencapsulation," *Oils and Fats*, vol. 65, no. 8, pp. 641-653, 2016.
- [257] S. Lin, K. Chen and H. Teng, "Functionality of protective colloids affecting the formation, size uniformity and morphology of drug-free PLA microspheres," *J Microencapsul*, vol. 15, pp. 383-390, 1998.

- [258] I. Grizzi, H. Garreau, S. Li and M. Vert, "Hydrolytic degradation of devices based on poly(DL-lactic acid) size dependence," *Biomaterials*, vol. 16, pp. 305-311, 1995.
- [259] H. Gasmi, F. Danede, J. Siepmann and F. Siepmann, "Does PLGA microparticle swelling control drug release? New insight based on single particle swelling studies," *Journal of Controlled Release*, vol. 213, pp. 120-127, 2015.
- [260] D. Ciombor, A. Jaklenec, A. Liu, C. Thanos, N. Rahman and P. Weston, "Encapsulation of BSA using a modified W/O/O emulsion solvent removal method," *Journal of Microencapsulation*, vol. 23, no. 2, pp. 183-194, 2006.
- [261] N. Rahman, Mathiowitz and E, "Localization of bovine serum albumin in double-walled microspheres," *Journal of controlled release*, vol. 94, pp. 163-175, 2004.
- [262] H. Tan and J. Ye, "Surface morphology and in vitro release performance of double-walled PLLA/PLGA microspheres entrapping a highly water-soluble drug," *Applied Surface Science*, vol. 255, pp. 353-356, 2008.
- [263] Lee, TH, J. Wang and C. Wang, "Double-walled microspheres for the sustained release of a highly water soluble drug: characterization and irradiation studies," *J Control Release*, vol. 83, no. 3, pp. 437-452, 2002.
- [264] A. Navaei, M. Rasoolian, A. Momeni, S. Emami and M. Rafienia, "Double-walled microspheres loaded with meglumine antimoniate: preparation, characterization and in vitro release study," *Drug Development and Industrial Pharmacy*, vol. 40, no. 6, pp. 701-710, 2014.
- [265] S. Bee, Z. Hamid, M. Mariatti, B. Yahaya, K. Lim, S. Bee and L. Sin, "Approaches to improve therapeutic efficacy of biodegradable PLA/PLGA microspheres: a review," *Polymer Reviews*, vol. 58, no. 3, pp. 495-536, 2018.
- [266] C. Xiao, X. Shen and L. Tao, "Modified emulsion solvent evaporation method for fabricating core-shell microspheres," *International Journal of Pharmaceutics*, vol. 452, pp. 227-232, 2013.
- [267] K. Pekarek, J. Jacob and E. Mathiowitz, "Double-walled polymer microspheres for controlled drug release," *Letters to Nature*, vol. 367, pp. 258-260, 1994.
- [268] C. Srinivasan, Y. Katare, T. Muthumaran and A. Panda, "Effect of additives on encapsulation efficiency, stability and bioactivity of entrapped lysozyme from biodegradable polymer particles," *Journal of Microencapsulation*, vol. 22, no. 2, pp. 127-138, 2005.
- [269] F. Ungaro, M. Biondi, I. d'Angelo, L. Indolfi, F. Quaglia, P. Netti and M. La Rotonda, "Microsphere-integrated collagen scaffolds for tissue engineering: effect of microsphere formulation and scaffold properties on protein release kinetic," *J Control Release*, vol. 113, pp. 128-136, 2006.
- [270] E. Tenorio-Neto, D. de Souza Lima, M. Guilherme, Lima-Tenorio, MK, D. Scariot, C. Nakamura, M. Kunita and A. Rubira, "Synthesis and drug release profile of a dual-responsive poly(ethylene glycol) hydrogel nanocomposite," *RSC Advances*, vol. 7, p. 27637, 2017.

- [271] E. da Silva, M. Guilherme, F. Garcia, C. Nakamura, L. Cardozo-Filho, C. Alonso, A. Rubira and M. Kunita, "Drug release profile and reduction in the in vitro burst release from pectin/HEMA hydrogel nanocomposites crosslinked with titania," *RSC Advances*, vol. 6, p. 19060, 2016.
- [272] Kamisetti and RR, "Formulation and in vitro evaluation of modified release oral hydrogel driven drug delivery systems of diethylcarbamazine citrate," *RGUHS Journal of Pharmaceutical Sciences*, vol. 5, no. 2, pp. 41-46, 2015.
- [273] W. Low, M. Kenward, M. Amin and C. Martin, "Ionically crosslinked chitosan hydrogels for the controlled release of antimicrobial essential oils and metal ions for wound management applications," *Medicines (Basel)*, vol. 3, no. 1, p. 8, 2016.
- [274] Z. Rao, R. Chen, H. Zhu, Y. Li, Y. Liu and J. Hao, "Carboxylic terminated thermo-responsive copolymer hydrogel and improvement in peptide release profile," *Materials (Basel)*, vol. 11, no. 3, p. 338, 2018.
- [275] P. Paradiso, R. Galante, L. Santos, A. C. R. Alves de Matos, A. Serro and B. Saramaggo, "Comparison of two hydrogel formulations for drug release in ophthalmic lenses," *J Biomed Mater Res B Appl Biomater*, vol. 102, no. 6, pp. 1170-1180, 2014.
- [276] K. Campbell, D. Hadley, D. Kukis and E. Silva, "Alginate hydrogels allow for bioactive and sustained release of VEGF-C and VEGF-D for lymphangiogenic therapeutic applications," *PLoS ONE*, vol. 12, no. 7, p. e0181484, 2017.
- [277] S. Bashir, Y. N. S. Teo, S. Ramesh and K. Ramesh, "pH responsive N-succinyl chitosan/Poly(acrylamide-co-acrylic acid) hydrogels and in vitro release of 5-fluorouracil," *PLoS ONE*, vol. 12, no. 7, p. e0179250, 2017.
- [278] R. S. A. Elhayek, P. Jarrett, S. Gueddez and C. Rosales, "Sustained release of bevacizumab from hydrogel depots for intravitreal injections," *Investigative Ophthalmology and Visual Science*, vol. 55, p. 5264, 2014.
- [279] H. Park, J. Temenoff, Y. Tabata, A. Caplan and A. Mikos, "Injectable biodegradable hydrogel composited for rabbit marrow mesenchymal stem cell and growth factor delivery for cartilage tissue engineering," *Biomaterials*, vol. 28, pp. 3217-3227, 2007.
- [280] A. Shamloo, M. Sarmadi, Z. Aghababaie and M. Vossoughi, "Accelerated full-thickness wound healing via sustained bFGF delivery based on a PVA/chitosan/gelatin hydrogel incorporating PCL microspheres," *International Journal of Pharmaceutics*, vol. 537, pp. 278-289, 2018.
- [281] X. Cao and M. S. Shoichet, "Delivering neuroactive molecules from biodegradable microspheres for application in central nervous system disorders," *Biomaterials*, vol. 20, pp. 329-339, 1999.
- [282] E. Tan, R. Lin and C. Wang, "Fabrication of double-walled microspheres for the sustained release of doxorubicin," *Journal of Colloid and Interface Science*, vol. 291, pp. 135-143, 2005.
- [283] J. Schindelin, I. Arganda-Carreras, E. Frise, V. Kaynig, M. Longair, T. Pietzsch, A. Preibisch, C. Rueden, S. Saalfeld, B. Schmid, J. Tinevez, D. White, V. Hartenstein, K.

- Eliceiri, P. Tomancak and A. Cardona, "Fiji: an open-source platform for biological-image analysis," *Nature Methods*, vol. 9, pp. 676-682, 2012.
- [284] Y. Wan, H. Luo, F. He, H. Liang, Y. Huang and X. Li, "Mechanical, moisture absorption, and biodegradation behaviours of bacterial cellulose fibre-reinforced starch biocomposites," *Composites Science and Technology*, vol. 69, pp. 1212-1217, 2009.
- [285] G. Schliecker, C. Schmidt, S. Fuchs, R. Wombacher and T. Kissel, "Hydrolytic degradation of poly(lactide-co-glycolide) films: effect of oligomers on degradation rate and crystallinity," *Int J Pharm*, vol. 266, pp. 39-49, 2003.
- [286] C. Witt, "Morphological characterization of microspheres, films and implants prepared from poly(lactide-co-glycolide) and ABA triblock copolymers: Is the erosion controlled by degradation, swelling or diffusion?," *Eur J Pharm Biopharm*, vol. 51, pp. 171-181, 2001.
- [287] I. Grizzi, H. Garreau, S. Li and M. Vert, "Hydrolytic degradation of devices based on poly(D,L-lactic acid) size dependence," *Biomaterials*, vol. 16, pp. 305-311, 1995.
- [288] A. Determan, B. Trewyn, V. Lin, M. Nilsen-Hamilton and B. Narasimhan, "Encapsulation, stabilization and release of BSA-FITC from polyanhydride microspheres," *Journal of controlled release*, vol. 100, pp. 97-109, 2004.
- [289] S. Ravi, K. Peh, Y. Darwis, B. Murthy, T. Raghu Raj Singh and C. Mallikarjun, "Development and characterization of polymeric microspheres for controlled release protein loaded drug delivery system," *Indian Journal of Pharmaceutical Sciences*, vol. 70, no. 3, pp. 303-309, 2008.
- [290] G. Wu, L. Chen, H. Li, C. Deng and X. Chen, "Comparing microspheres with different internal phase of polyelectrolyte as local drug delivery system for bone tuberculosis therapy," *BioMed Research International*, 2014.
- [291] J. Madan, V. Kadam, S. Bandavane and K. Dua, "Formulation and evaluation of microspheres containing ropinirole hydrochloride using biodegradable polymers," *Asian Journal of Pharmaceutics*, vol. 7, pp. 184-188, 2013.
- [292] R. Ansary, M. Rahman, A. Mohamed, K. Haliza, H. Hazrina, M. Farahidah, D. Abd and K. Yunus, "Preparation, characterization and in vitro release study of BSA-loaded double-walled glucose-poly(lactide-co-glycolide) microspheres," *Archives of Pharmacal Research*, vol. 39, no. 9, pp. 1242-1256, 2016.
- [293] A. Ding, L. Teng, Y. Zhou, P. Chen and W. Nie, "Synthesis and characterization of bovine serum albumin-loaded microspheres based on star-shaped PLLA with a xylitol core and their drug release behaviours," *Polym Bull*, vol. 75, pp. 2917-2931, 2018.
- [294] T. Kemala, E. Budiarto and B. Soegiyono, "Preparation and characterization of microspheres based on blend of poly(lactic acid) and poly( $\epsilon$ -caprolactone) with poly(vinyl alcohol) as emulsifier," *Arabian Journal of Chemistry*, vol. 5, no. 1, pp. 103-108, 2012.
- [295] Q. Xu, S. Chin, C. Wang and D. Pack, "Mechanism of drug release from double-walled PDLA(PLGA) microspheres," *Biomaterials*, vol. 34, no. 15, pp. 3902-3911, 2013.

- [296] L. Kokai, A. Ghaznavi and K. Marra, "Incorporation of double-walled microspheres into polymer nerve guides for the sustained delivery of glial cell line-derived neurotrophic factor," *Biomaterials*, vol. 31, pp. 2313-2322, 2010.
- [297] Y. Li, S. Wang, R. Huang, Z. Huang, B. Hu, W. Zheng, G. Yang and X. Jiang, "Evaluation of the effect of the structure of bacterial cellulose on full thickness skin wound repair on a microfluidic chip," *Biomacromolecules*, vol. 16, no. 3, pp. 780-789, 2015.
- [298] T. Hoare and D. Kohane, "Hydrogels in drug delivery: progress and challenges," *Polymer*, vol. 49, no. 8, pp. 1993-2007, 2008.
- [299] M. Amin, N. Ahmad, N. Halib and I. Ahmad, "Synthesis and characterization of thermo- and pH- responsive bacterial cellulose/acrylic acid hydrogels for drug delivery," *Carbohydrate Polymers*, vol. 88, pp. 465-473, 2012.
- [300] C. Brazel and N. Peppas, "Mechanisms of solute and drug transport in relaxing, swellable, hydrophilic glassy polymers," *Polymer*, vol. 40, pp. 3383-3398, 1999.
- [301] H. Ichikawa and Y. Fukumori, "A novel positively thermosensitive controlled-release microcapsule with membrane of nano-sized poly (N-isopropylacrylamide) gel dispersed in ethylcellulose matrix," *Journal of controlled release*, vol. 63, no. 1-2, pp. 107-119, 2000.
- [302] R. Zarzycki, Z. Modrzejewska and K. Nawrotek, "Drug release from hydrogel matrices," *Ecological Chemistry and Engineering*, vol. 17, no. 2, pp. 117-136, 2010.
- [303] K. Gelin, A. Bodin, P. Gatenholm, A. Mihranyan, K. Edwards and M. Stromme, "Characterization of water in bacterial cellulose using dielectric spectroscopy and electron microscopy," *Polymer*, vol. 48, pp. 7623-7631, 2007.
- [304] F. Jiang, T. Huang, C. He, H. Brown and H. Wang, "Interactions affecting the mechanical properties of acromolecular microsphere composite hydrogels," *The Journal of Physical Chemistry*, vol. 117, pp. 13679-13687, 2013.
- [305] B. Devrim and A. Bozkur, "Preparation and evolution of double-walled microparticles prepared with a modified water-in-oil-in-oil-in-water (w1/o/o/w3) method," *Journal of Microencapsulation*, vol. 30, no. 8, pp. 741-754, 2013.
- [306] F. Cui, D. Cun, A. Tao, M. Yang, K. Shi, M. Zhao and Y. Guan, "Preparation and characterization of melittin-loaded poly (DL-lactic acid) or poly (DL-lactic-co-glycolic acid) microspheres made by the double emulsion method," *J Control Release*, vol. 107, no. 2, pp. 310-319, 2005.
- [307] Y. Yang, H. Chia and T. Chung, "Effect of preparation temperature on the characteristics and release profiles of PLGA microspheres containing protein fabricated by double-emulsion solvent extraction/evaporation method," *Journal of Controlled Release*, vol. 69, no. 1, pp. 81-96, 2000.
- [308] B. Connor and M. Dragunow, "The role of neuronal growth factors in neurodegenerative disorders of the human brain," *Brain Research Reviews*, vol. 27, pp. 1-39, 1998.

- [309] Lee, KB, S. Lim, K. Kim, K. Kim, Y. Kim, W. Chang, J. Yeom, T. Kim and B. Hwang, "Six-month functional recovery of stroke patients: a multi-time-point study," *Int J Rehabil Res*, vol. 38, no. 2, pp. 173-180, 2015.
- [310] M. Protasoni, S. Sangiorgi, A. Cividini and e. al, "The collagenic architecture of human dura mater," *J Neurosurg*, vol. 114, pp. 1723-1730, 2011.
- [311] K. Deng, X. Ye, Y. Yang, M. Liu, A. Ayyad, Y. Zhao, Y. Yuyu, J. Zhao and T. Xu, "Evaluation of efficacy and biocompatibility of a new absorbable synthetic substitute as a dural onlay graft in a large animal model," *Neurological Research*, vol. 38, no. 9, pp. 199-808, 2016.
- [312] K. Yamata, S. Mryamoto, M. Takayama and e. al, "Clinical application of a new bioabsorbable artificial dura mater," *J Neurosurg*, vol. 96, pp. 731-735, 2002.
- [313] H. Kawai, I. Nakagawa, F. Nishimaura, Y. Motoyama, Y. Park, M. Nakamura, H. Nakase, S. Suzuki and Y. Ikada, "Effectiveness of a new gelatin sealant system for dural closure," *Neurological Research*, vol. 36, no. 10, pp. 866-872, 2014.
- [314] S. Bielecki, A. Krystynowicz, M. Turkiewicz and H. Kalinowska, "Bacterial Cellulose," *WILEY-VCH*, 2005.
- [315] N. Sunagawa, T. Fujiwara, T. Yoda, S. Kawano, Y. Satoh, M. Yao, K. Tajima and T. Dairi, "Cellulose complementing factor (Ccp) is a new member of the cellulose synthase complex (terminal complex) in *Acetobacter xylinum*," *Journal of Biosciences and Bioengineering*, vol. 115, no. 6, pp. 607-612, 2013.
- [316] S. Zang, Q. Zhuo, X. Chang, G. Qiu, Z. Wu and G. Yang, "Study of osteogenic differentiation of human adipose-derived stem cells (HASCs) on bacterial cellulose," *Carbohydr Polym*, vol. 104, pp. 158-165, 2014.
- [317] G. Helenius, H. Backdahl, A. Bodin, U. Nannmark, P. Gatenholm and B. Risberg, "In vivo biocompatibility of bacterial cellulose," *J Biomed Mater Res A*, vol. 76A, pp. 431-438, 2006.
- [318] C. Zhu, F. Li, X. Zhou, L. Lin and T. Zhang, "Kombucha-synthesized bacterial cellulose: Preparation, characterization, and biocompatibility evaluation," *J Biomed Mater Res A*, vol. 102, pp. 1548-1557, 2014.
- [319] M. Scherner, S. Reutter, D. Klemm, A. Sterner-Kock, M. Guschlbauer, T. Richter, G. Langebartels, N. Madershahian, T. Wahlers and J. Wippermann, "In vivo application of tissue-engineered blood vessels of bacterial cellulose as small arterial substitutes: proof of concept," *J Surg Res*, vol. 189, pp. 340-347, 2014.
- [320] T. Miyamoto, S. Takahashi, Ito, H, H. Inagaki and Y. Noishiki, "Tissue biocompatibility of cellulose and its derivatives," *J Biomed Mater Res*, vol. 23, pp. 125-133, 1989.
- [321] M. Risbud, S. Bhargava and R. Bhonde, "In vivo biocompatibility evaluation of cellulose macrocapsules for islet immunoisolation: implications of low molecular weight cut-off," *J Biomed Mater Res*, vol. 66, pp. 86-92, 2003.

- [322] R. Pertile, S. Moreira, R. Gil da Costa, A. Correia, L. Guardao, F. Gartner, M. Vilanova and M. Gama, "Bacterial cellulose: long-term biocompatibility studies," *Journal of Biomaterials: Science Polymer Edition*, vol. 23, pp. 1339-1354, 2012.
- [323] F. Andrade, N. Alexandre, I. Amorim, F. Gartner, A. Mauricio, A. Luis and M. Gamal, "Studies on the biocompatibility of bacterial cellulose," *Journal of Bioactive and Comptable Polymer*, vol. 28, pp. 97-112, 2013.
- [324] A. Bodin, S. Bharadwaj, S. Wu, P. Gatenholm, A. Atala and Y. Zhang, "Tissue-engineered conduit using urine-derived stem cells seeded bacterial cellulose polymer in urinary reconstruction and diversion," *Biomaterials*, vol. 31, no. 34, pp. 8889-8901, 2010.
- [325] H. Mohammadi, D. Boughner, L. Millon and W. Wan, "Design and simulation of a poly(vinyl alcohol)-bacterial cellulose nanocomposite mechanical aortic heart valve prosthesis," *Proc Inst Mech Eng H*, vol. 223, pp. 697-711, 2009.
- [326] E. Neto and J. Dolci, "Nasal septal perforation closure with bacterial cellulose in rabbits," *Braz J Otorhinolar*, vol. 76, pp. 442-449, 2010.
- [327] L. Salata, G. Craig and L. Brook, "In-vivo evaluation of a new membrane (Gengiflex(R)) for guided bone regeneration (Gbr)," *J Dent Res*, vol. 74, p. 825, 1995.
- [328] L. Nimeskern, H. Martinez Avila, J. Sundberg, P. Gatenholm, R. Muller and K. Stok, "Mechanical evaluation of bacterial nanocellulose as an implant material for ear cartilage replacement," *J Mech Behav Biomed*, vol. 22, pp. 12-21, 2013.
- [329] J. Kucinska-Lipka, I. Gubanska and H. Janik, "Bacterial cellulose in the field of wound healing and regenerative medicine of skin: recent trends and future perspectives," *Polymer Buletin*, vol. 72, pp. 2399-2419, 2015.
- [330] W. Czaja, A. Krystynowicz, S. Bielecki and R. Brown, "Microbial cellulose - the natural power to heal wounds," *Biomaterials*, vol. 27, pp. 145-151, 2006.
- [331] L. Fu, J. Zhang and G. Yang, "Present status and applications of bacterial cellulose-based materials for skin tissue repair," *Carbohyd Polym*, vol. 92, pp. 1432-1442, 2013.
- [332] A. Engler, S. Sen, H. Sweeney and D. Discher, "Matrix elasticity directs stem cell lineage specification," *Cell*, vol. 126, pp. 677-689, 2006.
- [333] T. Stumpf, R. Pertile, C. Rambo and L. Porto, "Enriched glucose and dextrin mannitol-based media modulates fibroblast behavior on bacterial cellulose membranes," *Mat Sci Eng C-Mater*, vol. 33, pp. 4739-4745, 2013.
- [334] J. Yang, X. Lv, S. Chen, Z. Li, C. Feng, H. Wang and Y. Xu, "In situ fabrication of a microporous bacterial cellulose/potato starch composite scaffold with enhanced cell compatibility," *Cellulose*, vol. 21, pp. 1823-1835, 2014.
- [335] H. Orelma, L. Morales, L. Johansson, I. Hoeger, I. Filpponen, C. Castro, O. Rojas and J. Laine, "Affibody conjugation onto bacterial cellulose tubes and bioseparation of human serum albumin," *Rsc Adv*, vol. 4, pp. 51440-51450, 2014.
- [336] H. Barud, H. Barud, M. Cavicchioli, T. do Amaral, O. de Oliveira, D. P. A. Santos, F. Celes, V. Borges, C. de Oliveira, P. de Oliveira, R. Furtado, D. Tavares and S. Ribeiro,

- "Preparation and characterization of a bacterial cellulose/silk fibroin sponge scaffold for tissue regeneration," *Carbohydr Polym*, vol. 128, pp. 41-51, 2015.
- [337] C. Gao, Y. Wan, C. Yang, K. Dai, T. Tang, H. Luo and J. Wang, "Preparation and characterization of bacterial cellulose sponge with hierarchical pore structure as tissue engineering scaffold," *J Porous Mat*, vol. 18, pp. 139-145, 2011.
- [338] I. Jipa, L. Dobre, M. Stroescu, A. Stoica-Guzun, S. Jinga and T. Dobre, "Preparation and characterization of bacterial cellulose-poly(vinyl alcohol) films with antimicrobial properties," *Mater Lett*, vol. 66, pp. 125-127, 2012.
- [339] G. Yang, J. Xie, F. Hong, Z. Cao and X. Yang, "Antimicrobial activity of silver nanoparticle impregnated bacterial cellulose membrane: Effect of fermentation carbon sources of bacterial cellulose," *Carbohydr Polym*, vol. 87, pp. 839-845, 2012.
- [340] L. Maria, A. Santos, P. Oliveira, A. Valle, H. Barud, Y. Messaddeq and S. Ribeiro, "Preparation and antibacterial activity of silver nanoparticles impregnated in bacterial cellulose," *Polimeros*, vol. 20, pp. 72-77, 2010.
- [341] F. Jebel and H. Almasi, "Morphological, physical, antimicrobial and release properties of ZnO nanoparticles loaded bacterial cellulose films," *Carbohydr Polym*, vol. 149, pp. 8-19, 2016.
- [342] F. Andrade, R. Costa, L. Domingues, R. Soares and M. Gama, "Improving bacterial cellulose for blood vessel replacement: Functionalization with a chimeric protein containing a cellulose-binding module and an adhesion peptide," *Acta Biomater*, vol. 6, pp. 4034-4041, 2010.
- [343] R. Pertile, S. Moreira, F. Andrade, L. Domingues and M. Gama, "Bacterial cellulose modified using recombinant proteins to improve neural and mesenchymal cell adhesion," *Biotechnol Prog*, 2011.
- [344] R. Pertile, F. Andrade, C. Alves and M. Gama, "Surface modification of bacterial cellulose by nitrogen-containing plasma for improved interaction with cells," *Carbohydr Polym*, vol. 82, pp. 692-698, 2010.
- [345] M. Rouabhia, J. Asselin, N. Tazi, Y. Messaddeq, D. Levinson and Z. Zhang, "Production of biocompatible and antimicrobial bacterial cellulose polymers functionalized by PGDC grafting groups and gentamicin," *ACS Appl Mater Inter*, vol. 6, pp. 1439-1446, 2014.
- [346] J. Wang, Y. Wan, H. Luo, C. Gao and Y. Huang, "Immobilization of gelatin on bacterial cellulose nanofibers surface via crosslinking technique," *Materials Science and Engineering C*, vol. 32, pp. 536-541, 2012.
- [347] J. Wang, Y. Wan, J. Han, X. Lei and T. G. C. Yan, "Nanocomposite prepared by immobilising gelatin and hydroxyapatite on bacterial cellulose nanofibers," *Micro Nano Lett*, vol. 6, pp. 133-136, 2011.
- [348] H. Luo, J. Zhang, G. Xiong and Y. Wan, "Evolution of morphology of bacterial cellulose scaffolds during early culture," *Carbohydr Polym*, vol. 111, pp. 722-728, 2014.

- [349] B. Fang, Y. Wan, T. Tang, C. Gao and K. Dai, "Proliferation and osteoblastic differentiation of human bone marrow stromal cells on hydroxyapatite/bacterial cellulose nanocomposite scaffolds," *Tissue Eng Pt A*, vol. 15, pp. 1091-1098, 2009.
- [350] S. Shi, S. Chen, X. Zhang, W. Shen, X. Li, W. Hu and H. Wang, "Biomimetic mineralization synthesis of calcium-deficient carbonate-containing hydroxyapatite in a three-dimensional network of bacterial cellulose," *J Chem Technol Biot*, vol. 84, pp. 285-290, 2009.
- [351] J. Li, Y. Wan, L. Li, H. Liang and J. Wang, "Preparation and characterization of 2,3-dialdehyde bacterial cellulose for potential biodegradable tissue engineering scaffolds," *Mat Sci Eng C Bio S*, vol. 29, pp. 1635-1642, 2009.
- [352] V. Kuzmenko, T. Kalogeropoulos, J. Thunberg, S. Johannesson, D. Hagg, P. Enoksson and P. Gatenholm, "Enhanced growth of neural networks on conductive cellulose-derived nanofibrous scaffolds," *Materials Science and Engineering C*, vol. 58, pp. 14-23, 2016.
- [353] M. Sureshkumar, D. Siswanto and C.-K. Lee, "Magnetic antimicrobial nanocomposite based on bacterial cellulose and silver nanoparticles," *Journal of Materials Chemistry*, vol. 20, pp. 6948-6955, 2010.
- [354] J. Gutierrez, S. Fernandes, I. Mondragon and A. Tercjak, "Multifunctional hybrid nanopapers based on bacterial cellulose and sol-gel synthesized titanium/vanadium oxide nanoparticles," *Cellulose*, vol. 20, pp. 1301-1311, 2014.
- [355] I. Reyes-Moreno and R. Verheggen, "Time-sparing and effective procedure for dural closure in the posterior fossa using a vicryl mesh (Ethisorb)," *Neurocirugia*, vol. 17, pp. 527-531, 2006.
- [356] F. Andrade, S. Moreira, L. Domingues and F. Gama, "Improving the affinity of fibroblasts for bacterial cellulose using carbohydrate-binding modules fused to RGD," *J Biomed Mater Res A*, vol. 92A, pp. 9-17, 2010.
- [357] P. Ross, R. Mayer and M. Benziman, "Cellulose biosynthesis and function in bacteria," *Microbiol Rev*, vol. 55, pp. 35-58, 1991.
- [358] C. Haigler, A. White, R. Brown and K. Cooper, "1982," *Alteration of in vivo cellulose ribbon assembly by carboxymethylcellulose and other cellulose derivatives*, vol. 94, pp. 64-69, *J Cell Biol*.
- [359] W. Czaja, D. Kyrlyiuk, C. DePaula and D. Buechter, "Oxidation of gamma-irradiated microbial cellulose results in bioresorbable, highly conformable biomaterial," *Journal of Applied Polymer Science*, p. 39995, 2013.
- [360] H. Backdahl, B. Risberg and P. Gatenholm, "Observations on bacterial cellulose tube formation for application as vascular graft," *Materials Science and Engineering C*, vol. 31, pp. 14-21, 2011.
- [361] A. Massensini, H. Ghuman, L. Saldin, C. Medberry, T. Keane, F. Nicholls, S. Velankar, S. Badylak and M. Mado, "Concentration-dependent rheological properties of ECM hydrogel for intracerebral delivery to a stroke cavity," *Acta Biomaterialia*, vol. 27, pp. 116-130, 2015.

- [362] M. Ma, Y. Ma, X. Yi, R. Guo, W. Zhu, X. Fan, G. Xu, W. Frey and X. Liu, "Intranasal delivery of transforming growth factor-beta1 in mice after stroke reduces infarct volume and increases neurogenesis in the subventricular zone," *BMC Neuroscience*, vol. 9, p. 117, 2008.
- [363] L. Fletcher, S. Kohli, S. Sprague, R. Scranton, S. Lipton, A. Parra, D. Jimenez and M. Digicaylioglu, "Intranasal delivery of erythropoietin plus insulin-like growth factor-I for acute neuroprotection in stroke: laboratory investigation," *Journal of Neurosurgery*, vol. 111, no. 1, pp. 164-170, 2009.
- [364] C. Brackmann, M. Zaborowska, J. Sundberg, P. Gatenhol and A. Enejder, "In situ imaging of collagen synthesis by osteoprogenitor cells in microporous bacterial cellulose scaffolds," *Tissue Eng Part C Methods*, 2012.
- [365] I. Zarkesh, M. Ghanian, M. Azami, F. Bagheri, H. Baharvand, J. Mohammadi and M. Eslaminejad, "Facile synthesis of biphasic calcium phosphate microspheres with engineered surface topography for controlled delivery of drugs and proteins," *Colloids and Surfaces B: Biointerfaces*, vol. 157, pp. 223-232, 2017.
- [366] Z. W, G. Zhou, Y. Gao, Y. Zhou, J. Liu, L. Zhang, A. Long, L. Zhang and P. Tang, "A sequential delivery system employing the synergism of EPO and NGF promotes sciatic nerve repair," *Colloids and Surfaces B: Biointerfaces*, vol. 159, pp. 327-336, 2017.
- [367] A. Henslee, S. Shah, M. Wong, A. Mikos and F. Kasper, "Degradable, antibiotic releasing poly(propylene fumarate)-based constructs for craniofacial space maintenance applications," *J Biomed Mater Res Part A*, vol. 103A, pp. 1485-1497, 2015.
- [368] Y.-Y. Tseng, Y.-C. Wang, C.-H. Su and S.-J. Liu, "Biodegradable vancomycin-eluting poly(D,L-lactide-co-glycolide) nanofibres for the treatment of postoperative central nervous system infection," *Scientific Reports*, vol. 5, p. 7849.
- [369] D. Hoover and A. Mahmood, "Ossification of autologous pericranium used in duraplasty: case report," *J Neurosurg*, vol. 95, pp. 350-352, 2001.
- [370] A. C. A. Ostendorf, "Medical management of eosinophilic meningitis following bovine graft duraplasty for Chiari malformation type I repair: case report," *J Neurosurg Pediatr*, vol. 12, pp. 357-359, 2013.
- [371] G. Sabatino, G. Della Pepa, F. Bianchi, G. Capone, L. Rigante, A. Albanese and e. al, "Autologous dural substitutes: a prospective study," *Clin Neurol Neurosurg*, vol. 116, pp. 20-23, 2014.
- [372] H. Ito, T. Kimura, T. Sameshima, H. Aiyama, K. Nishimura, C. Ochiai and e. al, "Reinforcement of pericardium as a dural substitute by fibrin sealant," *Acta Neurochir (Wien)*, vol. 153, pp. 2251-2254, 2011.
- [373] F. Biroli, M. Fusco, G. Bani, A. Signorelli, O. de Divitiis and e. al, "Novel equine collagen-only dural substitute," *Neurosurgery*, vol. 62(suppl 1), pp. 273-274, 2008.
- [374] R. Menger, D. J. Connor, M. Hefner, G. Caldito and A. Nanda, "Pseudomeningocele formation following Chian decompression: 19-year retrospective review of predisposing and prognostic factors," *Surg Neurol Int*, vol. 6, p. 70, 2015.

- [375] P. Narotam, J. Van Cellen, K. Bhoola and D. Raidoo, "Experimental evaluation of collagen sponge as a dural graft," *Br J Neurosurg*, vol. 7, pp. 635-641, 1993.
- [376] A. Cohen, S. Aleksic and J. Ransohoff, "Inflammatory reaction to synthetic dural substitute. Case Report," *J Neurosurg*, vol. 70, pp. 633-635, 1989.
- [377] T. Ng, K. Chan, S. Leung and K. Mann, "An unusual complication of silastic dural substitute: case report," *Neurosurgery*, vol. 27, pp. 491-493, 1990.
- [378] D. Simpson and A. Robson, "Recurrent subarachnoid bleeding in association with dural substitute, report on three cases," *J Neurosurg*, vol. 60, pp. 408-409, 1984.
- [379] M. Nunes and e. al, "Identification and isolation of multipotential neural progenitor cells from the subcortical white matter of the adult human brain," *Nat Med*, vol. 9, pp. 439-447, 2003.
- [380] S. Pluchino and e. al, "Injection of adult neurospheres induces recovery in a chronic model of multiple sclerosis," *Nature*, vol. 422, pp. 688-694, 2003.
- [381] S. Savitz and e. al., "Stem cell therapy as an emerging paradigm for stroke (STEPS) II," *Stroke*, vol. 42, pp. 825-829, 2011.
- [382] H. Park, X. Guo, J. Temenoff, Y. Tabata, A. Caplan, F. Kasper and A. Mikos, "Effect of swelling ratio of injectable hydrogel composited on chondrogenic differentiation of encapsulated rabbit mesenchymal stem cells in vitro," *Biomacromolecules*, vol. 10, no. 3, p. 5410546, 2009.
- [383] S. Gorham, T. Hyland, D. French and M. Willins, "Cellular invasion and breakdown of three different collagen films in the lumbar muscle of the rat," *Biomaterials*, vol. 11, pp. 113-118, 1990.
- [384] M. Boon, J. Ruijgrok and M. Vardaxis, "Collagen implants remain supple not allowing fibroblast ingrowth," *Biomaterials*, vol. 16, pp. 1089-1093, 1995.
- [385] W. Friess, "Collagen - biomaterial for drug delivery," *European Journal of Pharmaceutics and Biopharmaceutics*, vol. 45, no. 2, pp. 113-136, 1998.
- [386] Y. Nishiyama, J. Sugiyama, H. Chanzy and P. Langan, "Crystal structure and hydrogen bonding system in cellulose I alpha synchrotron x-ray and neutron fiber diffraction," *Journal of American Chemical Society*, vol. 125, pp. 14300-14306, 2003.
- [387] A. Rice, A. Khaldi, H. Harvey and e. al, "Proliferation and neuronal differentiation of mitotically active cells following traumatic brain injury," *Exp Neurol*, vol. 183, pp. 406-417, 2003.
- [388] S. Savitz, D. Rosenbaum, J. Dinsmore, L. Wechsler and L. Caplan, "Cell transplantation for stroke," *Neurological Progress*, vol. 52, no. 3, 2002.

## Appendix

Figure 21 shows the release profile of the 1:1 polymer ratio DWMS.

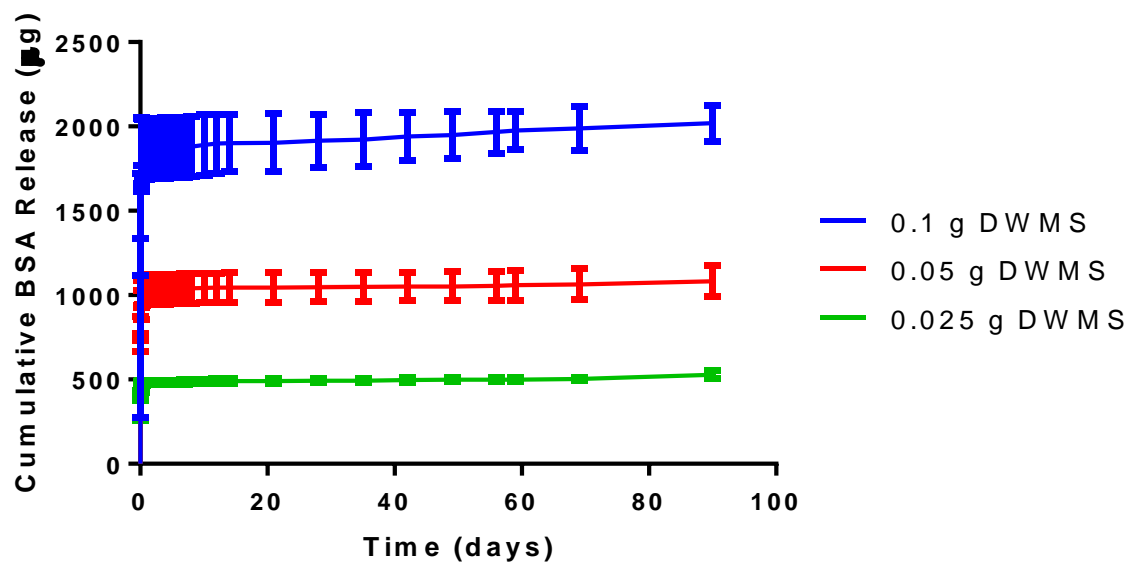


Figure 21. Cumulative BSA released from various amounts of 1:1 DWMS (N=6).

Figure 22 shows an alternative way to present the composite membrane release data.

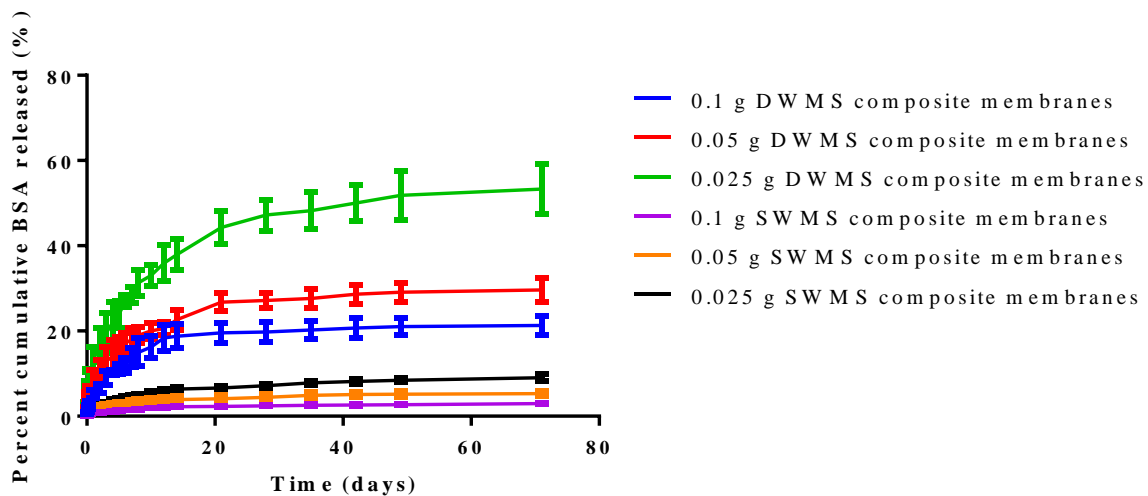


Figure 22. Percent cumulative BSA release from various amounts of SWMS and DWMS incorporated into the composite membranes (N=6).